Petrography and depositional environments of the Lower Ordovician El Paso Formation

by Russell E. Clemons

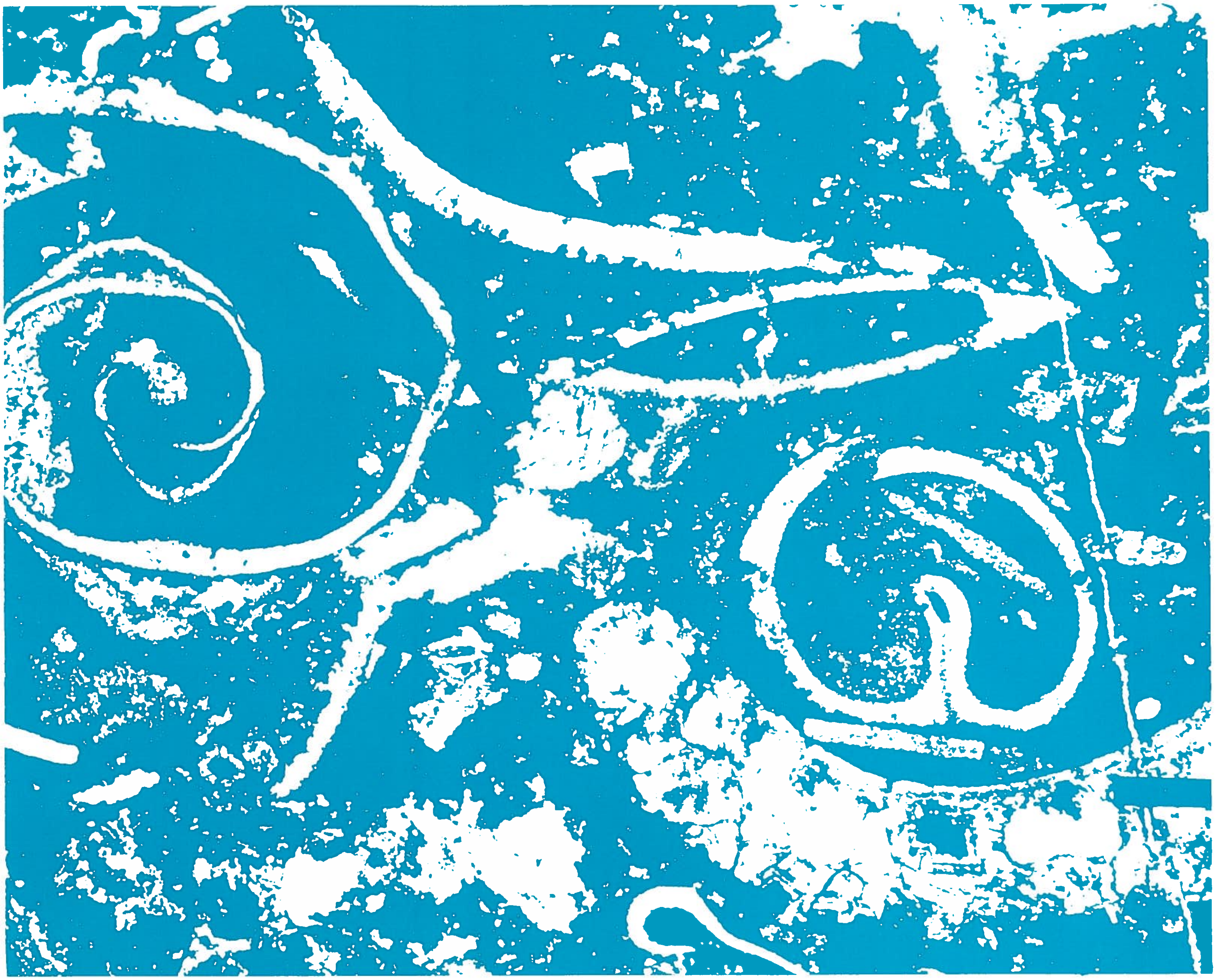

Bulletin 125 New Mexico Bureau of Mines & Mineral Resources 1991

A DIVISION OF

NEW MEXICO INSTITUTE OF MINING & TECHNOLOGY

Bulletin 125

New Mexico Bureau of Mines & Mineral Resources

A DIVISION OF
NEW MEXICO INSTITUTE OF MINING & TECHNOLOGY

Petrography and depositional environments of the Lower Ordovician El Paso Formation

by Russell E. Clemons

New Mexico State University
Las Cruces, New Mexico 88003

SOCORRO 1991

Original Printing

Published by Authority of State of New Mexico, NMSA 1953 Sec. 63-1-4
Printed by University of New Mexico Printing Services, August 1991

Contents

ABSTRACT 5
INTRODUCTION 5
PROCEDURES 5
NOMENCLATURE 5
PREVIOUS WORK *10*
AGE AND THICKNESSES 10
REGIONAL CORRELATIONS 12
ACKNOWLEDGMENTS 13
SEDIMENTARY STRUCTURES 14
***SPONGE-CALATHIUM* MOUNDS** 14
CRYPTALGAL MOUNDS 15
ONCOLITES 17
CRYPTALGAL LAMINITES 18
STYLOLITES 19
BURROWS 19
SCOUR AND FILL 20
CROSSBEDDING 21
PETROGRAPHY 23
TERRIGENOUS CONSTITUENTS 23
ALLOCHEMICAL CONSTITUENTS 23
Bioclasts 23
Brachiopods 23
Calathium 24
Cephalopods 24
Echinoderms 25
Gastropods 25
Girvanella 25
Nuia 28
Ostracods 29
Pulchrilamina spinosa 29
Sponge spicules 29
Trilobites 32
Intraclasts 32
Ooids 33
Pellets and peloids 33
ORTHOCHEMICAL CONSTITUENTS 34
Micrite 34
Spar 35
Dolomite 35
Quartz 36
Other minerals 36
DOLOMITIZATION 38
Origins 38
DEPOSITIONAL ENVIRONMENTS 41
CONCLUSIONS 44
REFERENCES 45
APPENDICES 49
A—OTHER EL PASO FORMATION SECTIONS 49
B—QUANTITATIVE ANALYSES OF THIN SECTIONS 50

Tables

1—Thicknesses of Hitt Canyon, Jose, McKelligon, and Padre Members and total El Paso Formation at 38 sections sampled 8
2—Criteria used for interpretation of depositional environments 42
3—Sedimentary features observed in the El Paso Formation 43
Al—Approximate thicknesses of other El Paso Formation sections 49
B1–B29—Percentages of allochemical, terrigenous, and orthochemical constituents in thin sections 50

Figures

1—Index map of 38 sections sampled 6
2—Chart of stratigraphic nomenclature 7
3A—Isopach map of El Paso Formation 10
3B —Isopach map of Hitt Canyon Member 11
3C—Isopach map of Jose Member 12
4—Outcrop of Jose Member 13
5—Map showing some correlative Cambrian/Ordovician rock units 13
6—Sponge-Calathium mounds 14
7—Locations of *sponge-Calathium* mounds and stacked hemispheroidal stromatolites 15
8—Digitate algae and calcareous channel fill 15
9—Thin section of digitate algae 16
10—Stacked hemispheroidal stromatolites 16
11—Tops of stacked-hemispheroidal-stromatolite columns 17
12—Thin section of stromatactis in stacked hemispheroidal stromatolite 17
13—Oncolites 18
14—Thin section of an oncolite 18
15—Cryptalgal laminites 18
16—Stylolites 19
17—Burrows 19
18—Thin sections of burrow fill 20
19—Chert horizons 20
20—Scour-and-fill intraclastic grainstone 21
21—Thin sections of intraclastic grainstone 21
22—Crossbedding in sandstone and sandy dolostone 22
23—Thin section of grainstone from channel fill 23
24—Calathium 24
25—Thin sections of silicified *Calathium* walls 24
26—Thin section of spicule packstone 25
27—Silicified cephalopods 26
28—Thin sections of echinoderm grainstone 27
29—Silicified gastropods 27
30—Thin sections of gastropods 28
31—Girvanella 29
32—Nuia 30
33—Ostracods 31
34—Pulchrilamina in *sponge-Calathium* mound 31
35—Thin section of *Pulchrilamina spinosa* double layers 31
36—Sponge spicules 32
37—Trilobite fragments 32
38—Gastropod chambers 33
39-0olite 33
40—Ooids 34

41—Concentric ooids 35
42—Radial ooids 35
43—Thin sections of *Nuia* grainstone 36
44—Zoned euhedral dolomite rhombs replacing burrow fill 36
45—Authigenic euhedral quartz in ooid 37
46—Thin section of green clay(?) or glauconite(?) grains 37
47—Distribution of limestone and dolostone at 38 sections sampled 38
48—Interpreted position of Equator during Early Ordovician time 39
49—Beds in upper part of Padre Member **42**

Abstract

The Lower Ordovician (Canadian) El Paso Formation conformably overlies Bliss Sandstone across most of southern New Mexico and west Texas. Locally, lower El Paso beds overlie plutonic and volcanic rocks. Field examination, sampling, and petrographic study of 38 stratigraphic sections from southeastern Arizona, across southern New Mexico, to Van Horn, Texas, indicate the El Paso was deposited in shallow waters near a shoreline to the north. The southwestern edge of the North American craton had subsided gradually throughout most of Canadian time, receiving the up-to420-m-thick El Paso carbonate blanket.

The El Paso Formation is subdivided by lithology into four members that are recognized throughout the region. In ascending order, the members are the Hitt Canyon (33-136 m), the Jose (3-33 m), the McKelligon (45-190 m), and the Padre (35-117 m). The gradually decreasing sand content upward through the Hitt Canyon Member indicates the Hitt Canyon was deposited farther from shore in waters that became deeper as the seas transgressed northward. *Girvanella* oncolites are locally abundant. Stromatolite mounds near the top of the Hitt Canyon and the presence of sand, ooids, and rounded bioclasts in the Jose Member record a shoaling environment. The McKelligon Member contains little or no sand; at several locales *sponge-Calathium* mounds and stromatolite mounds are prominent. The Padre contains a more restricted fauna that includes traces of ostracods. Beds in the lower part of the Padre Member are silty to sandy and locally contain thinly laminated zones.

There is no correlation between stratigraphic members of the El Paso Formation and occurrences of dolostone. Beds in the lower part of the Hitt Canyon Member are typically dolostone, but are limestone at 25% of the sections studied. The El Paso Formation is mostly to completely dolostone at Beach Mountain near Van Horn, Texas, at Bishop Cap, and in the Sacramento, San Andres, Oscura, and Pedregosa Mountains. The El Paso is predominantly limestone at San Diego Mountain and in the Caballo and Mud Springs Mountains, 60 km west of the Bishop Cap—San Andres—Oscura Mountains trend. At other locales, the limestone/dolostone ratios vary with no apparent geographic relationship. Locally, single beds of dolostone are interbedded with limestone sections. More typically, dolostone or limestone prevails for tens of meters of section. Evidence of supratidal dolostone is lacking except in some beds in the Jose and Padre Members. Hydrothermal dolostone is common in several sections.

Pervasive bioturbation of El Paso Formation beds and a varied biota of echinoderms, sponges, gastropods, trilobites, *Nuia, Calathium,* cephalopods, and algae (plus minor brachiopods, *Pulchrilamina,* and ostracods) indicate a predominantly shallow-subtidal environment. Intertidal conditions prevailed intermittently, and possibly supratidal deposition took place during parts of Jose and early Padre times. Low-energy platform environments, in which a large volume of micritic muds accumulated, were often disturbed by storms that produced abundant thin, poorly washed biosparite, intrasparite, and intrasparrudite (bioclastic and intraclastic grainstone) lenses.

Introduction

The El Paso Formation is one of many time-correlative units deposited on the North American craton in shallow Early Ordovician (Canadian) seas. It crops out in most mountain ranges from southeast Arizona to west Texas. Parts of it have been investigated in biostratigraphic detail. The regional knowledge of the formation has also been summarized (Kottlowski, 1963; Hayes, 1975a). The purposes of this paper are: (1) to describe the sedimentary structures, textures, and compositions of the El Paso at 38 locales between Willcox, Arizona, and Van Horn, Texas (Fig. 1); (2) to consider possible origins of dolomitization; and (3) to interpret the depositional environments.

Procedures

Outcrops of the El Paso Formation at 54 locales were investigated and compared with sections described in the literature (Table 1, Appendix A). From the investigations and published descriptions, representative sections at 38 locales (Fig. 1) were chosen for detailed examination and for sampling for petrographic study. Because S. Thompson and A. D. Jacka are doing a separate study of Mescal Canyon, the less well-documented Ram Gorge section (about 1 km north of Mescal Canyon) was chosen as the representative section in the Big Hatchet Mountains. The Scenic Drive section and the El Paso type section were sampled in the southern Franklin Mountains to check for variations over short lateral distances.

Sections were measured with a Jacob's staff and were sampled at varying intervals. Whether limestone portions were sampled at U.5- or 10-m intervals depended on outcrop lithology. That is, if a limestone section appeared uniform in composition, then it was sampled every 10 m; whereas if the lithology changed, each variation in composition was sampled to ensure that all lithology in the section would be represented. The Capitol Dome and Victorio Canyon sections were sampled at 2-3-m intervals as part of another project. From the samples taken from the 38 locales, more than 1,200 thin sections were examined and most (912) were point counted; from the Capitol Dome and Victorio Canyon sections, thin sections were examined, but only about one-third were point counted. Thin sections were described using the classifications of Folk (1959a) and Dunham (1962) and were point counted using grain-solid measurements and a 300-point grid (Flügel, 1982; Appendix B).

Nomenclature

The El Paso Limestone was named by Richardson (1904) for all exposures of Ordovician limestone in the southern Franklin Mountains near El Paso, Texas. Richardson (1908, 1909) later redefined the El Paso to include only the lower "1,000 ft" of Ordovician limestone. Darton (1916, 1917) extended the usage of El Paso Limestone westward into Luna County, New Mexico. Cloud and Barnes (1948) divided the El Paso in the type area into units A, B, and C, in ascending order (Fig. 2). They correlated the El Paso with other Lower Ordovician (Canadian) formations, most notably the Ellenburger Group of west and central Texas (Barnes et al., 1959). Cloud and Barnes (1948) also referred to the El Paso as a

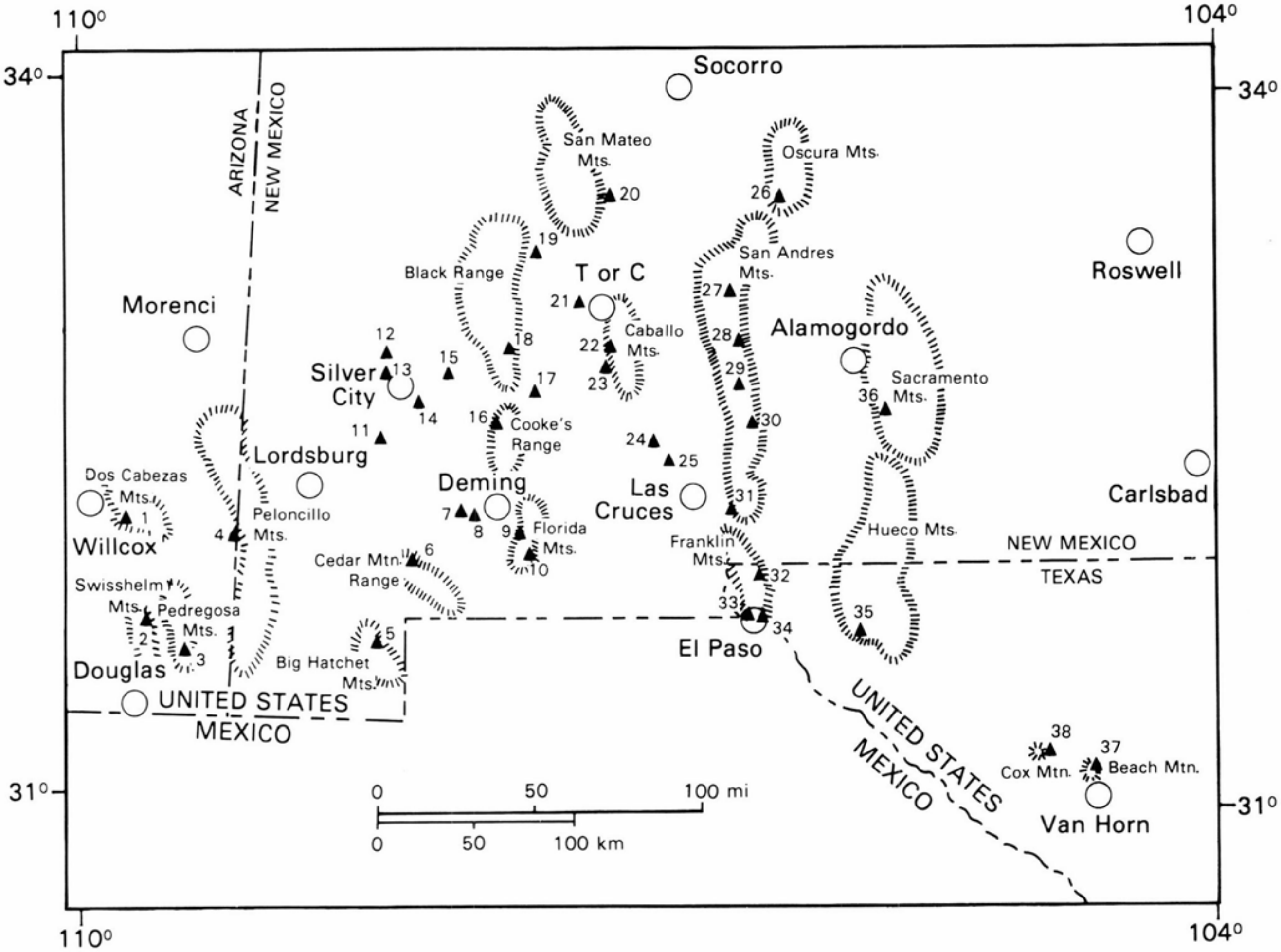

FIGURE 1—Index map of the 38 sections sampled. See Table 1 for locations and references to the sections.

formation rather than as a limestone because regional field studies showed that the El Paso contains a varied lithology of "limestone, dolomite, minor sandstone, and local shale beds" (Cloud and Barnes, 1948: p. 61).

The El Paso Formation was raised to group status by Kelley and Silver (1952). From the lithology observed in the Mud Springs Mountains and at Cable Canyon in the Caballo Mountains, they divided the El Paso Group into two units, the lower Sierrite Limestone and the upper Bat Cave Formation (Fig. 2). Flower (1958, 1959) recognized distinct faunal zones in the El Paso Group and later applied geographic names to the faunal units (Flower, 1964), which then became known as formal formations (Fig. 2). Flower (1969) and LeMone (1969, 1975, 1980) continued to use these formational names. Lucia (1968) established six lithic formational units for the El Paso Group in the Franklin Mountains and correlated these units with Flower's faunal zones. When Harbour (1972) mapped the Franklin Mountains, he maintained the name El Paso Formation, but described six informal units that closely coincided with Lucia's formations. Neither Lucia's nor Harbour's terminology has been accepted by later workers.

Hayes (1975a, b) presented a new formational subdivision of the El Paso Group based on three lithic units recognized from southeastern Arizona to west Texas. The three units are the Hitt Canyon, McKelligon, and Padre Formations (in ascending order). The Hitt Canyon was named by Hayes for its type section, described by Harbour (1972), on the east side of the northern Franklin Mountains. The Hitt Canyon is equivalent to unit A used by Cloud and Barnes (1948) and to five formations used by Flower (1964) in the Franklin Mountains. For the middle unit, Hayes used the name McKelligon, a formation named by Flower (1964) for a section at McKelligon Canyon in the southern Franklin Mountains that was later assigned by LeMone (1969) as a type section. Hayes's McKelligon unit is equivalent to units B, and B_2 of Cloud and Barnes (1948) and to the McKelligon Canyon, Snake Hills, and Mud Springs Mountain Formations of Flower (1964). The Padre, the upper unit, was named by Hayes for Padre Canyon in the Hueco Mountains, 45 km east of the El Paso type section. The Padre is equivalent to units B_2, and C used by Cloud and Barnes (1948) in the type area and to the Scenic Drive and Florida Mountains Formations of Flower (1964).

With slight modifications (Fig. 2), Hayes's units are considered the most appropriate for areal mapping and regional studies. The changes presented in this report are based in part on the recommendation of the American Commission on Stratigraphic Nomenclature (1961) and the North American Commission on Stratigraphic Nomenclature (1983) that formations be mappable at the scale of geologic mapping practiced in this region (1:24,000). Although recognizable throughout the region, subdivisions of the El Paso are not mappable at this scale in southern New Mexico. The

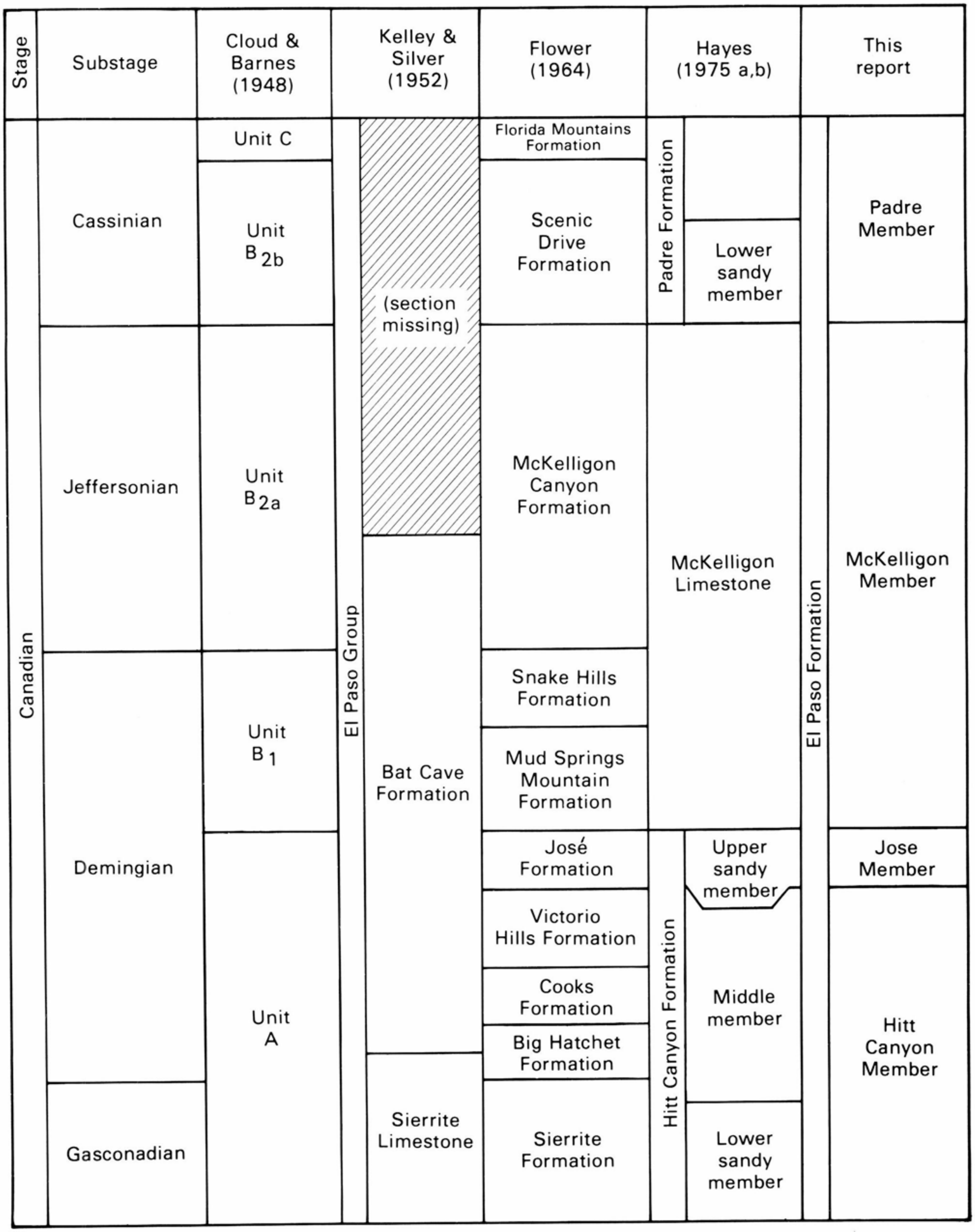

FIGURE 2—Stratigraphic nomenclature of the Lower Ordovician El Paso Formation.

TABLE 1—Thicknesses (in m) of Hitt Canyon, Jose, McKelligon, and Padre Members and total El Paso Formation at 38 sections sampled. Section numbers correspond with those in Figures 1 and 47 and Appendix B.

Section (with location and references)	Hitt Canyon	Jose	McKelligon	Padre	Total
1. **Dos Cabezas Mountains** West edge of Dos Cabezas village, southwest flank of Dos Cabezas Mountains (Jones and Bacheller, 1953; Cooper, 1960; Hayes, 1972).	89	12	10	0	111
2. **North Swisshelm Mountains** Northeastern Swisshelm Mountains, about 40 km north of Douglas (Epis and Gilbert, 1957; Hayes, 1972).	128	12	0	0	140
3. **South Pedregosa Mountains** Southwestern Pedregosa Mountains, north side of Buck Creek, about 3.2 km southeast of Boss Ranch headquarters (Epis and Gilbert, 1957).	?	?	?	?	256
4. **Central Peloncillo Mountains** South side of west end of Wood Canyon, central Peloncillo Mountains (Gillerman, 1958; Armstrong et al., 1978; Drewes and Thorman, 1980a).	120	20	35	0	175
5 **Ram Gorge** 1 km northwest of Mescal Canyon, Big Hatchet Mountains—note Ram Gorge is in sec. 29 T30S R15W, which is not the same location of the Ram Gorge section on plate 1 of Zeller (1965).	136	14	155	0	305
6. **Klondike Hills** Composite section, south end of Klondike Hills, 50 km southwest of Deming (Rupert, 1986).	70+	10+	76+	82+	238+
7. **Victorio Mountains** East end of Victorio Mountains, 32 km west of Deming (Kottlowski, 1960, 1963; Lynn, 1975).	100+	18	6+	0	124+
8. **Snake Hills** Composite section, Snake Hills, 15 km southwest of Deming (Lynn, 1975).	33+	12	80+	15+	140+
9. **Capitol Dome** Northwest end of Florida Mountains (Lochman-Balk, 1958; Lynn, 1975; Clemons, 1984, in press).	76	5	169+	40+	290+
10. **Victorio Canyon** Composite section, north and south sides of Victorio Canyon, near southeast end of Florida Mountains (Brown, 1982; Clemons and Brown, 1983; Clemons, in press).	94	3	171	82	350
11. **Werney Hill** 40 km south of Silver City (Ballman, 1960; Hedlund, 1978).	78+	0	0	0	78+
12. **Bear Mountain** 1.5 km south of Bear Mountain, northwest of Silver City (Paige, 1916; Blankenship, 1972; Cunningham, 1974).	83	9	43	0	135
13. **Chloride Flat** 1.7 km northwest of Chloride Flat, west of Silver City (Paige, 1916; Blankenship, 1972; Cunningham, 1974).	77	6	49	0	132
14. **Lone Mountain** West slope of Lone Mountain, 6.5 km west of Hurley (Jones et al., 1967; Pratt, 1967).	81	15	54	0	150
15. **San Lorenzo** North side of highway, 3.2 km west-southwest of San Lorenzo, west side of Mimbres valley (Jones et al., 1967; Hedlund, 1977).	63	24	59	0	146
16. **Northwest Cooke's Range** Northwest flank of Cooke's Range, 5 km north of Cooke's Peak (Jicha, 1954; Hayes, 1975b).	80	12	131	0	223
17. **Quartzite Ridge** North side of Quartzite Ridge, 3.5 km north-northwest of Lake Valley (Jicha, 1954).	56+	33	45	0	134+
18. **Kingston** South Percha Creek, 3.3 km southwest of Kingston (Kuellmer, 1954; Hedlund, 1977).	120+	6	23	0	149+
19. **Winston** North end of Cuchillo Mountains, 3.5 km east of Winston (Jahns, 1955; Hayes, 1975b).	57	6	12	0	75
20. **Eaton Ranch** Northeast of Bell Hill, 5.6 km north of Nogal Canyon, 56 km north of Truth or Consequences (Kelley and Furlow, 1965).	22	0	0	0	22

TABLE 1—(continued)

Section (with location and references)	Hitt Canyon	Jose	McKelligon	Padre	Total
21. Mud Springs Mountains Southwest flank of Mud Springs Mountains, west of Truth or Consequences (Kelley and Silver, 1952; Hill, 1956; Hayes, 1975b).	113	17	42	0	172
22. Cable Canyon Southern Caballo Mountains, 6.5 km northeast of Caballo Dam (Kelley and Silver, 1952; Hayes, 1975b).	82	15	52 +	0	149 +
23. Red Hills Northeastern Red Hills, 6 km southeast of Caballo Dam (Kelley and Silver, 1952).	111	11	12 +	0	134 +
24. San Diego Mountain Southeast end of San Diego Mountain (Seager et al., 1971).	88 +	0	0	0	88 +
25. Robledo Mountains Northeast end of Robledo Mountains (Kottlowski et al., 1953).	?	?	48 +	4	52 +
26. South Oscura Mountains Southern Oscura Mountains (Bachman, 1968).	39	0	0	0	39
27. Rhodes Canyon Northern San Andres Mountains (Kottlowski et al., 1956).	66	14	15	0	95
28. Hembrillo Canyon North-central San Andres Mountains (Kottlowski et al., 1956).	75	20	82	0	177
29. San Andres Canyon South-central San Andres Mountains (Kottlowski et al., 1956; Bachman and Myers, 1969; Hayes, 1975b).	62	29	115	3	209
30. Ash Canyon Southern San Andres Mountains (Kottlowski et al., 1956; Bachman and Myers, 1969).	60	29	113	35	237
31. Bishop Cap Southeast end of Bishop Cap, southeast of Las Cruces (Seager, 1973).	?	?	190 +	58	248 +
32. Hitt Canyon Head of Hitt Canyon, northern Franklin Mountains (Harbour, 1972; Hayes, 1975a).	66	32	176	81	355
33. El Paso type section 0.4 km north of Pistol Range Quarry at southeast end of Franklin Mountains (Cloud and Barnes, 1948).	130	25	160	105	420
34. Scenic Drive Parallel to, and 0.4 km south of, the El Paso type section (parts have been described by Lucia (1968), LeMone (1976a, b), and Toomey (1970)).	132	22	130	96	380
35. South Hueco Mountains Composite section, southern Hueco Mountains, in approximate areas of Hayes (1975a); "Pasotex Section" (King et al., 1945; Aluka, 1984).	98	27	178	117	420
36. Sacramento Mountains Agua Chiquita Canyon, southern Sacramento Mountains (Pray, 1961).	33	18	45	36	132
37. Beach Mountain Northeast slope of Beach Mountain, 11 km north of Van Horn (Cloud and Barnes, 1948; King, 1965).	50	27	162	101	340
38. Cox Mountain 6 km east-northeast of Cox Mountain, 36 km northwest of Van Horn (King, 1965).	25 +	20	48 +	?	93 +

formational subdivision of the El Paso used by Hayes is therefore abandoned. The Hitt Canyon, the McKelligon, and the Padre are here considered members of the El Paso Formation.

Specifically, Hayes's Hitt Canyon Formation is here redefined as the Hitt Canyon Member, which includes his lower sandy and middle members. Hayes's upper sandy member of the Hitt Canyon, which is equivalent to the Jose Formation of Flower (1964) and LeMone (1969), is here named the Jose Member. Hayes's McKelligon Limestone and Padre Formation are here called the McKelligon Member and Padre Member. The El Paso Formation is thus subdivided into four lithic units (in ascending order): the Hitt Canyon, the Jose, the McKelligon, and the Padre.

Although the Jose Member is very thin and is not mappable at a 1:24,000 scale, the sandy, oolitic unit is easily rec-

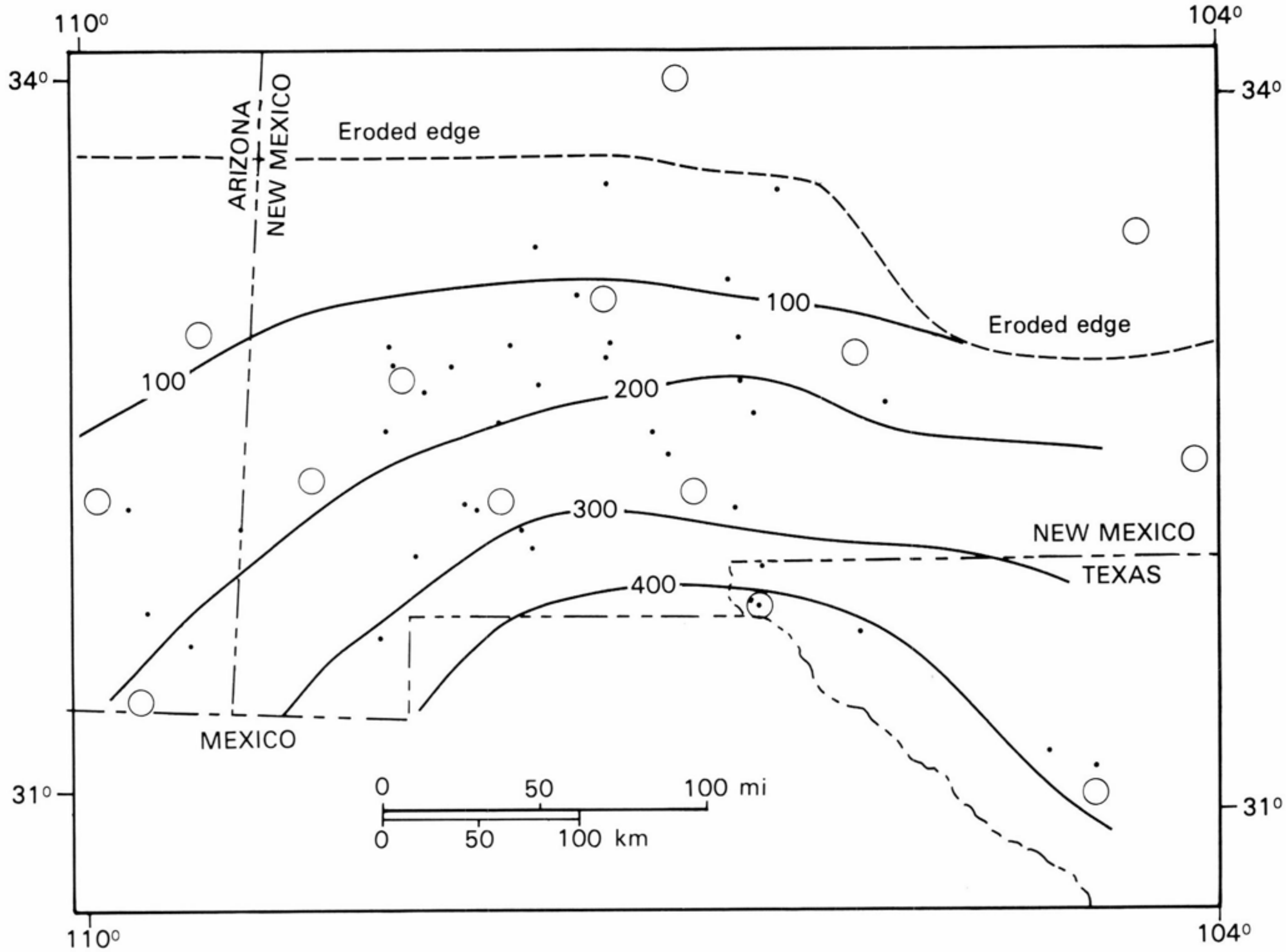

FIGURE 3A—Isopach map of the El Paso Formation. Closed dots show locations of 38 sections sampled; open circles represent cities. For section and city identification, see Figure 1 and Table 1. Contour interval = 100 m

ognizable throughout southern New Mexico. The name Jose has been used for 25 years; the lithic unit to which the name is applied is well understood. It is therefore appropriate to use "Jose Member" for this sandy unit rather than to introduce a new name. The Geologic Names Committee of the U.S. Geological Survey would not, however, accept "Jose" for this unit because Jose is the name of a mining district, not a recognizable geographic feature (Hayes, 1975a).

Previous work

Regional relations and correlations of the El Paso Formation were discussed by Kottlowski (1963), Hayes (1975a), and Aluka (1984). Ethington and Clark (1964) and Repetski (1982) described conodonts from the El Paso Formation in the southern Franklin Mountains. Toomey and Klement (1966), Klement and Toomey (1967), Toomey and Ham (1967), and Toomey (1970) studied the fauna of carbonate mounds and associated strata in the El Paso Formation of west Texas. LeMone (1969, 1974, 1976a, b) summarized and supplemented Flower's faunal units and presented several detailed descriptions of units in the southern Franklin Mountains and the uppermost unit in the southeastern Florida Mountains.

Descriptions of outcrops in varying degrees of detail also accompany the mapping of the El Paso Formation in the Van Horn area (King, 1965), Hueco Mountains (King et al., 1945), Sacramento Mountains (Pray, 1961), Organ Mountains (Seager, 1973, 1981), San Andres Mountains (Kottlowski et al., 1956; Bachman, 1965, 1968; Bachman and Myers, 1969), Caballo Mountains (Kelley and Silver, 1952; Mason, 1976), Mud Springs Mountains (Hill, 1956), San Diego Mountain (Seager et al., 1971), southeastern San Mateo Mountains (Kelley and Furlow, 1965), Black Range (Kuellmer, 1954; Jahns, 1955; Hedlund, 1977), Snake Hills and Victorio Mountains (Kottlowski, 1960; Lynn, 1975), Silver City area (Paige, 1916; Jones et al., 1967; Pratt, 1967; Cunningham, 1974), eastern Big Burro Mountains (Ballman, 1960; Hedlund, 1978), Cooke's Range (Jicha, 1954; Clemons, 1982), Florida Mountains (Lochman-Balk, 1958; Corbitt, 1971; Clemons and Brown, 1983; Clemons, 1984, 1985), Klondike Hills (Rupert, 1986), Big Hatchet Mountains (Zeller, 1965), Peloncillo Mountains (Gillerman, 1958; Armstrong et al., 1978; Drewes and Thorman, 1980a, b), Pedregosa and Swisshelm Mountains (Epis and Gilbert, 1957), and Dos Cabezas Mountains (Jones and Bacheller, 1953).

Age and thicknesses

The El Paso Formation conformably and gradationally overlies the Bliss Sandstone in southern New Mexico and west Texas and the Coronado Sandstone in southeastern Arizona. The Early Ordovician age of the El Paso Formation in southern New Mexico and west Texas has been well documented by Flower (1958, 1959, 1964, 1969), Kottlowski (1963), LeMone (1969, 1974, 1975, 1976a, b), and Hayes

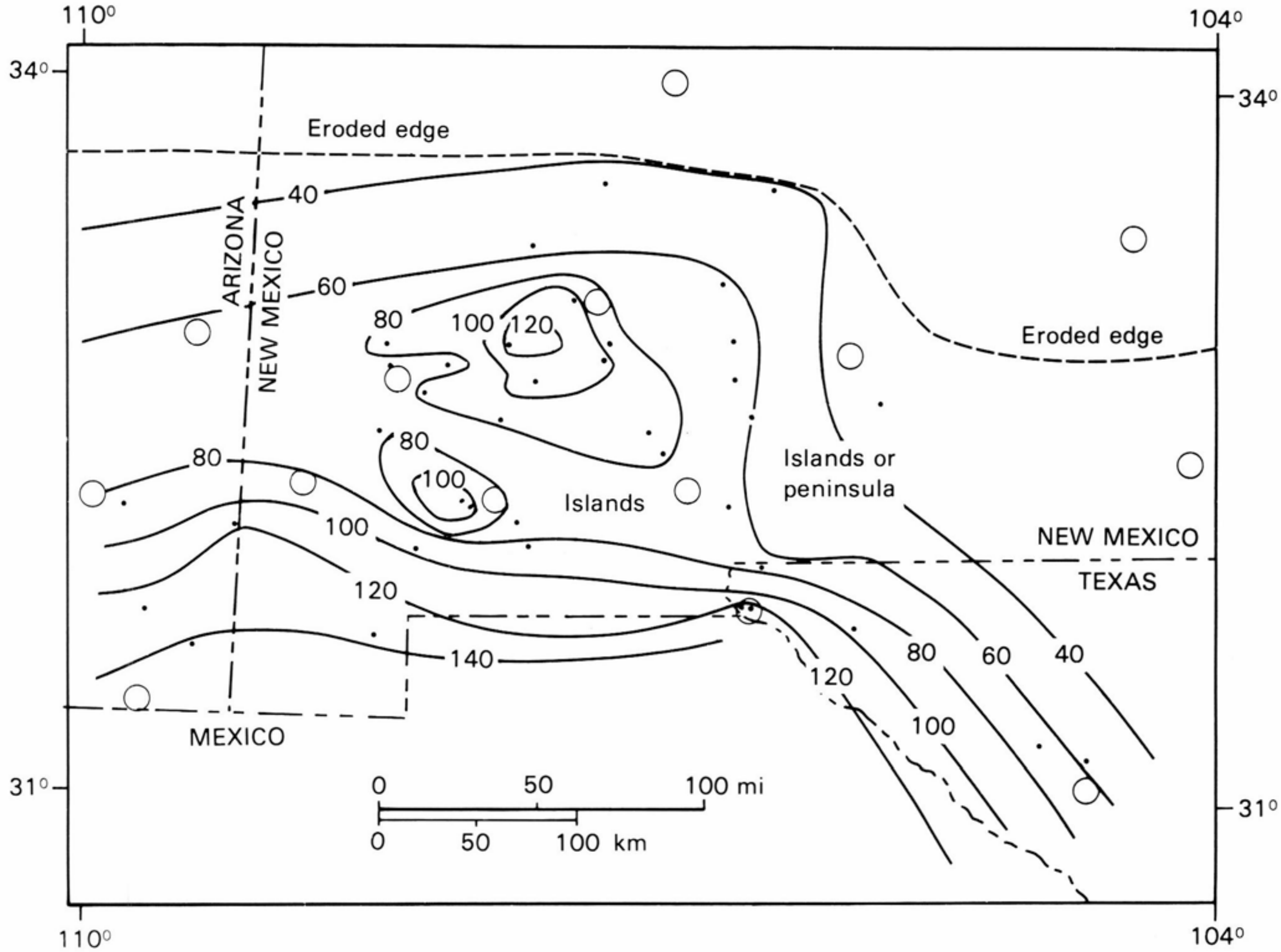

FIGURE 3B—Isopach map of the Hitt Canyon Member. Closed dots show locations of 38 sections sampled; open circles represent cities. For section and city identification, see Figure 1 and Table 1. Contour interval = 20 m.

(1975a). Lindgren (1905), Epis and Gilbert (1957), Sabins (1957), Gillerman (1958), Krieger (1968), and Hayes (1972, 1975a), however, interpreted that the El Paso of eastern Arizona and westernmost New Mexico is of Late Cambrian and Early Ordovician age. The El Paso has been described as diachronous, the lower beds being older in the west and younger in the east. In the Florida Mountains, the El Paso overlies Bliss Sandstone, which was deposited on Cambro-Ordovician (503 Ma) granite and syenite (Evans and Clemons, 1987, 1988). At this locale, the Bliss Sandstone and the El Paso Formation are younger than 503 Ma (Evans and Clemons, 1987).

Although the lowermost Lower Ordovician may be represented by the Bliss Sandstone in some locations (such as the Florida Mountains, mentioned above), almost the entire Lower Ordovician is represented by the El Paso Formation. The lowermost El Paso, the Hitt Canyon Member, was deposited during early Canadian (late Gasconadian) time and the uppermost preserved beds of the Padre Member were deposited during late Canadian (Cassinian) time. A period of erosion preceded deposition of the Montoya Formation during Late Ordovician (Cincinnatian?) time.

Preserved thicknesses of the El Paso Formation range from zero in the southern San Mateo and Oscura Mountains to about 420 m along the U.S.—Mexico border (Fig. 3A). The northward-thinned wedge has been attributed chiefly to erosion during early Middle Ordovician (Chazyan to Mohawkian) time (Darton, 1928; Kelley and Silver, 1952; Kottlowski et al., 1956; Kottlowski, 1963). The thicknesses of the southern sections are partly due to greater depositional thicknesses of the Hitt Canyon and Jose Members (Figs. 3B, 3C). Because Padre Member strata are preserved in only 14 of the 38 locales studied, seven of which are virtually complete, an isopach map of the Padre could not be made. An isopach map of the McKelligon Member also was not drawn. The McKelligon, like the Hitt Canyon and Jose, probably thickens southward as indicated by measurements of 113 m at Ash Canyon in the southern San Andres Mountains, 176 m at Hitt Canyon in the northern Franklin Mountains, 160 to 178 m at five other southern sections, and 190 m or more at Bishop Cap (Table 1). Lack of data on the El Paso Formation in the subsurface of northern Chihuahua and northeastern Sonora prevents positively extending the Lower Ordovician platform farther southward.

Most previous workers have referred to the Bliss Sandstone and El Paso Formation as an eastward transgressive unit on the North American craton. Schuchert (1955) and Stauffer (1962) indicated an east-trending shoreline lay north of Truth or Consequences during the Early Ordovician. Recent work by Clemons and Osburn (1986) and by Stageman (1987) also suggested an east-trending shoreline in southern New Mexico during deposition of the Bliss Sandstone. Although Ross (1976) indicated transgression was more likely from the southwest during Early Ordovician time, isopach

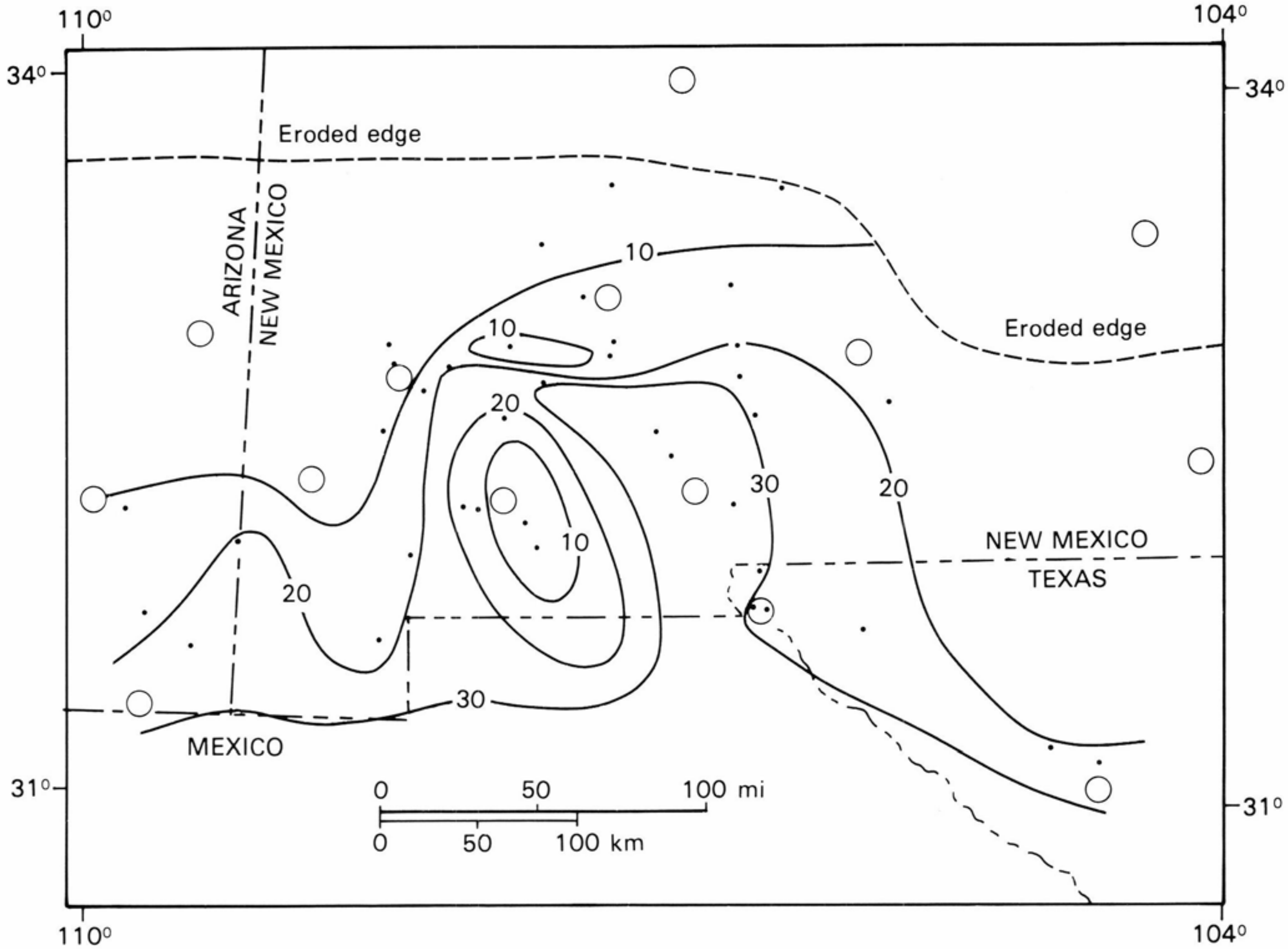

FIGURE 3C—Isopach map of the Jose Member. Closed dots show locations of 38 sections sampled; open circles represent cities. For section and city identification, see Figure 1 and Table 1. Contour interval = 10 m.

maps of the Hitt Canyon and Jose Members strongly suggest transgression from the south. The northward depositional thinning of the Hitt Canyon and Jose Members and the lithology of the Jose suggest an east-west-trending shoreline lay to the north.

The Jose Member is a thin unit (3-33 m) and changes little in lithology from Willcox, Arizona, to Van Horn, Texas, or from its southernmost to northernmost exposures. The Jose is apparently (nearly?) identical in age throughout this 120,000 km^2 area of the Lower Ordovician platform, but precise ages are lacking. The only published conodont study of the Jose is on the El Paso type section in the Franklin Mountains (Repetski, 1982). Additional studies at other sections are needed to verify age relations. Furthermore, a distinct mottled, oolitic lithology (Fig. 4) is easily recognized in the Hembrillo Canyon, Red Hills, Cable Canyon, and Kingston sections. Coincidentally(?), this easterly trend of oolitic strata in the Jose closely parallels the oolitic—hematitic lithotope of the Bliss Sandstone (Kelley, 1951). The northwest-trending thickening and thinning features of the Jose (Fig. 3C) may represent tidal channels or possibly long-shore sand waves. Oriented-grain analyses by Stauffer (1962) showed a north-south alignment in the long axes of elongate grains from the El Paso Formation in the Caballo Mountains. Stauffer attributed the possible cause of the alignment to tidal currents.

Regional correlations

Kottlowski et al. (1956) presented a concise correlation summary of the El Paso Formation. Subsequently, Flower (1964, 1965, 1969) and LeMone (1969) also correlated the El Paso with Canadian-age sections in Arkansas, Missouri, and Utah. The lowest part of the El Paso Formation in southern New Mexico and west Texas is continuous to the west with the Upper Cambrian Copper Queen Member of the Abrigo Formation in Arizona (Hayes, 1975a). To the east, the El Paso is continuous with the Ellenburger Group to central Texas and the Marathon Limestone in the Big Bend region (Cloud and Barnes, 1948; Toomey, 1964, 1970, 1978; Toomey and Nitecki, 1979).

Cloud and Barnes (1948) subdivided the Ellenburger Group into the Tanyard, Gorman, and Honeycut Formations (in ascending order). The upper part of the Tanyard and most of the Gorman appear to correlate with the Hitt Canyon Member of this report. The uppermost Gorman and lowermost Honeycut beds are approximately equivalent to the Jose Member, as suggested by similarities in lithology, fauna, and erosional surfaces. The Jose is a distinct sandy, oolitic unit throughout southern New Mexico. Folk (1959b) stated that an oolitic zone near the Gorman—Honeycut contact is the only stratigraphic horizon traceable in the subsurface Ellenburger. Umphress (1977) also recognized a sandy zone with concentric oolites at the top of the Gorman in Reagan

FIGURE 4—Outcrop of the Jose Member showing mottled, oolitic lithology. From Cable Canyon section, southern Caballo Mountains.

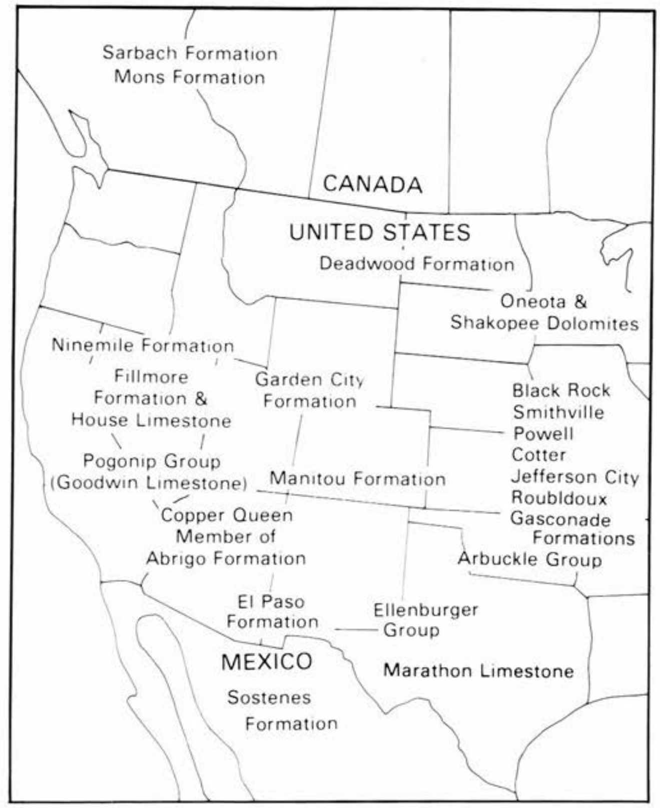

FIGURE 5—Map showing distribution of some Cambrian/Ordovician rock units considered correlative with the El Paso Formation.

County, Texas. Hendricks (1964) interpreted the Gorman-Honeycut contact as an erosional surface. LeMone (1969) and Toomey and Nitecki (1979) correlated most of the McKelligon Member of this report with the Honeycut Formation in central Texas. They considered that the upper part of the McKelligon and the Padre Member are postHoneycut.

Cloud and Barnes (1948), Ethington and Clark (1971), and Toomey (1978) further demonstrated faunal and lithologic correlation of the El Paso, Ellenburger, and Marathon units with the Arbuckle Group in Oklahoma. Toomey (1964, 1%7), Flower (1964, 1969), and LeMone (1969) extended the correlation of the El Paso with Canadian-age Gasconade, Roubidoux, Jefferson City, Cotter, Powell, and Smithville units in Missouri and with the Black Rock Formation in Arkansas (Fig. 5). Northward the El Paso appears correlative with the Oneota and Shakopee Dolomites in Wisconsin and Minnesota, the Manitou Formation in Colorado, and the Deadwood Formation in the eastern Montana—Dakotas region (Toomey, 1978; Ross, 1976). Other correlative units, at least partly based on identification of conodonts and related fauna, include Fillmore Formation and House Limestone in western Utah, Garden City Formation in northeastern Utah, Ninemile Formation and Goodwin Limestone in central Nevada, Sarbach and Mons Formations in British Columbia, St. George Group in Newfoundland, and Beekmantown Group in the Appalachian region (Church, 1974; Hintze, 1973; Pratt and James, 1982; Rigby, 1965; Ross, 1976; Stricker and Carozzi, 1973; Toomey, 1978).

Correlations of the El Paso Formation with southern units is presently not possible. The southern extent of the El Paso and its equivalents are buried by more than 4,900 m of Pedregosa basin fill. Relations between the El Paso and small, poorly exposed outcrops of Lower Ordovician rocks in Sonora and Baja California (Gastil and Miller, 1981; Lopez-Ramos, 1969; Stewart et al., 1984) and the Sostenes Formation in Chihuahua (Bridges, 1964) are poorly understood.

Major funding for this project was provided by the New Mexico Bureau of Mines and Mineral Resources. I am indebted to Frank E. Kottlowski, Director, and the Bureau for continued support of my geologic studies in southern New Mexico. A minigrant from the Arts and Sciences Research Center at New Mexico State University helped to defray costs for some petrographic and photographic work. Discussions with Dave LeMone, Greg Mack, and Sam Thompson III aided in interpretation of the data. A day in the field with Rousseau Flower was especially helpful in recognizing the faunal zones. Greg Dozer provided petrographic data on several of the measured sections. Manuscript quality has benefited greatly from comments by Phil Hayes, Steve Rowland, and Don Toomey.

Sedimentary structures

Sponge-Calathium mounds

Large (up to 6 m high and 13 m long) carbonate mounds are conspicuous in the lower part of the McKelligon Member near the El Paso type section (Fig. 6A). Large sponge-*Calathium* mounds are well developed in the type section and Scenic Drive, Ash Canyon, Cable Canyon, and Lone Mountain sections (Fig. 7). The large mounds are less common at most other locales and with few exceptions are restricted to the McKelligon Member throughout the study area (Fig. 6B). Smaller (less than 1 m high and 1.5 m long) mounds are present throughout the McKelligon and occur in about one-third of the sections studied. A couple of sponge-*Calathium* mounds are present in the Jose Member and one occurs in the uppermost part of the Hitt Canyon Member. None has been reported in the Padre Member.

The *sponge-Calathium* mounds are composed chiefly of lime mud. Toomey (1970) estimated that about 60 to 75% of the mounds are composed of lime mudstone and wackestone. Bioclasts, which may comprise up to 25% of the mound rock, are fragments of mostly echinoderms, spicules and spines, trilobites, and gastropods; *Girvanella, Nuia*, and brachiopods are scarce. The skeletal framework is dominated by siliceous lithistid sponges (Fig. 6C) and *Calathium*, a problematical organism regarded as a quasi-sponge (Toomey, 1970), a receptaculitid alga (Church, 1974), or upright alga (Toomey and Babcock, 1983). In the lower part of the McKelligon at the El Paso type section, the upper "climax stage" of the larger mounds contains abundant *Pulchrilamina spinosa* (Toomey and Ham, 1967). *Pulchrilamina* was not positively identified at any other sections in the study area, although it may be present in the Quartzite Ridge section near Lake Valley. Digitate stromatolites (Figs. 8, 9), where present, are near the bases of *sponge-Calathium* mounds, overlying dolomitized, mottled, burrowed wackestone.

Some *sponge-Calathium* mounds were cut by irregular channels (Fig. 8) before overlying beds were deposited. The channel fills are dark and are composed of bioclastic and intraclastic grainstone (biosparite, intrasparite) and minor packstone (biomicrite). Many large channels have cross-bedded fillings that contain broken and abraded sponges, *Calathium*, and silicified cephalopod siphuncles. Rounded

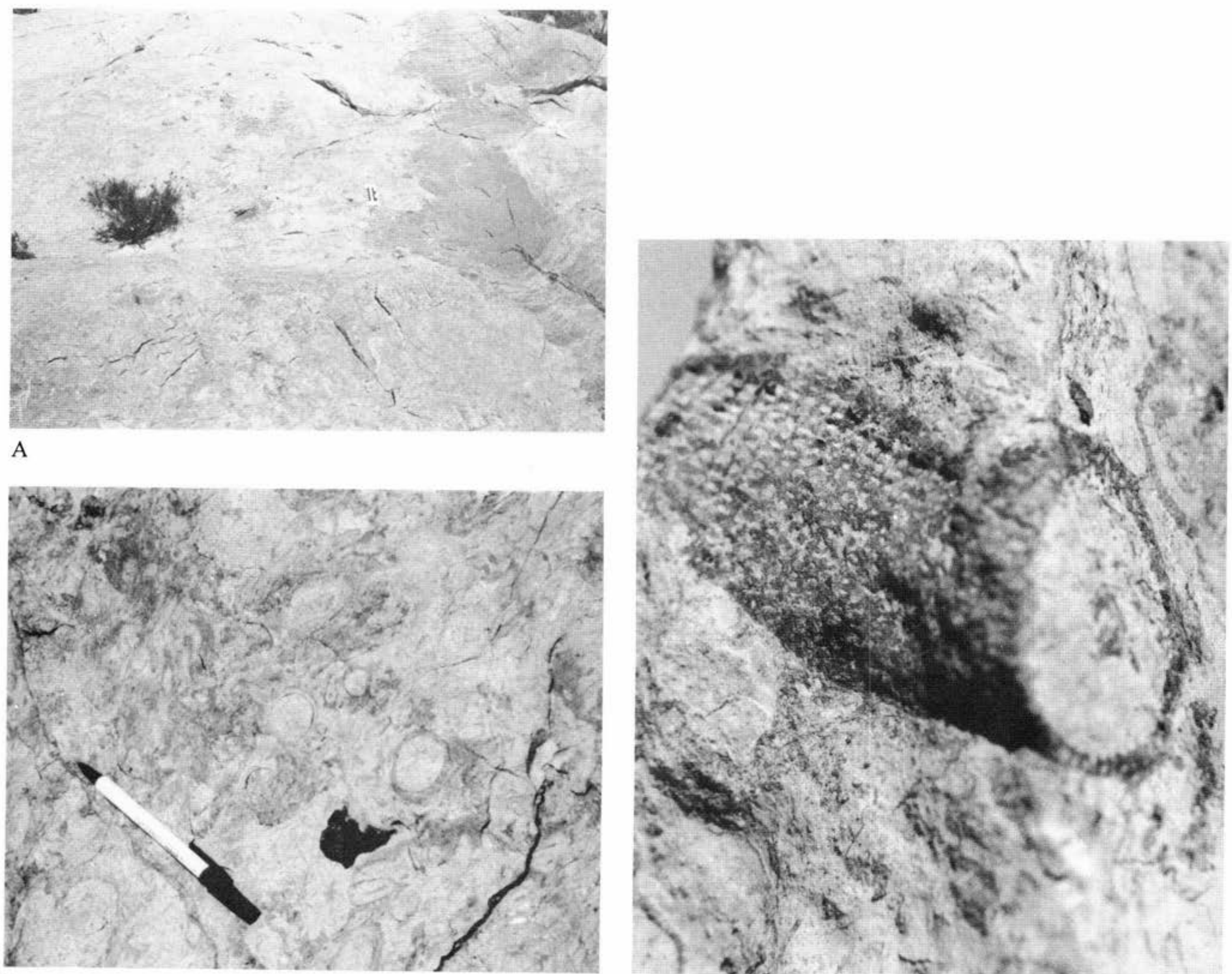

A B C

FIGURE 6—Sponge-*Calathium* mounds. (A) From lower part of McKelligon Member, Scenic Drive section, southern Franklin Mountains. Lechuguilla mound of Toomey (1970). (B) From lower part of McKelligon Member, Klondike Hills section. Pen is 15 cm long. (C) Sponge fragment in sponge-*Calathium* mound from lower part of McKelligon Member, Capitol Dome section, northwestern Florida Mountains. Diameter of sponge is 3 cm.

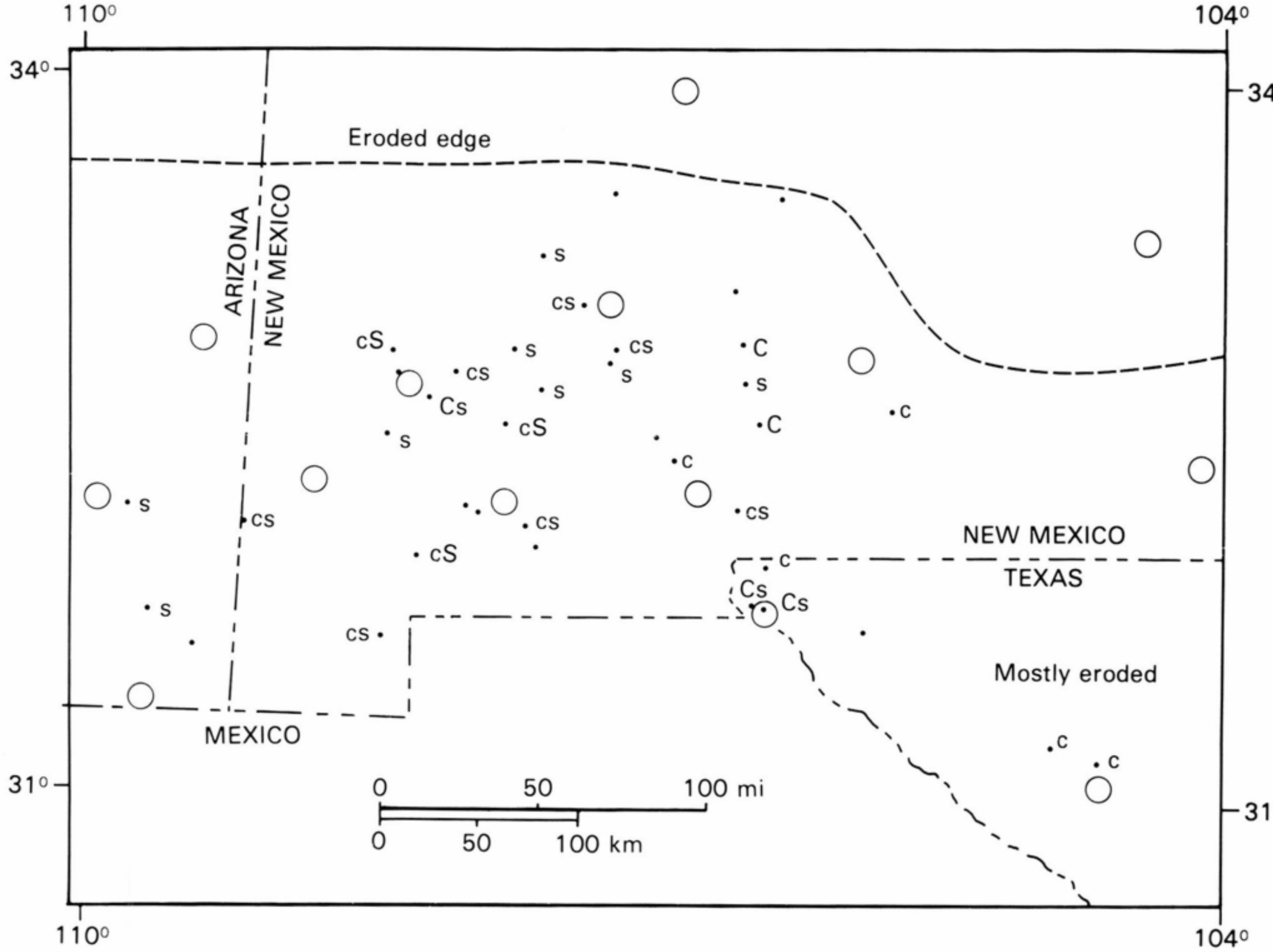

FIGURE 7—Map showing distribution of sponge-*Calathium* mounds (C), and stacked hemispheroidal stromatolites (S). Closed dots show locations of 38 sections sampled; open circles represent cities; large letters indicate abundant large mounds; and small letters indicate scarce small mounds.

intraclasts of mound rock and intermound beds commonly have micritized rims. In many channels, intraclasts are also partly to almost completely replaced by large euhedral dolomite rhombs. Bioclasts include abundant *Nuia* and the skeletal components of the mounds.

Cryptalgal mounds

A second type of carbonate mound in the El Paso Formation are the stacked hemispheroidal stromatolites (Fig. 10A). These cryptalgal mounds are built on bioturbated dolomitic packstone and are common in the upper part of the Hitt Canyon Member; a few occur in the Jose Member and in the lower part of the McKelligon Member, where they are associated with the *sponge-Calathium* mounds. Stacked hemispheroidal stromatolites were not observed in the lower part of the Hitt Canyon, in the upper part of the McKelligon, or in the Padre Member.

Most of the stromatolites are domes of constant radii and no walls. All five types described by Pratt and James (1982)

FIGURE 8—Digitate algae (below scale) and calcareous channel fill (dark zone above scale). From lower part of McKelligon Member, Scenic Drive section, southern Franklin Mountains.

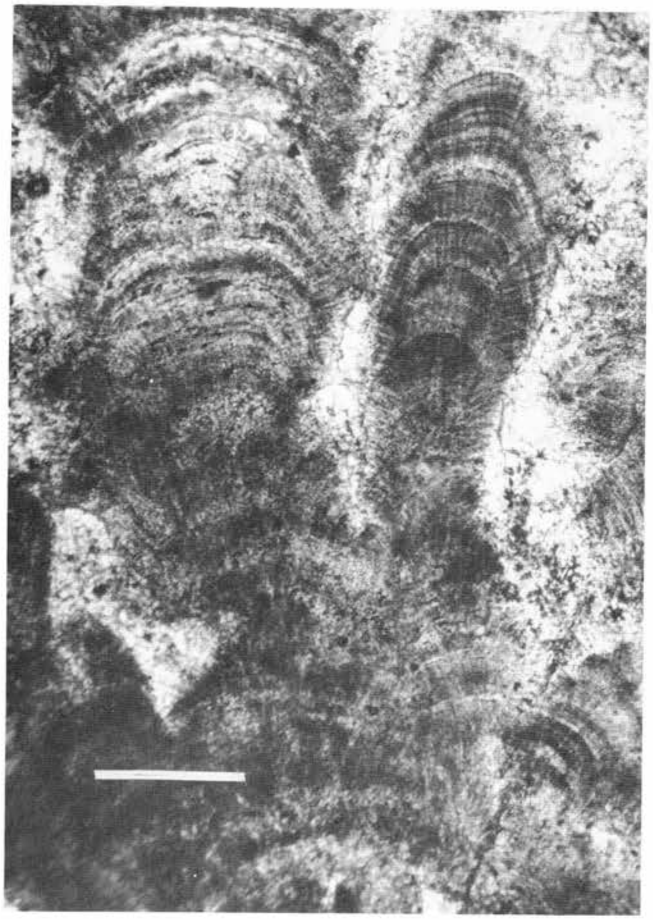

FIGURE 9—Thin section of digitate algae. From lower part of McKelligon Member, Cable Canyon section, southern Caballo Mountains. Bar = 1 mm.

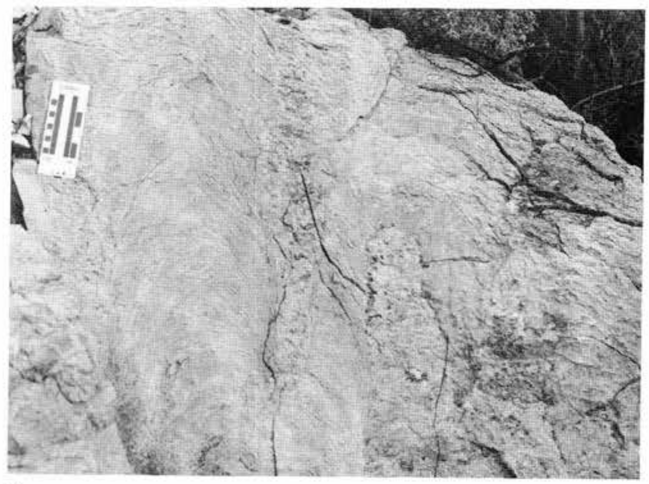

B

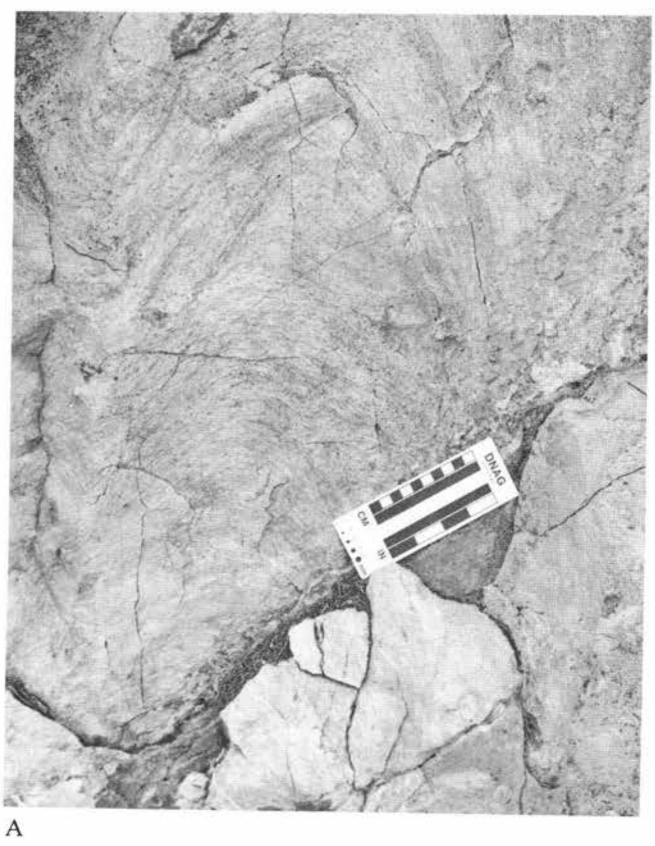

A

C

FIGURE 10—Stacked hemispheroidal stromatolites. (A) From upper part of Hitt Canyon Member, Red Hills section. Stromatactis (spar-filled voids) are subparallel to laminations. (B) Columns of stacked hemispheroidal stromatolites. From upper part of Hitt Canyon Member, northwest Cooke's Range section. (C) Stromatolite mound complex that contains the mound in A. Geologist with 1.5-m Jacob's staff at base of mound complex (bottom center) for scale.

FIGURE 11—Tops of stacked- hemispheroidal-stromatolite columns exposed on bedding plane. From upper part of Hitt Canyon Member, Klondike Hills section. Pen is 15 cm long.

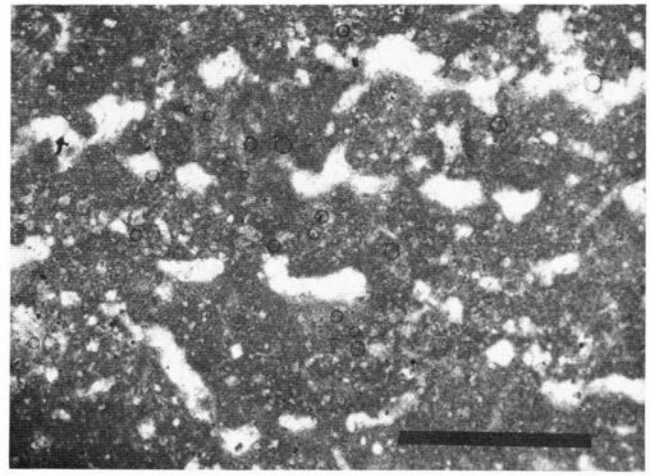

FIGURE 12—Thin section of stromatactis in stacked hemispheroidal stromatolite. From upper part of Hitt Canyon Member, Werney Hill section. Bar = 1 mm.

in the Lower Ordovician St. George Group in western Newfoundland are locally present. Many are built into closely spaced columns that are up to 1 m high and 10 to 30 cm wide (Fig. 10B). In some of the stromatolite complexes, laterally linked hemispheroids connect the columns. In the Red Hills section, one stromatolite column tapers slightly to a cone-top 1.5 m above a 35-cm-wide base. The largest and best developed stromatolites are in the upper part of the Hitt Canyon Member in the Red Hills, Caballo Mountains, Cooke's Range, and Klondike Hills sections. Kelley and Silver (1952) described stromatolitic masses 12 m high and 120 m long in the southern Caballo Mountains. A stromatolite mound complex in the northern Red Hills is shown in Figure 10C.

Stromatolite columns are prominent in the Cooke's Range and Klondike Hills (Fig. 11), where they occur within thick beds at several horizons rather than as convex buildups. These horizons are just below and just above the Jose Member. No stromatolites were seen in the Snake Hills and Victorio Mountains sections, midway between the Cooke's Range and Klondike Hills sections (Fig. 7). Stromatolites occur only as rare small, conical forms in the lowermost part of the McKelligon in the Florida Mountains.

The stromatolite rock in mud mounds is typically lime mudstone or wackestone; it probably accumulated from blue-green algal binding of locally derived sediment and from bioclasts that slowly settled out of suspension (Logan et al., 1964; Pratt, 1982). The only evidence of algal binding in the cryptalgal rock is dark and light laminations, in which the dark color is probably due to algal content. Bioclasts, which comprise 3 to 18% of the rock, are embedded in micrite or microspar. Spicules are the most abundant small bioclasts, followed by traces to a few percent of echinoderms, *Nuia*, trilobites, and *Girvanella*.

The cryptalgal laminated rock typically contains up to 10% spar-filled voids (stromatactis) that are commonly subparallel to the laminations (Fig. 10A). The fenestral fabric of the stromatactis microstructure (Fig. 12) may have been caused by gas escape, organic decay, or desiccation. Spar subsequently filled the 0.2-0.7-mm voids. The cryptalgal laminated rock usually contains a trace to 3% of fine- to coarse-grained quartz silt.

Interstromatolite fillings in the mound complexes are composed of bioclastic and intraclastic grainstone and packstone. Abraded fragments of echinoderms, *Nuia*, and trilobites are abundant; gastropods and brachiopods are sparse. The intraclasts are rounded clasts of cryptalgal laminated rock and spicular wackestone. Scattered euhedral dolomite rhombs are common and traces of small (0.10-0.15 mm) iron oxide cubes (probably pseudomorphs of pyrite) are present in a few thin sections.

Oncolites

Oncolites, spheroidal and ellipsoidal cryptalgal structures that are 0.5 to 1.5 cm in diameter, are common in the Hitt Canyon Member at some locales. Brown (1982) used oncolites as an indicator of "lower El Paso" (Hitt Canyon) when he mapped in the Florida Mountains; they are abundant in the middle and upper parts of the Hitt Canyon at most exposures in the Florida Mountains. Lochman-Balk (1958) and Lynn (1975) referred to the oncolites in the middle and upper parts of the Hitt Canyon as *Girvanella* algal spheres. A graded-bedding appearance is produced at Capitol Dome by repeated sequences of coarse-crystalline, yellowish-brown dolostone separated by a sharp contact from overlying medium-crystalline, medium-gray, oncolite-bearing dolostone.

Oncolites are prominent in the upper part of the Hitt Canyon Member in the Klondike Hills (Fig. 13) as noted by Rupert (1986). Similar oncolites are exposed in the Hitt Canyon at Chaney Canyon on the southwest side of the Big Hatchet Mountains; they are scarce to absent in the Ram Gorge and Mescal Canyon sections in the northeastern Big Hatchet Mountains. Another occurrence of abundant oncolites is in the Ash Canyon section in the southern San Andres Mountains. The oncolite zone there extends from

FIGURE 13—Oncolites. From upper part of Hitt Canyon Member, Klondike Hills section. Oeh letters are 3 cm high.

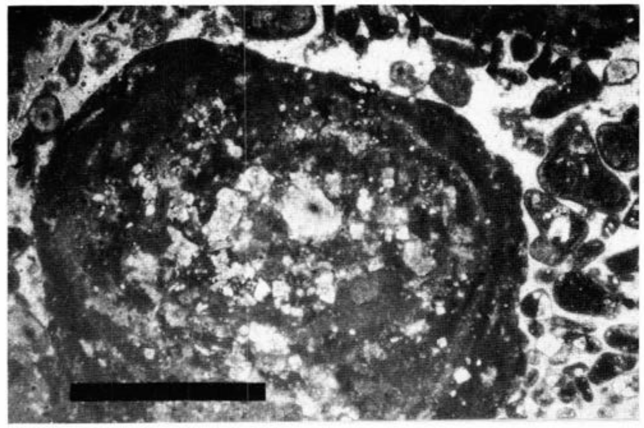

FIGURE 14—Thin section of an oncolite, grapestone, and *Nuia* grains. From Jose Member, Cox Mountain section. Bar = 1 mm.

the uppermost part of the Hitt Canyon into the Jose Member. Oncolites are conspicuous in the Jose northeast of Cox Mountain. Oncolites have not been observed in the McKelligon or Padre Members.

Oncolites have concentric, thin (0.1-0.5 mm) laminae often arranged asymmetrically around intraclast and bioclast nuclei. Many are without distinct nuclei and consist mostly of tangled masses of *Girvanella* (Fig. 14). Micritization and neomorphism of the oncolites have destroyed most of the *Girvanella(?)* tubular structures, but similar morphology in a few oncolites that have remains of *Girvanella* tubules suggests all have a similar origin. Most of the oncolites occur in dolomitized rock where microstructures are not preserved.

Cryptalgal laminites

Thinly laminated (0.5-3.0 mm), silty, fine-crystalline (0.020.06 mm) dolostone and dolomitic siltstone beds are common in the lower part of the Padre Member in the southern Hueco and Franklin Mountains, at Bishop Cap, and in the southern San Andres Mountains (Fig. 15). This lithology is not seen in the Padre in the Florida Mountains. Similar laminated rock occurs locally in the Jose Member in some sections.

The slightly undulating cryptalgal laminites appear to be stratiform stromatolites. Scattered thin (0.5-1.5 cm), discontinuous interlaminae of fine-crystalline dolostone, mudcracks, rip-up clasts, and brecciated layers are common in these stromatolites. Hayes (1975a) interpreted that intraclasts in the lower part of the Padre Member in the Hueco Mountains are desiccation chips of algal-mat dolomite.

Lucia (1971) described cryptalgal laminites in the lower part of the Padre Member, the tidal flat unit that he called the Cindy Formation. The lower laminites in this unit are dark gray to very dark gray and are underlain by about 15 m of crossbedded dolomitic sandstone and 8 m of thin-bedded sandy dolostone.

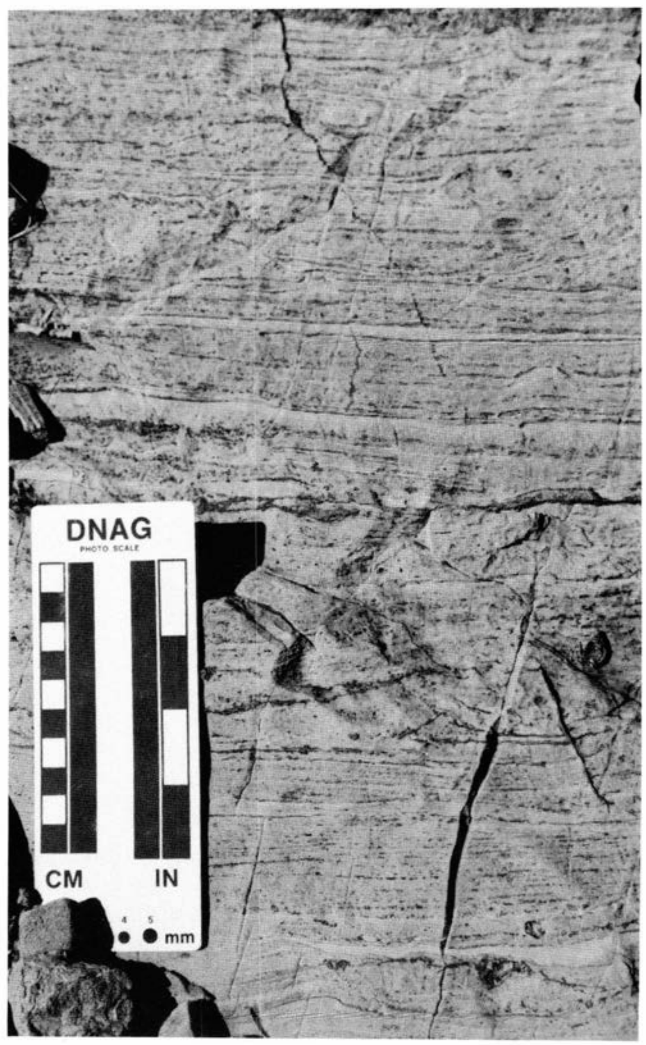

FIGURE 15—Cryptalgal laminites with sandy interlaminae. From lower part of Padre Member, Bishop Cap section.

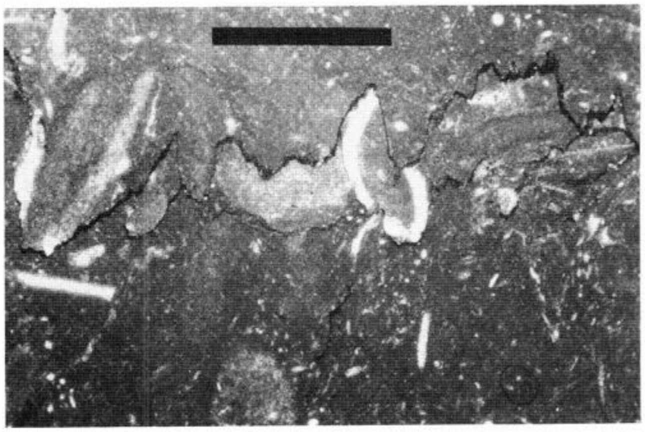

FIGURE 16—Thin section of stylolites in wackestone. From middle part of McKelligon Member, northwest Cooke's Range section. Bar = 1 mm.

Stylolites

Stylolites are abundant throughout the El Paso Formation. Only two or three of the more than 1,000 thin sections examined lack stylolites (Fig. 16). The stylolites are typically parallel or subparallel to bedding. They vary from slightly undulating seams to jagged, seismogram-like lines with vertical columns up to 1 cm high. They are commonly filled with unidentified opaque insoluble material, iron oxides, silt, and some euhedral dolomite rhombs.

In many sections stylolites cut spar veinlets, but in other sections veinlets cut across stylolites. The stylolites obviously formed by solution after lithification because they cut bioclasts, intraclasts, ooids, dolomite rhombs, spar cement, and micrite matrix indiscriminantly. It is interesting to speculate how much dissolved material has been removed from the El Paso and how much of the original thickness of lithified rock has been preserved.

The dolomitic, clay-rich, insoluble residues along stylolites stand out in relief on bedding faces. Hill (1956) and Zeller (1965) referred to this insoluble material as "silty chert laminae" and Kelley and Silver (1952) referred to it as "chert laminations." Many previous workers, including Pray (1961), Kelley and Silver (1952), and Kottlowski (1963), noted its reticulated appearance.

Burrows

Burrows are ubiquitous in carbonate rocks in the El Paso Formation. They stand out in relief on weathered surfaces (Fig. 17A, B) forming the "twiggy" appearance on bedding planes in at least parts of all El Paso sections studied. Several previous authors referred to these features as mottling and fucoidal markings (Jones et al., 1967; Pratt, 1967; Lucia, 1968; Zeller, 1965). Zeller (1965) also referred to them as

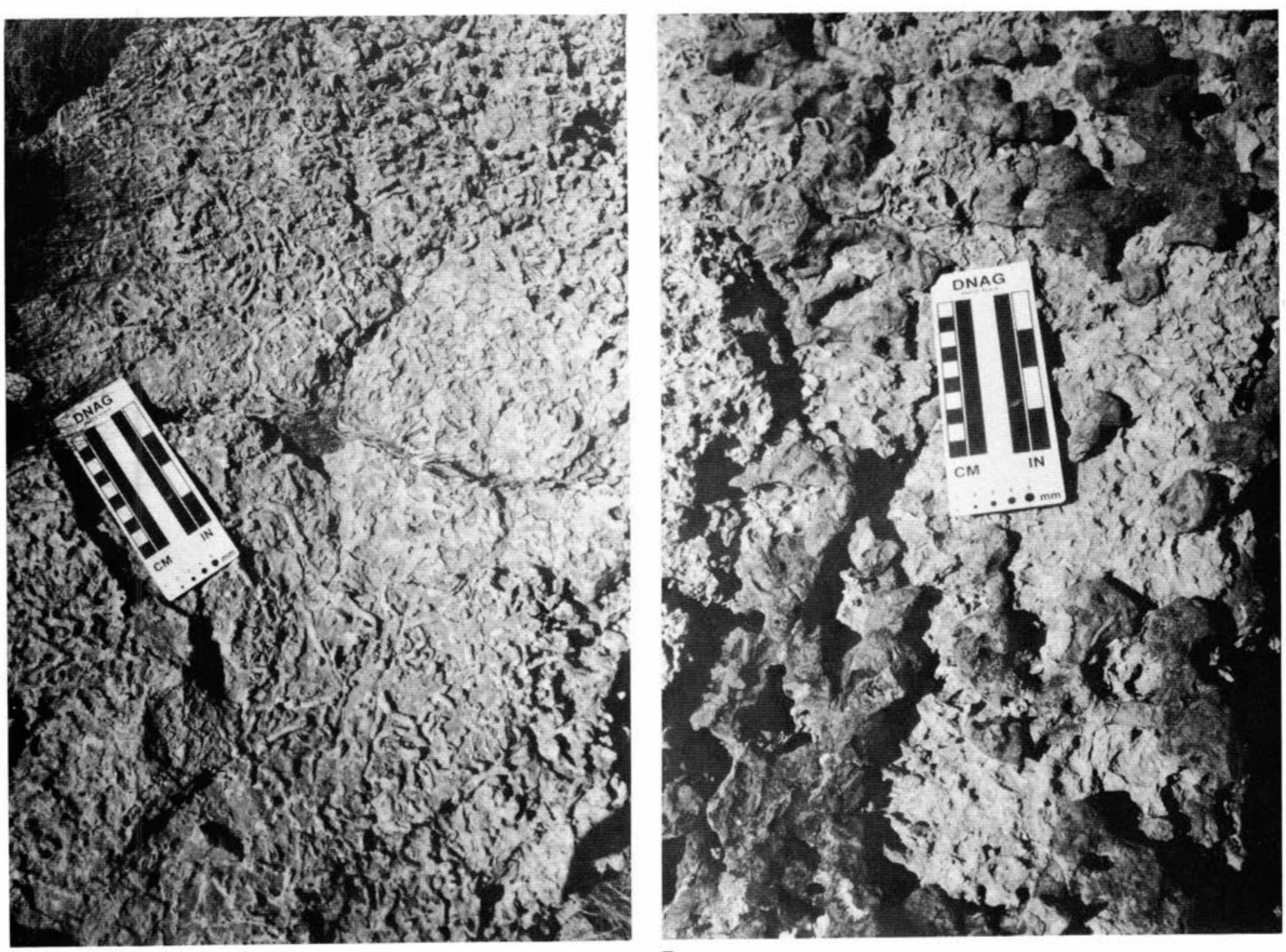

A B

FIGURE 17—Burrows. (A) Small burrows on bedding plane. From upper part of Hitt Canyon Member, Cable Canyon section, southern Caballo Mountains. (B) Ropy chert resembling large burrows on bedding plane. From upper part of Hitt Canyon Member, Cable Canyon section, southern Caballo Mountains.

worm trails or burrows in the upper part of the El Paso in the Big Hatchet Mountains. Lochman-Balk (1958) described these features as "twig-like algal structures." The light yellowish-gray burrow fillings are characteristically dolomitic and often slightly silty and micritic (Fig. 18A). However, burrows filled with bioclasts and spar occur locally (Fig. 18B).

Three sizes of burrows are present in some sections but at different stratigraphic horizons. The burrows most abundant are 0.3 to 1.0 cm in diameter. Smaller burrows (0.10.3 cm in diameter) locally occur with them or alone. The largest burrows(?) are 1.5 to 5.0 cm in diameter and are pervasively replaced by chert. On bedding faces, the brown-weathering chert appears as circular to ellipsoidal chert nodules concentrated in a few zones parallel to bedding (Fig. 19). When seen on bedding planes, the nodules are cross sections of a tubular network. All three types of burrows are mostly horizontal and parallel to bedding and form branching and anastomosing networks (Fig. 17A, B). A few of the smaller burrows may locally traverse bedding as much as 6 cm. The dolomitic and calcitic surfaces of the burrow fills normally show marked differences when weathered; the distinct dolomitic burrow fills are more conspicuous than the calcitic. Locally, intense bioturbation has churned the original sediments to such an extent that individual burrows cannot be distinguished in the mottled textures of bioturbated dolomitic material and "undisturbed" calcitic sediment.

Identity of the creatures that formed the burrows is unknown. Similar occurrences have been attributed by Kendall (1977) to *Spongeliomorpha* and by Sheehan and Schiefelbein (1984) to *Thalassinoides.* Brett and Brookfield (1984) illustrated similar small burrows that they identified as borings by *Trypanites* and intermediate-size burrows as borings by *Thalassinoides.*

Scour and fill

Small-scale erosional surfaces and hardgrounds are common features throughout the El Paso Formation and are especially conspicuous in the McKelligon Member. Relief on scoured erosional surfaces is generally 1 to 5 cm (Fig. 20A) and rarely more than 10 cm. Overlying scoured surfaces of wackestone and packstone are lenses of intraclastic grainstone (intrasparrudite). These lenses average about 3 cm thick; a few are up to 15 or 20 cm thick. The thin lenses pinch out laterally within a few meters, whereas one 20cm-thick lens was traced 100 m to a covered area. Three-dimensional views of the lenses are provided at many exposures. The intraclastic grainstone lenses appear as shallow "basins" rather than as channels. Earlier reports (Kelley and Silver, 1952; Jones et al., 1967; Lynn, 1975; Lochman-Balk, 1958) referred to the intraclastic grainstone as limestone-pebble and intraformational conglomerates and as calcirudite.

The intraclasts in the grainstone lenses average about 1 cm in length, range from 1 mm to 3 cm, and rarely are as much as 10 cm long. They are predominantly well rounded and subelongated, but shapes may vary from equant to discoidal (Fig. 20B). The intraclasts must have been fairly rigid when deposited because none appears to be bent or squashed by adjoining grains. Intraclasts are wackestone, packstone, and lime mudstone (micrite and biomicrite). The

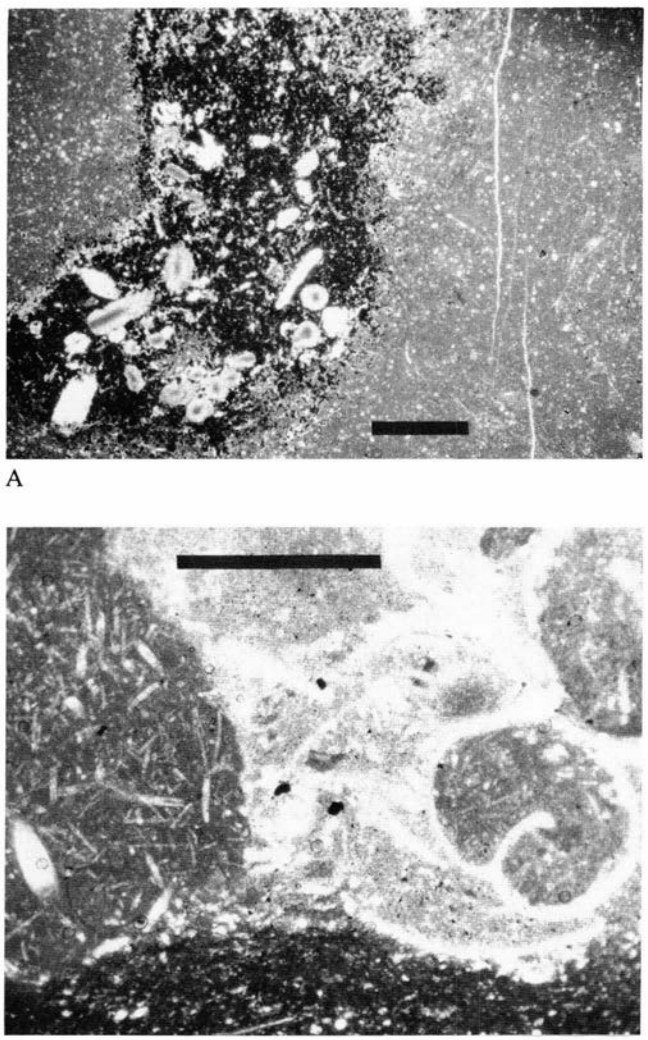

FIGURE 18—Thin sections of burrow fill in spicular wackestone. (A) Dolomitized burrow fill (dark) with *Nuia*. From upper part of Hitt Canyon Member, Werney Hill section. (B) Gastropod-spar burrow fill. From McKelligon Member, San Lorenzo section. Bars = 1 mm.

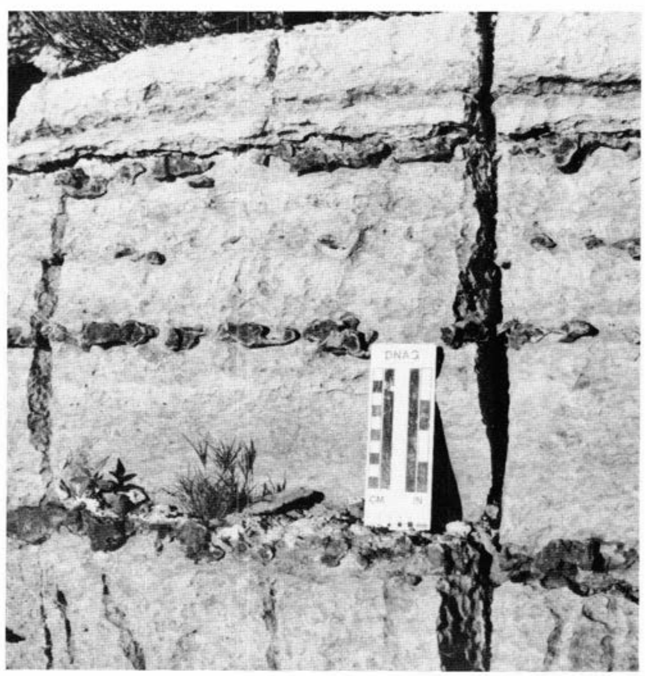

FIGURE 19—Chert horizons. From lower part of McKelligon Member, El Paso type section, southern Franklin Mountains.

type of intraclast that is predominant in each grainstone lens is correlative with the composition of the scoured bed. Spicular wackestone and *Nuia* wackestone are especially common (Fig. 21A). Commonly associated with the intraclasts are skeletal fragments of mud-filled gastropods and trilobites (Fig. 21B). The intraclasts are partly dolomitized in some sections, and typically contain zoned euhedral rhombs confined to the micritic material. These intraclastic grainstone lenses are here interpreted as storm deposits.

Crossbedding

Crossbedding and low-angle cross-laminations are prominent in dolomitic sandstone and sandy dolostone in the basal part of the Hitt Canyon Member at many locales, in the Jose Member in the Franklin, Sacramento, and San Andres Mountains (Fig. 22A), and in the basal part of the Padre Member in the Franklin and southern San Andres Mountains (Fig. 22B). They are also conspicuous in the lower part of the Hitt Canyon at Beach Mountain near Van Horn, Texas, and in the lower part of the Padre at Bishop Cap. Less prominent cross-laminations are exposed in the southern Hueco Mountains. Cross-lamination is directly related to sand content in the El Paso; the less sandy southwestern sections have fewer cross-laminated zones.

A

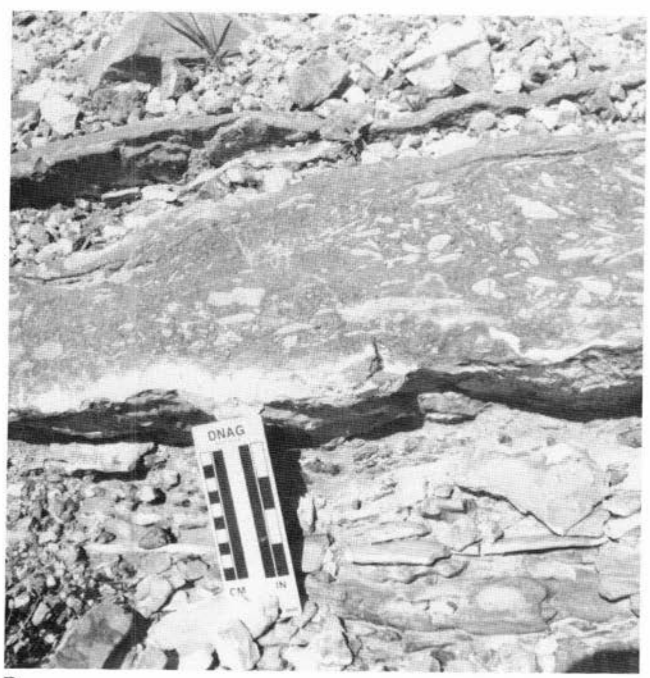

B

FIGURE 20—Intraclastic grainstone. (A) Scour-and-fill intraclastic grainstone (dark) above hardground. From Padre Member, El Paso type section, southern Franklin Mountains. (B) Intraclastic grainstone bed. From near top of Padre Member, El Paso type section, southern Franklin Mountains.

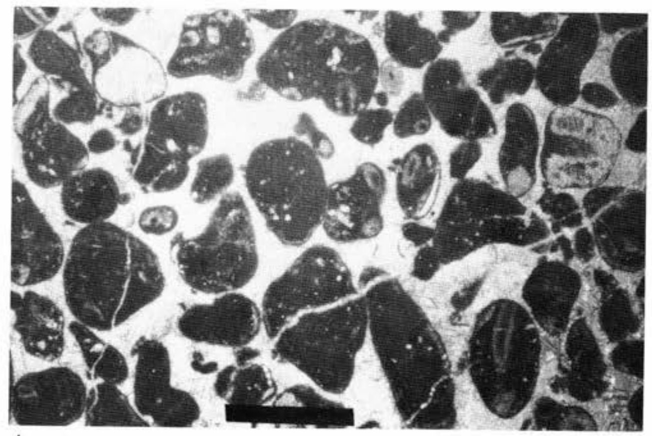

A

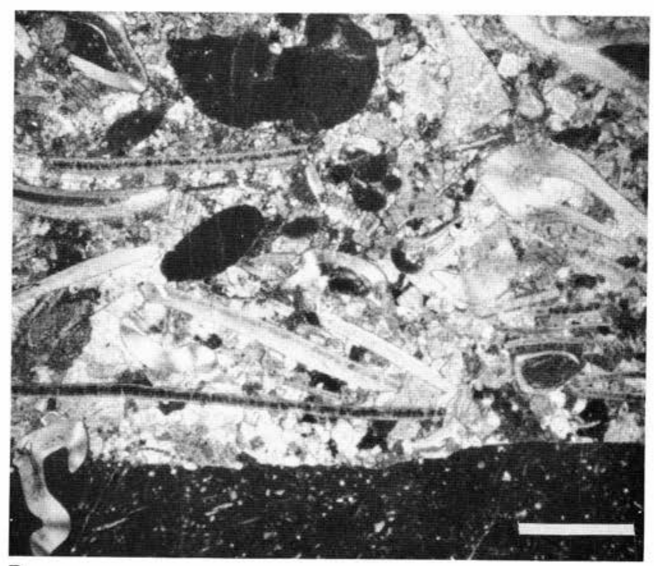

B

FIGURE 21—Thin sections of intraclastic grainstone. (A) The intraclasts are *Nuia* wackestone with few echinoderm fragments. From Jose Member, Klondike Hills section. (B) Trilobite-intraclastic grainstone above hardground developed on spicule wackestone. One trilobite fragment (lower left) projects above hardground surface. From lower part of Padre Member, Victorio Canyon section, southeastern Florida Mountains. Bars = 1 mm.

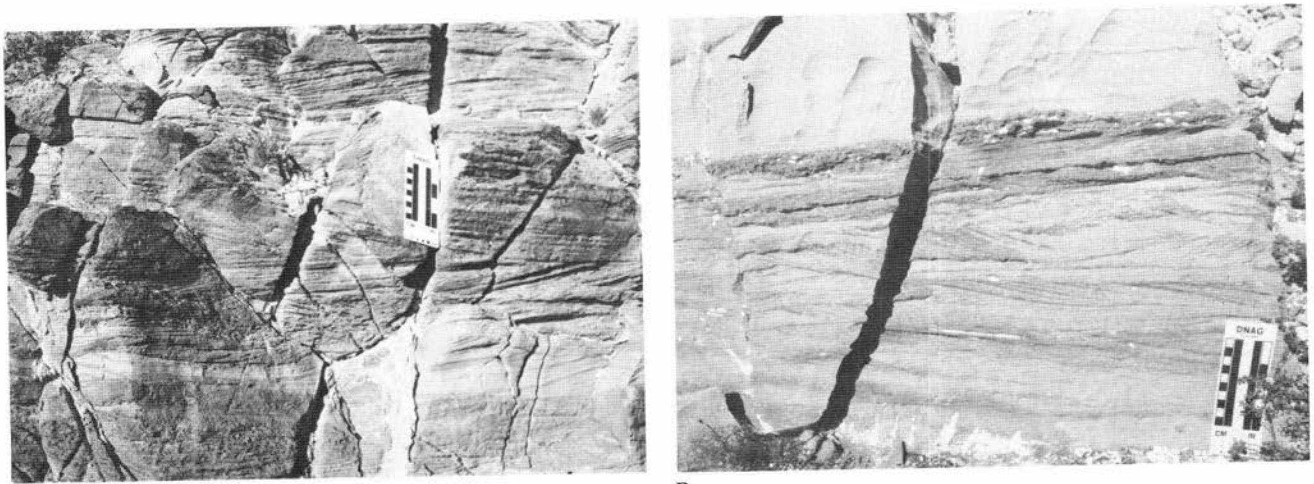

A B

FIGURE 22—Crossbedding. (A) Crossbedded sandstone. From upper part of Jose Member, Scenic Drive section, southern Franklin Mountains. (B) Cryptalgal laminites underlain by low-angle crossbedding in sandy dolostone. From lower part of Padre Member, Scenic Drive section, southern Franklin Mountains.

Cross-lamination sets range in thickness from 10 to 30 cm and have bi-directional dips typical of swash and back-wash deposits. Locally, ripple laminations underlie the thicker cross-laminated beds. Some of these sandy beds have been interpreted as beach deposits (Lucia, 1968). LeMone (1976a) and Stageman (1987) interpreted that the lenticular sand bodies are tidal-channel deposits and the laterally continuous sand bodies are storm-surge and storm-surge ebb deposits.

Petrography

Terrigenous constituents

Terrigenous minerals are minerals that were deposited in a basin as solids, but were derived from the erosion of a land area outside the basin of deposition (Folk, 1959a). Generally, the El Paso Formation contains little terrigenous material. Terrigenous sand and silt are present in the basal part of the Hitt Canyon and Padre Members and in the Jose Member. Sand and silt are generally visible in crossbedded dolomitic sandstone and sandy dolostone (as noted above in section on crossbedding). Most of the sand and silt are made up of well-rounded, well-sorted, medium-grained quartz. Feldspars and volcanic and metamorphic rock fragments are locally scarce to common.

Quartz grains are both monocrystalline and polycrystalline and undulose and non-undulose. Monocrystalline quartz grains are non-undulose and well rounded and contain abundant microlites. Polycrystalline quartz grains are typically undulose and may contain elongated crystals, sutured intergranular boundaries, and deformation lamellae. Feldspar grains are predominantly subrounded microcline and perthite. Plagioclase is rare. The potassium feldspars may be sericitized; plagioclase, where present, is typically kaolinized. A few angular perthite grains are scattered throughout the dolomitic Hitt Canyon Member in the southeastern Florida Mountains.

Lithic terrigenous fragments are also present. Lithic quartz-feldspar grains are subangular, relatively large fragments of monocrystalline quartz and microcline. Volcanic rock fragments have a felted texture, are stained by sodium cobaltinitrite, and thus are rhyolitic in composition. A few well-rounded, large chert grains occur in a couple of sections, indicating a sedimentary source (Stageman, 1987).

The abundance of terrigenous monocrystalline quartz and potassium feldspars in El Paso Formation sandstones indicates a dominantly granitic source; polycrystalline quartz and its particular textures suggest a metamorphic source. The most probable granitic and metamorphic sources for these sands are the Precambrian and Cambro-Ordovician plutons of southern New Mexico. Remnant islands of Precambrian and Cambrian rock were common in the Ordovician and served as sources of detritus for Paleozoic seas (Kottlowski et al., 1969, 1973). In the Franklin Mountains, potassium-rich volcanic rock fragments are present and were derived from the nearby Thunderbird rhyolite, which served as a source of volcanic detritus for the area. Precambrian metasedimentary rocks that are exposed in the Sacramento Mountains were probably the source of the minor sedimentary detritus.

Allochemical constituents

Allochems are constituents that formed by chemical precipitation within the basin of deposition and organized into discrete aggregates (Folk, 1959a). Allochems occur in various stages of preservation throughout the El Paso Formation. They are easily visible in all thin sections of limestone, except in a few from cryptalgal mounds. In dolostone, however, only vague allochem ghosts remain. An allochem ghost is recognizable by the presence of a dusty brown area within the dolomite-crystal mosaic. The brownish appearance is attributed in part to organic matter, but more commonly it is due to the presence of abundant fluid-filled vacuoles in the replacing dolomite (Folk, 1959b). Because most allochems in dolostone have been obliterated and are difficult to identify, only the less intensely dolomitized sections were sampled for detailed study and only about 100 thin sections of dolostone were examined. All allochem percentages in the tables of Appendix B are based on grain-solid analyses (Flügel, 1982) of 300 points for each thin section. A trace indicates that allochems are present in a thin section, but represented no more than 1 point in the count.

Bioclasts

Paleontology of the El Paso Formation has been discussed by many workers, including Cloud and Barnes (1948, 1957), Ethington and Clark (1964), Flower (1953, 1957, 1964, 1969), Hayes (1975a), Jones et al. (1967), Kottlowski et al. (1956), LeMone (1969, 1974, 1976a, b), Pratt (1967), Repetski (1982), Toomey (1970), Toomey and Ham (1967), Toomey and Mement (1966), and Yochelson and Bridge (1957). Flower (1969) noted that the faunal succession in the El Paso is difficult to determine because of poor fossil preservation and a lack of weathering that frees fossils from the carbonate matrix of rocks. Limited collections have yielded specimens of brachiopods, cephalopods, gastropods, sponges, and trilobites. This report concentrates on fossil fragments seen in thin sections.

Brachiopods—Brachiopods are relatively scarce in the El Paso Formation as indicated by the fact that 76% of the thin sections contain no brachiopod fragments. Two thin sections from channels cut in *sponge-Calathium* mounds in the southern Franklin Mountains contain 8 and 15% brachiopod fragments (Fig. 23). Apparently these thin sections represent local concentrations because other thin sections contain no more than 4% brachiopod fragments, and the vast majority have only a trace or none (Appendix B).

The brachiopods are chiefly impunctate types. A few pseudopunctate valves were observed. Locally, as in the San Lorenzo section, thin brachiopod valves are chitino-phosphatic. In other sections, some of the calcareous valves are partly replaced by chalcedony (micro-prismatic silica). Although there does not appear to be any systematic stratigraphic variation in brachiopod content in the El Paso, more

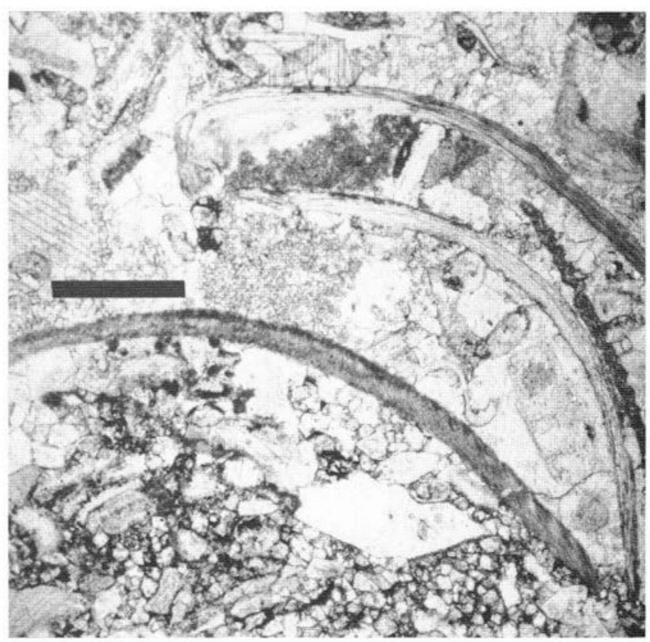

FIGURE 23—Thin section of brachiopod-echinoderm grainstone filling channel cut in sponge-*Calathium* mounds. From lower part of McKelligon Member, southern Franklin Mountains. Bar = 1 mm.

A

B

FIGURE 24—*Calathium*. (A) Longitudinal section of 6-cm-long *Calathium* cone in mound. From near base of McKelligon Member, Scenic Drive section, southern Franklin Mountains. (B) Transverse sections of 3-5-cm wide *Calathium* fragments showing double wall structure. From near base of McKelligon Member, southern Franklin Mountains.

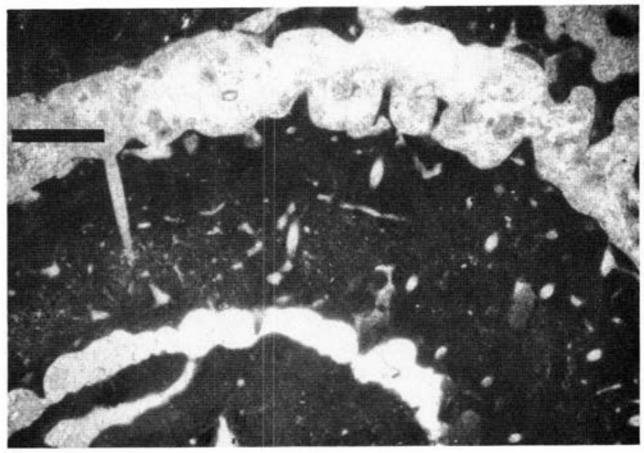

A

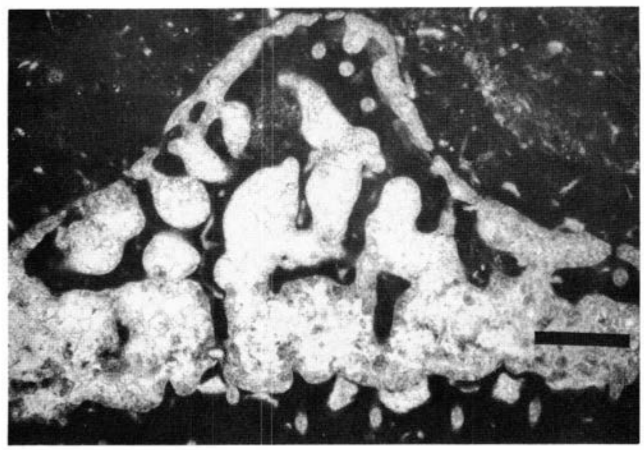

B

FIGURE 25—Thin sections of *Calathium*. (A) Silicified *Calathium* walls and sponge spicules in micrite matrix. From southern Franklin Mountains. (B) Protuberance on silicified outer *Calathium* wall. From southern Franklin Mountains. Bars = 1 mm.

detailed study may show that variations in brachiopod content are related to occurrences of mounds and shoaling episodes.

Calathium—*Calathium* is only present in and near the *sponge-Calathium* mounds, and thus its occurrence is restricted to the McKelligon Member and rare small mounds in the Jose Member. *Calathium* was apparently a rather sturdy organism because *Calathium* fragments are also found in channel fills in mounds and immediately adjacent to mound flanks.

Previously called an upright alga (Toomey and Babcock, 1983), a quasi-sponge (Toomey, 1970), and problematical organism or receptaculitid alga (Toomey, 1981; Church, 1974), *Calathium* is now classified as a receptaculitid (Nitecki, 1986). In growth position, *Calathium* has a downward-tapering cone shape with a root-like system for attachment (Toomey and Nitecki, 1979; Nitecki, 1986). Specimens are up to 12 to 15 cm high and 5 to 6 cm wide at their tops. They are typically silicified on weathered rock surfaces and have grid-network wall structures (Fig. 24A) and characteristic double walls (Fig. 24B). Their spines(?) and walls in transverse section (Fig. 24B) are easily distinguished from sponge spicules by size (Fig. 25A, B).

Calathium was not counted as a separate allochem because of its restricted occurrence. Traces seen in flank beds (Fig. 26) were included with sponge spicules (Appendix B).

Cephalopods—Flower (1964) described the cephalopods in the El Paso Formation. They are represented chiefly by silicified siphuncles (Fig. 27A), but a few outcrops contain whole fossil outlines and septa (Fig. 27B, C). They are scarce

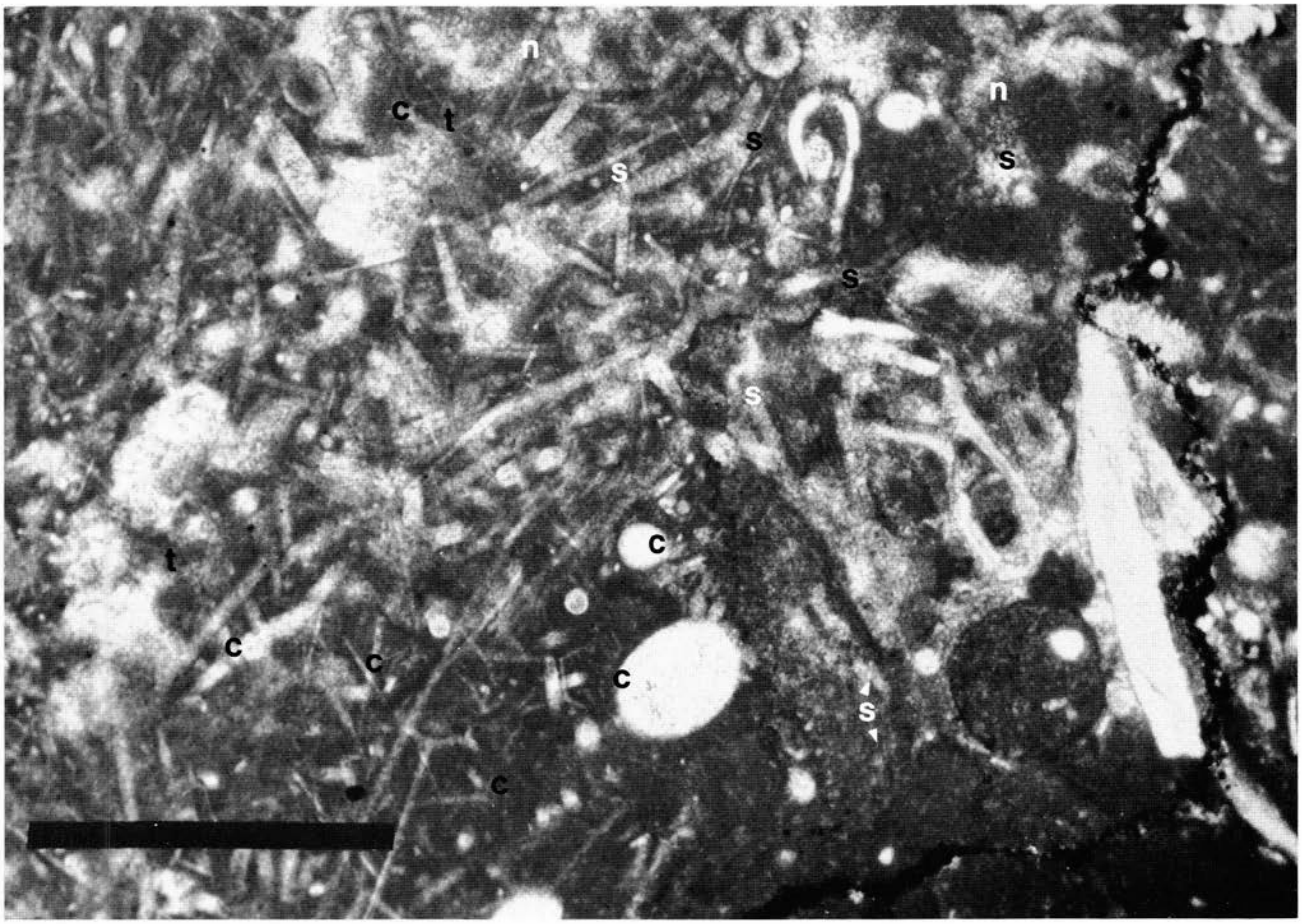

FIGURE 26—Thin section of spicule packstone with both sponge (s) and *Calathium* (c) spicules. Few fragments of trilobites (t), *Nuia* (n) below the stylolite. Bar = 1 mm.

in the Jose and Padre Members, but are common in the upper two-thirds of the Hitt Canyon Member and throughout the McKelligon Member. Their distribution does not appear to vary regionally; cephalopods may be concentrated near mounds, but many siphuncles occur in beds far from any observed mounds.

Cephalopods were not counted as allochems because (1) their size is relatively large and (2) fragments are often unidentifiable. A cephalopod can easily occupy a whole thin section, and so rocks were sectioned to avoid even the siphuncles, which are typically 1 to 3 cm in diameter. In most samples, fragments of original shell material were fragmented beyond positive recognition and were dissolved and replaced by spar or silica.

Echinoderms—Bioclasts herein referred to as echinoderms are organisms composed of stalked and unstalked forms that attached themselves to the sea bottom (pelmatozoans). Predominant ossicle and calyx fragments in the El Paso are probably those of crinoids and some cystoids (Toomey, 1970; Toomey and Nitecki, 1979; Toomey and Babcock, 1983).

Echinoderms are among the most abundant bioclasts in the El Paso Formation. They are present to some extent in most thin sections (Appendix B). Thin sections have an average content of about 5 to 10% and range up to 59% echinoderm fragments (Fig. 28A). The echinoderm fragments are typically bored and have micritized rims (Fig. 28B, C), which Klement and Toomey (1967) interpreted as work of the alga *Girvanella*. Syntaxial overgrowths on the echinoderm fragments are abundant in most thin sections. Locally, the bioclasts are partly replaced by chalcedony. Echinoderm fragments are very well rounded in the Jose Member (Fig. 28C) and some form the nuclei of ooids. There does not appear to be any significant variation in regional or vertical distribution of echinoderms throughout the El Paso.

Gastropods—Gastropods are another important constituent in most thin sections (Fig. 29). A few thin sections contain up to 26% gastropod fragments, but most thin sections average about 2 to 3% (Appendix B).

Gastropods probably made up a larger proportion of original El Paso Formation sediments. Most gastropod shells were originally composed of aragonite, which was dissolved during diagenesis and which left molds. If preserved, the molds were then filled with mosaics of sparry calcite (Fig. 30A, B). Otherwise the organisms were obliterated from the geologic record. The gastropod in Figure 30C appears to have very thin inner- and outer-shell layers of calcite, which enclosed the central aragonite layer that was dissolved and replaced by the spar mosaic.

Gastropods are significantly not common or are absent in grainstone most likely because the shells break up in environments of more agitated waters, where finer grains are winnowed out (Fig. 30D), and are not easily recognized. Both planospiral *(Lecanospira?, Maclurites?)* and high-spired *(Hormotoma?)* gastropods are well represented in the thin sections.

Girvanella—The blue-green alga *Girvanella* apparently was very abundant in original El Paso Formation sediments. Its tubular filaments that are 10 to 16μ in diameter may occur as loose threads (Fig. 31A, B), intertwined felt-like masses, tightly coiled nodular aggregates (oncolites), or as encrustations (Fig. 31C). More typically *Girvanella* occurs as col-

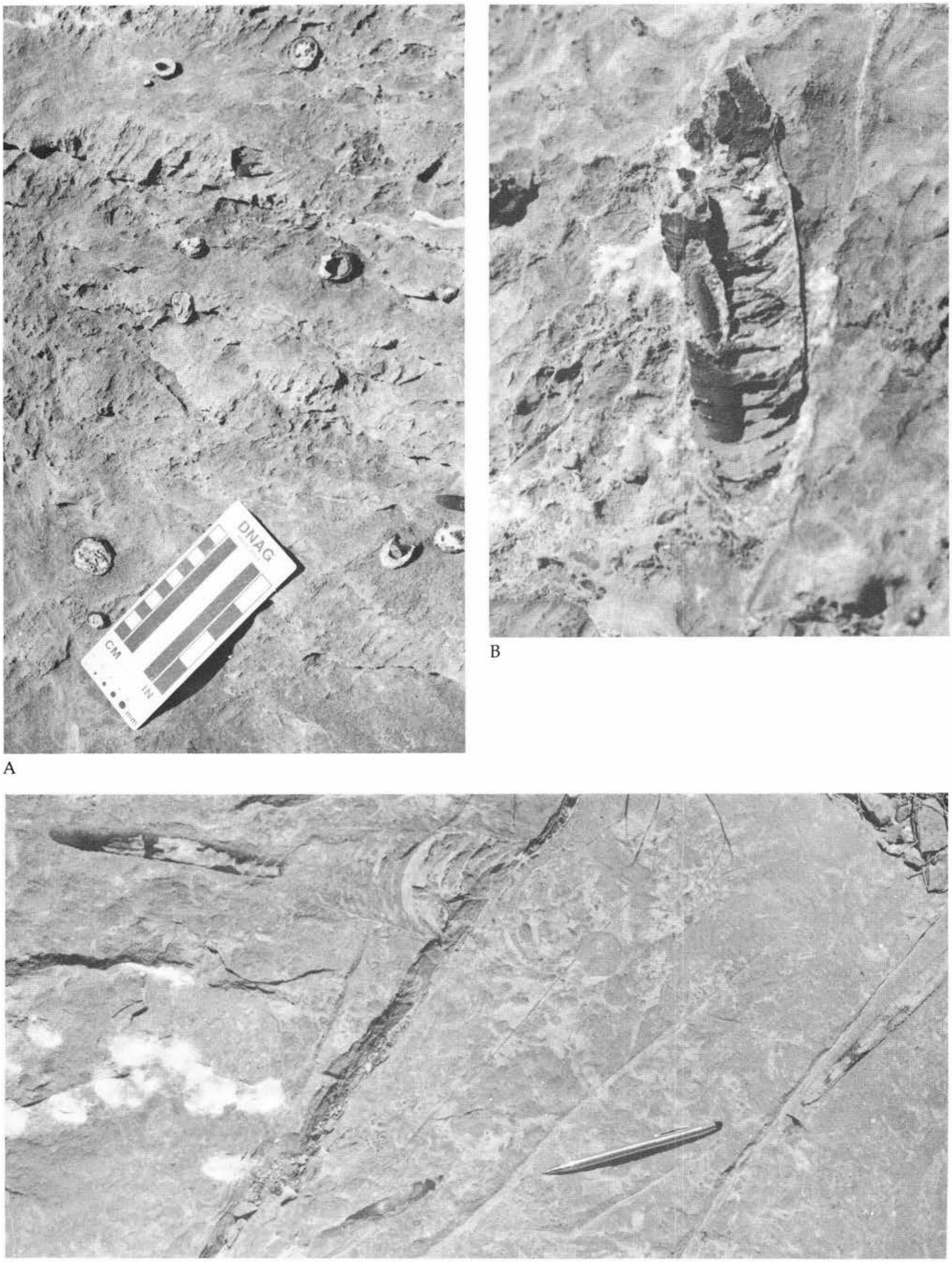

FIGURE 27—Silicified cephalopods. (A) Silicified cephalopod siphuncles. From McKelligon Member, Hitt Canyon section, northern Franklin Mountains. (B) Silicified cephalopod with part of siphuncle and septa preserved. From McKelligon Member, Klondike Hills section (scale unknown). (C) Vague outline of cephalopod with enclosed silicified siphuncle exposed on bedding plane. From upper part of Hitt Canyon Member, Victorio Mountains section. Two other silicified siphuncles are at opposite ends of 15-cm-long pen.

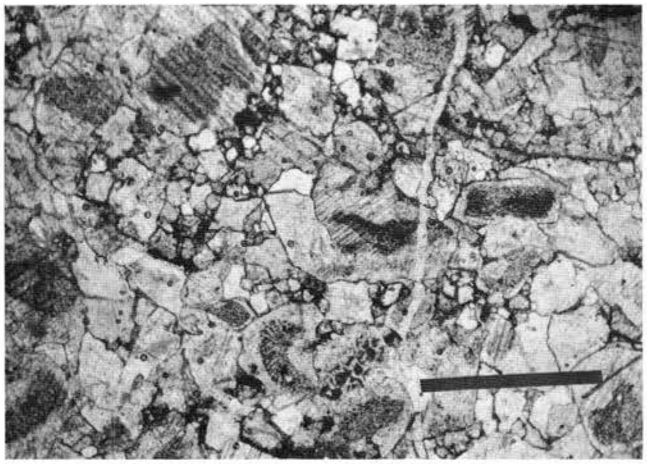

A

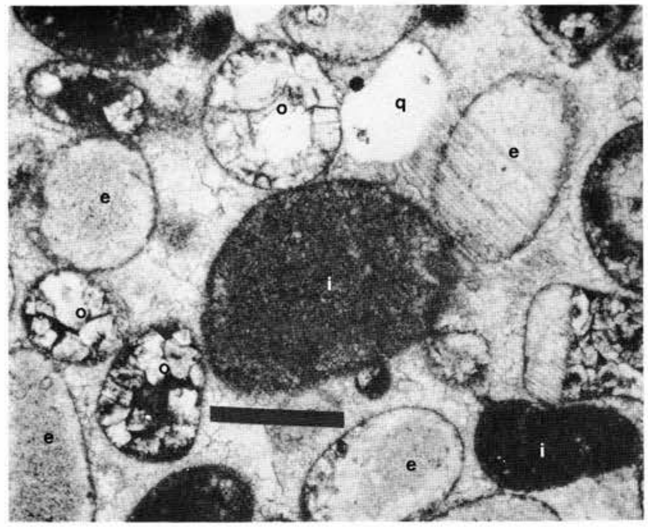

B

FIGURE 28—Thin sections of echinoderm grainstone. (A) Neomorphosed echinoderm grainstone. From Hitt Canyon Member, Bear Mountain. (B) Echinoderm-trilobite grainstone. From Hitt Canyon Member, northwest Cooke's Range section. Several of the echinoderm fragments have large syntaxial overgrowths. (C) Grainstone with rounded echinoderm (e) fragments, dolomitized ooids (o), intraclasts (i) (all with micritized rims), and quartz (q) grains. From Jose Member, Capitol Dome section, northwestern Florida Mountains. Bars = 1 mm.

FIGURE 29—Silicified gastropods on bedding plane. From Padre Member, Bishop Cap section.

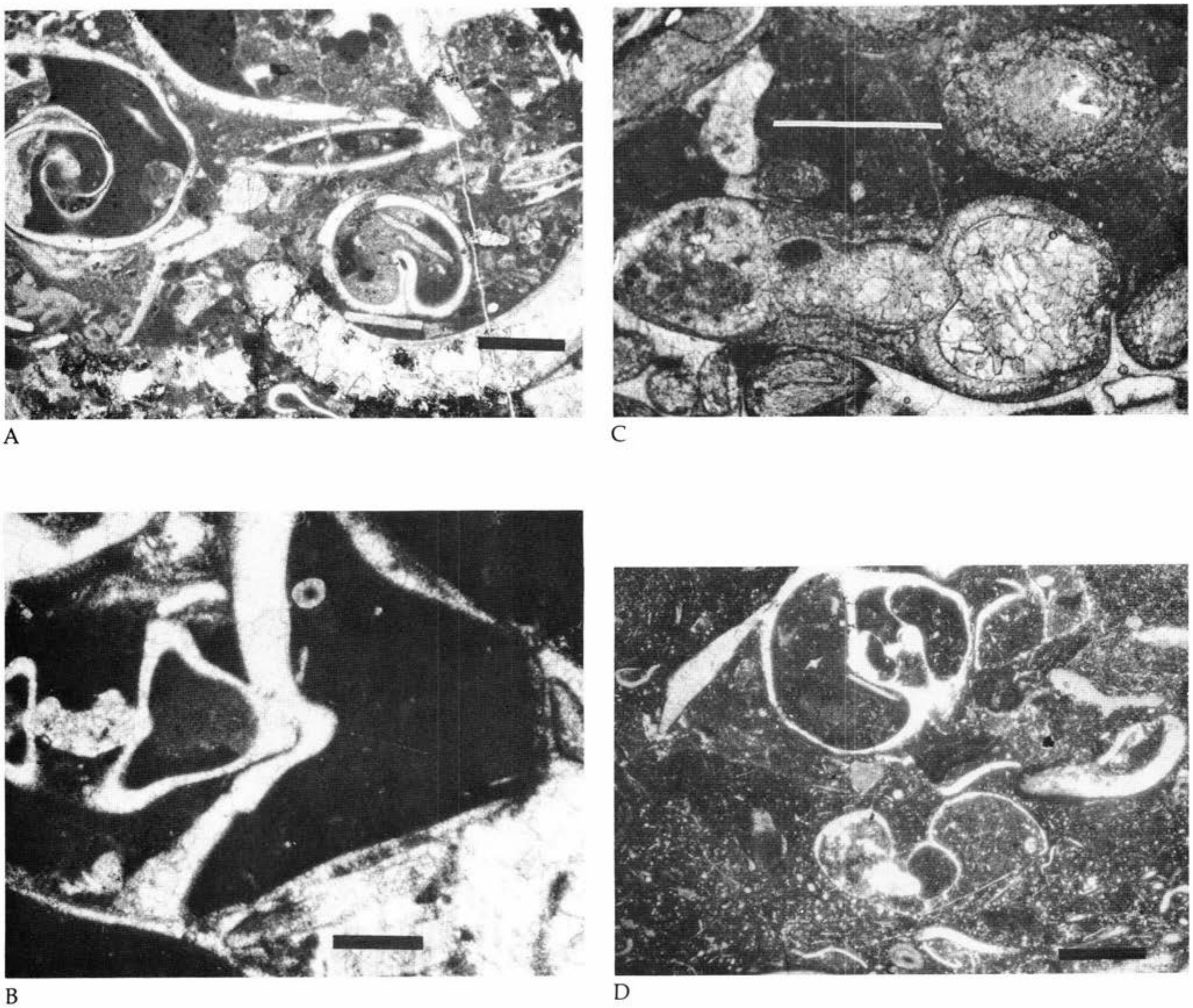

FIGURE 30—Thin section of gastropods. (A) Gastropod packstone with *Nuia*, echinoderm and trilobite fragments, and intraclasts. Dolomite replaced some spar in large gastropod cast; several trilobite fragments possess *Girvanella*(?) bored rims. From lower part of McKelligon Member, Snake Hills section. (B) Planospiral gastropod spar cast and micrite chamber fillings; single *Nuia* in upper part of large chamber. From McKelligon Member, Capitol Dome section. (C) Planospiral gastropod and concentric ooids. Upper right ooid has trilobite-fragment nucleus. From Jose Member, northwest Cooke's Range section. (D) Gastropod-spicule wackestone with *Nuia* and trilobite fragments. From Hitt Canyon Member, Victorio Canyon section. Bars = 1 mm.

lapsed dark, micritic tubules in which the characteristic outlines are destroyed.

Klement and Toomey (1967) described the corrosion of allochems and micritic rims on allochems and interpreted that the corroded features were bored and perforated by *Girvanella*. *Girvanella* was not point counted because positive identification could be made in only a few thin sections. Much of the micrite matrix seen in thin sections probably comprises *Girvanella* material.

Nuia—A problematical micro-organism known as *Nuia siberica* (Maslov, 1956) is the most abundant and characteristic bioclast in the El Paso Formation. *Nuia siberica* Maslov has straight or curved tubes with dark central canals. The single and multiple walls are composed of radially arranged, hyaline calcite prisms (Fig. 32A). Transverse sections are circular (up to 0.8 mm in diameter), oblique sections are elliptical, and longitudinal sections are elongate (up to 3 mm in length). Mamet and Roux (1982) illustrated *Nuia siberica* as an upright stalked form with dichotomous ramifications and encasing or budding growths, which could produce sections seen in Figure 32B.

Previous to 1965, several workers, including Folk (1959b) and Stauffer (1962), referred to *Nuia* grains in the Ellenburger Group and El Paso Formation as oolites. Umphress (1977) also referred to *Nuia* grains in the Ellenburger as oolites. Flower (1964) reported "an unnamed hollow tubular alga" in the El Paso Formation. Swett (1964) reported and illustrated questionable algal grains in the Lower Ordovician Manitou Formation of Colorado. Toomey (1965) and Toomey and Klement (1966) recognized these grains as *Nuia* and reported the occurrence of *Nuia* in the El Paso in the southern Franklin Mountains.

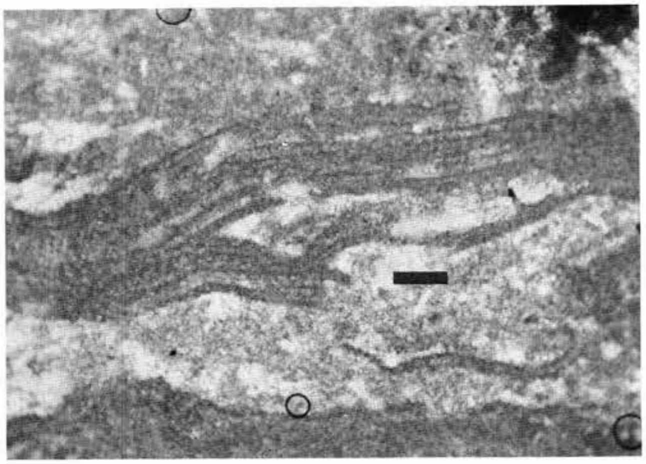

A

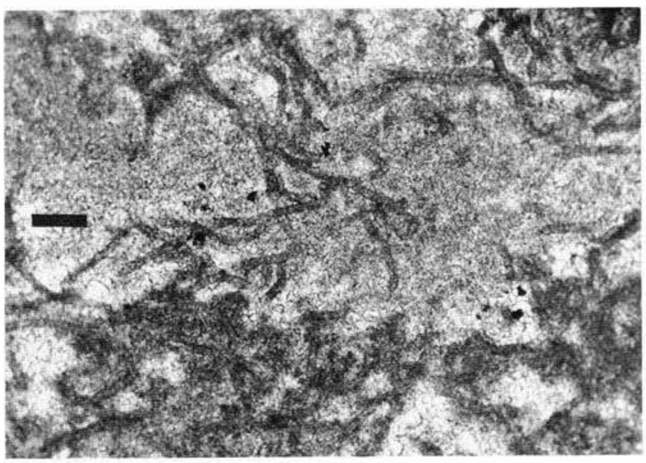

B

C

FIGURE 31—Thin sections of Girvanella. (A) From Hitt Canyon Member, San Lorenzo section. (B) From McKelligon Member, southern Hueco Mountains section. (C) *Girvanella* with trilobite and gastropod fragments. From Hitt Canyon Member, Cable Canyon section, southern Caballo Mountains. Bars = 0.1 mm.

Nuia is present in about 80% of the thin sections (Appendix B). *Nuia* averages about 5 to 10%, but commonly comprises 15 to 20% of a thin section and up to 66% of one thin section from Ash Canyon. Typically, *Nuia* is most abundant in the Hitt Canyon Member. *Nuia* is a common skeletal component in the Jose and McKelligon Members, but is scarce in the Padre Member. *Nuia* grains are equally common in grainstone (Fig. 32C) and packstone or wackestone (Fig. 32D). Toomey and Klement (1966) noted the incompatible relation between *Nuia* and the questionable blue-green alga *Renalcis* (Riding and Toomey, 1972; Pratt, 1984). Neither *Renalcis* nor a common *Renalcis* associate, *Epiphyton*, were observed in any thin sections from the El Paso.

Ostracods—Ostracods are a minor constituent in the El Paso Formation. They were observed only in the Padre Member (Fig. 33A, B), where they are present generally in trace amounts in about one-third of the thin sections (Appendix **B).** The ostracods occur mostly as disarticulated valves 0.4 to 0.6 mm long. One thin section from Klondike Hills contains 4% disarticulated valves. This large occurrence probably represents a local concentration of reworked valves.

Pulchrilamina spinosa—Another minor constituent in the El Paso Formation is *Pulchrilamina spinosa*. Toomey and Ham (1967) described and illustrated this newly recognized species where it occurs in the El Paso type section in the Franklin Mountains and in the correlative unit in the Arbuckle Group in southern Oklahoma.

Pulchrilamina is a massive colonial organism that produces structures that resemble stacked, wavy hemispheroidal stromatolites (Fig. 34). The laminae are convex upward and vary in thickness laterally; some pinch out, some bifurcate (Fig. 35). The upper surfaces bear randomly arranged, sharply pointed spines (Fig. 35). The laminae and spines are typically replaced by mosaics of sparry calcite (Fig. 35) so that no microstructures are preserved. On surface exposures, the laminae and spines are commonly replaced by silica and stand out in relief.

Pulchrilamina is believed to be a primitive coelenterate (Toomey and Ham, 1967; Toomey and Babcock, 1983; Webby, 1986). *Pulchrilamina spinosa* was observed only in the sponge*Calathium* mounds in the McKelligon Member in the El Paso type section. It was not seen in outcrops or in thin sections from *sponge-Calathium* mounds elsewhere within the region studied. D. Toomey (written commun. 1987) stated it is present in the Caballo Mountains.

Sponge spicules—Sponge spicules (Fig. 36A) are prominent biotic constituents throughout the El Paso Formation. They are present in about 75% of the thin sections. The sponge spicules came chiefly from siliceous lithistid sponges (Figs. 6A, 36B). There are many excellent photographs of these sponges and spicules in Toomey and Babcock (1983) and Toomey and Nitecki (1979). The sponges are replaced by sparry calcite, and so most spicules appear as solid circular, ellipsoidal, or acicular spar mosaics. Diameters vary from 0.01 to 0.04 mm and lengths are typically less than 1 mm. Some larger spicules or spines also are present, but they probably came from *Calathium* (Fig. 36B).

There appears to be no systematic variation in abundance regionally, except that possibly sponge spicules are slightly less abundant in the westernmost sections (Dos Cabezas and central Peloncillo Mountains). Rock sections were cut to avoid obvious, large sponge fragments, but some sections contain small sponge bioclasts. When point counted, the small sponge fragments were included with spicules. Consequently, although the contents of thin sections are rarely greater than 10% sponge spicules, some counts show up to 40% sponge spicules (Appendix B). Grainstone contains few or no spicules probably because the spicules are broken into pieces too small to recognize or were possibly winnowed out.

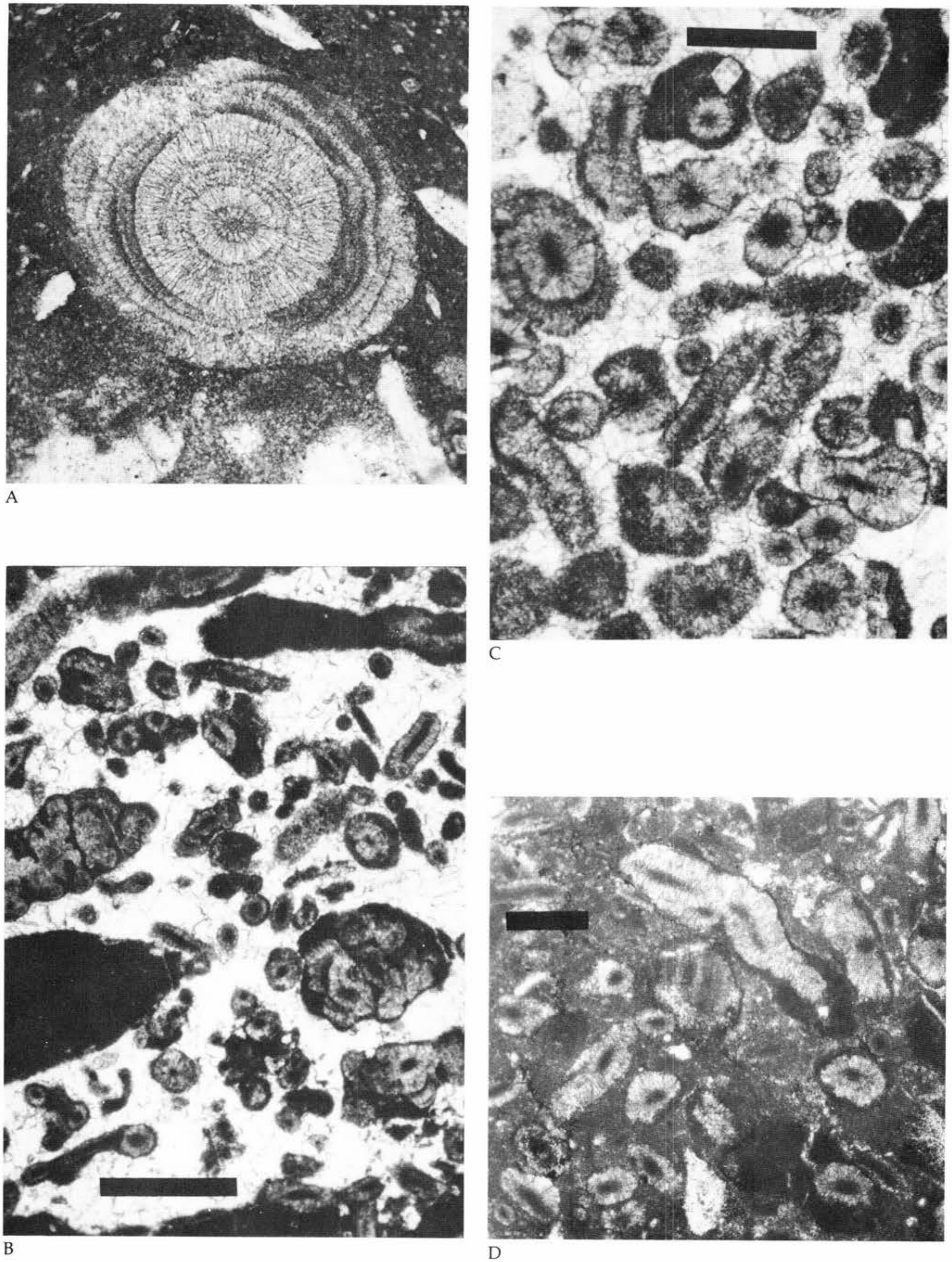

FIGURE 32—Thin sections of *Nuia*. (A) Transverse section of multilayered *Nuia* showing well-developed radial structure and dark central canal. From Capitol Dome section. Maximum diameter of the *Nuia* grain is 0.8 mm. (B) *Nuia* grainstone showing several atypical grains, as well as the more characteristic circular, elliptical, and elongate *Nuia* grains, and a large intraclast (lower left). From Hitt Canyon Member, Red Hills section. (C) *Nuia* grainstone. From Hitt Canyon Member, Cable Canyon section, southern Caballo Mountains. (D) *Nuia* packstone. From Hitt Canyon Member, Bear Mountain section. Bars = 1 mm.

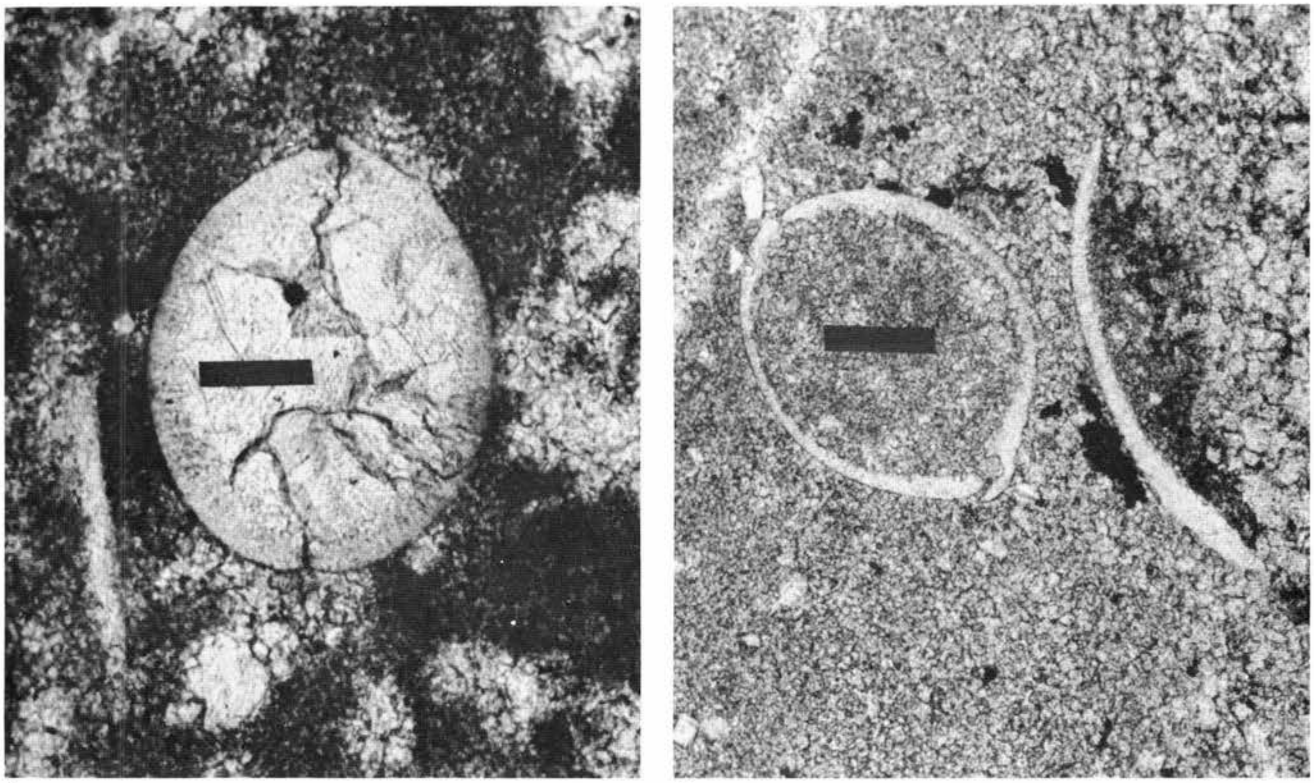

A B

FIGURE 33—Thin sections of ostracods. (A) Ostracod in peloidal matrix. From Padre Member, Victorio Canyon section, southeastern Florida Mountains. (B) Ostracod and disarticulated valve in neospar matrix. From Padre Member, Victorio Canyon section, southern Florida Mountains. Bars = 1 mm.

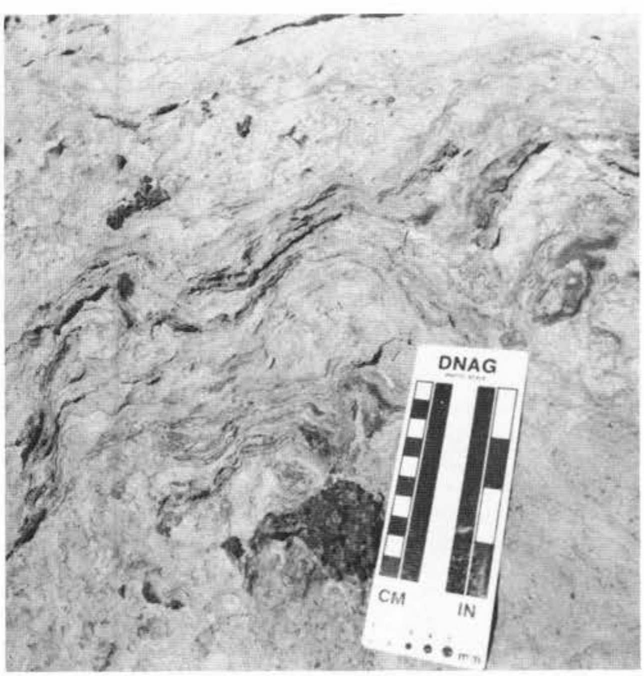

FIGURE 34—*Pulchrilamina* in sponge-*Calathium* mound. From McKelligon Member, Scenic Drive section, southern Franklin Mountains.

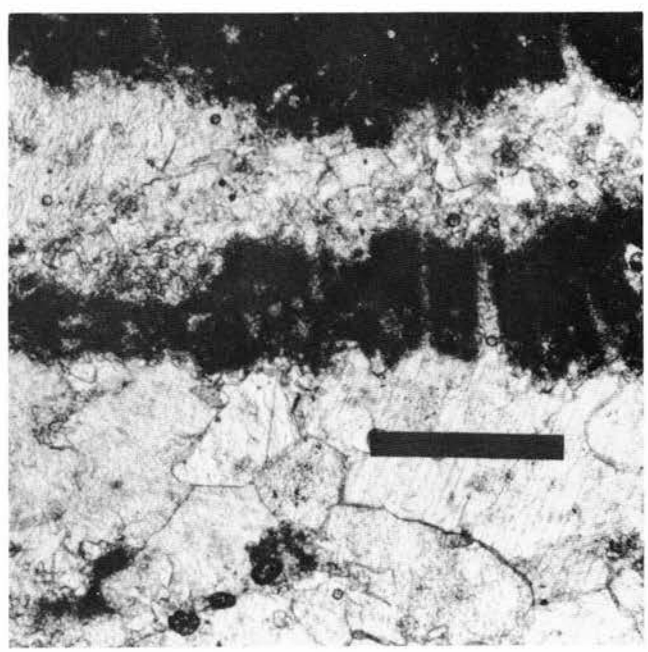

FIGURE 35—Thin section of *Pulchrilamina spinosa* double layers and upward-projecting spines replaced by spars. From sponge-*Calathium* mound, lower part of McKelligon Member, Scenic Drive section, southern Franklin Mountains. Bar = 1 mm.

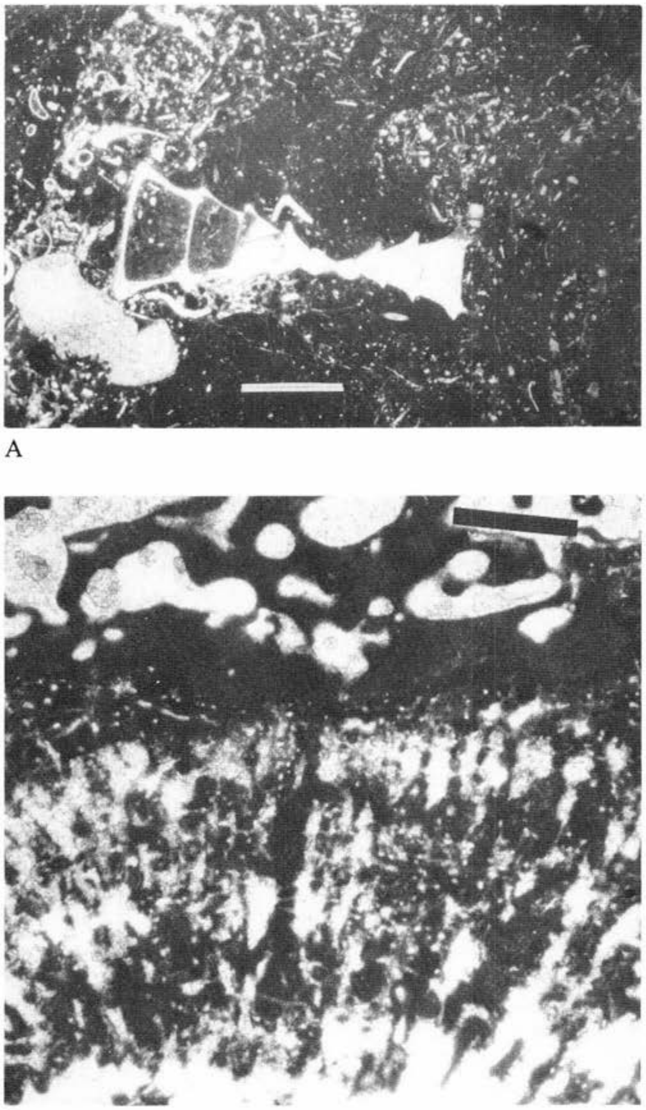

FIGURE 36—Thin sections of spicules. (A) Spicule wackestone with few fragments of gastropods, echinoderms, and trilobites. From upper part of Hitt Canyon Member, Quartzite Ridge section. (B) Fragments of *Calathium* (above) and sponge (below) showing relative sizes of spicules. From lower part of McKelligon Member, Scenic Drive section, southern Franklin Mountains. Bars = 1 mm.

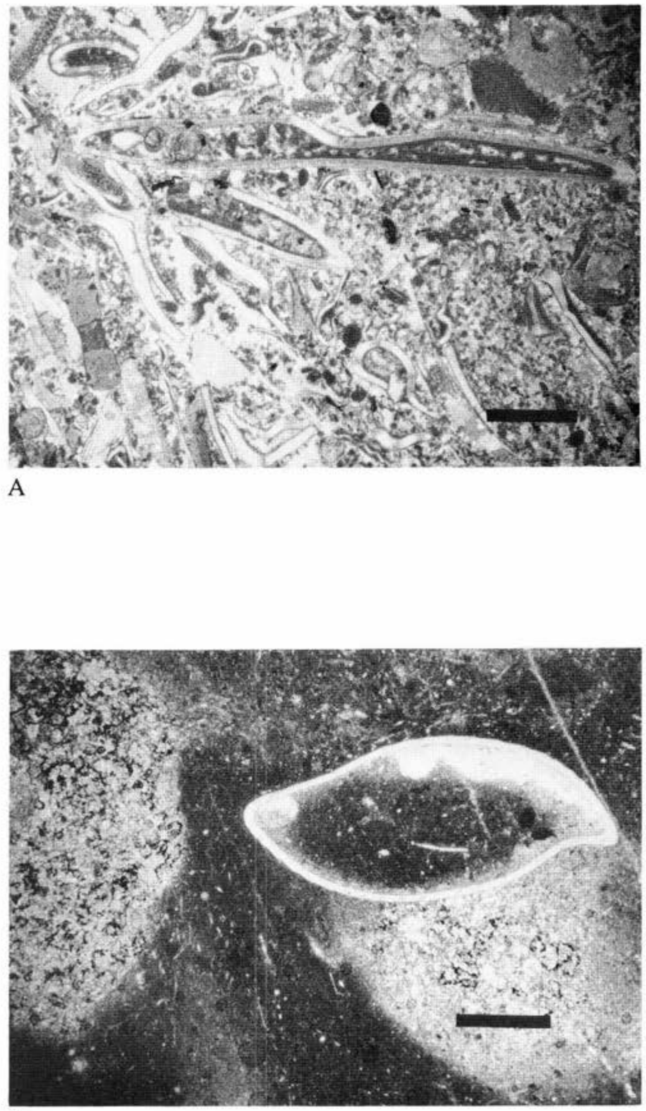

FIGURE 37—Thin sections of trilobite fragments. (A) Trilobite-echinoderm grainstone. From Hitt Canyon Member, San Lorenzo section. (B) Trilobite geopetal in bioturbated lime mudstone. From McKelligon Member, Ram Gorge section, Big Hatchet Mountains. Bars = 1 mm.

Trilobites—Trilobite fragments are ubiquitous in the El Paso Formation and typically average only about 2 to 3% of each thin section. A few thin sections contain 10 to 12% trilobite fragments and one from the San Lorenzo section contains 21% (Fig. 37A). No whole fossils were seen, but, locally, thin (5-10 cm) beds in the Jose Member contain pygidia concentrations. A sample of one of these beds is pictured in Clemons (in press: fig. 22D). Typically the trilobite fragments are unaltered (Fig. 37B), except in grainstone, where they are rounded and have micritized rims, presumably formed by *Girvanella* borings.

Intraclasts

Intraclasts occur throughout the El Paso Formation and are abundant in thin sections from all 38 locales sampled. Percentages vary greatly because lime mudstone contains virtually no intraclasts, whereas grainstone may contain up to 72% intraclasts. In general, the Jose Member contains the greatest concentration of intraclasts per unit volume and the Padre Member the least. At some locales, the McKelligon Member has more intraclastic grainstone (intrasparrudite) lenses; at others, the Hitt Canyon Member has more; and in some locales, the units contain equal amounts.

The intraclasts average 0.5 to 1.0 mm long, although many are as long as 2 cm and a few reach 12 to 15 cm in length. They are predominantly subelongated, but vary from equant to discoidal. Almost all have well-rounded corners. Apparently, the intraclasts were moderately rigid when deposited because only a few appear to be squashed between adjoining grains. Most of the intraclasts are lime mudstone, wackestone, and packstone (Fig. 21A). In many thin sections, the composition of the intraclasts is identical to that of the bed beneath the grainstone in which they occur. Many "intraclasts" in some thin sections appear to have the

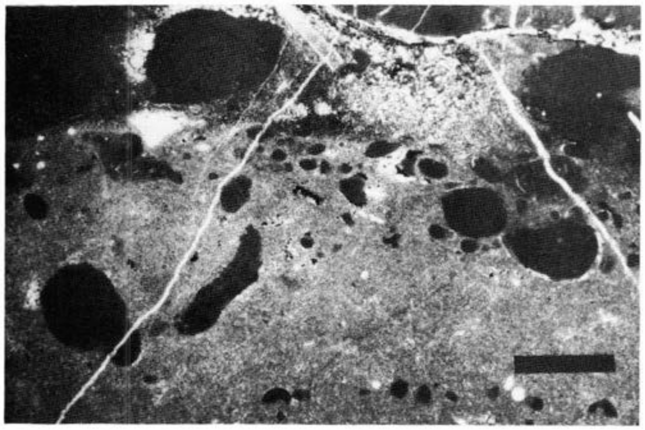

FIGURE 38—Thin section of probable gastropod steinkerns reflecting various chamber sizes. From lower part of McKelligon Member, northwest Cooke's Range section. Bar = 1 mm.

FIGURE 39—Oolite. From Jose Member, Hitt Canyon section, northern Franklin Mountains. Intraclast in bottom center is 2.5 cm long.

same shapes and sizes as gastropod chambers (Fig. 38) in subjacent beds. This similarity in shape indicates that the gastropod chambers were lithified to the extent that they survived the destruction of the bioclast without being deformed.

Ooids

Ooids are common in two horizons within the El Paso Formation: the Jose Member is characterized by its oolite beds (Fig. 39) and an oolite zone occurs about 35 to 40 m above the base of the Hitt Canyon Member near Kingston and Lake Valley. Several previous workers, including Aluka (1984), Hayes (1975a), and Stauffer (1962), reported oolites elsewhere in the El Paso, but they were not observed in this study.

Ooids in the Jose Member occur together with well-rounded quartz grains and well-rounded fragments of echinoderms and trilobites with micritized rims (Fig. 40A, B). The ooids are well sorted (Fig. 39), average about 0.5 mm in diameter, but range from 0.2 to 1.2 mm wide. Most ooids are spherical; some are slightly elongate (Fig. 40C). They typically show an original concentric structure where preserved. More commonly, the ooids have an oomoldic dolomitic composition and thin micritized rims (Fig. 40C). Some neomorphosed ooids occur with well-rounded, micritized echinoderm fragments (Fig. 40D) and partly dolomitized intraclasts (Fig. 40E). Some concentric ooids appear to be partly changed to oomoldic ooids (Fig. 41A, B).

Ooids in the Hitt Canyon Member near Kingston and Lake Valley possess a radial structure (Fig. 42A) or radial and concentric structures (Fig. 42B). Some oolite beds in the Jose Member northeast of Cox Mountain contain concentric ooids, although at least one bed in the Jose has radial ooids. As seen in thin sections from the Jose and the Hitt Canyon, many ooid nuclei are echinoderm, trilobite, gastropod, and *Nuia* fragments. Quartz silt or sand grains are scarcely seen as nuclei.

If the concentric and oomoldic structures represent original aragonite and the radial structure represents original radial fibrous calcite and high-magnesium calcite (Shoji and Folk, 1964; Sandberg, 1975, 1983), conditions must have been present during early Canadian time for both to occur. Some radial ooid cortices appear continuous with *Nuia* nuclei (Fig. 42A), but other radial cortices are built over other bioclasts. The oscillating trend, described by Sandberg (1983) for Phanerozoic non-skeletal carbonate mineralogy, may be suspect because Sandberg's Ordovician ooid (University of Texas, TC 630) is from Oklahoma (probably from the Arbuckle Group, which is correlative with the El Paso). Sandberg's Early Cambrian oomoldic ooid (University of Indiana, A215) is from the Mural Limestone in British Columbia. Through the courtesy of P. E. Horowitz, the University of Indiana thin section of Mural Limestone, illustrated in Horowitz and Potter (1971: pp. 286-287), was examined and several *Nuia*, but no ooids or "oolith ghosts," were recognized.

Pellets and peloids

Pellets are structureless, rounded micritic allochems smaller than 0.15 to 0.20 mm (Folk, 1959a) that probably represent fecal material. They are rare, if present at all, in the thin sections of this study. Peloids are any small micritic allochems, irrespective of size or origin. Most peloids counted in the thin sections of the El Paso Formation (Appendix B) are probably small (<0.2 mm) intraclasts and micritized *Nuia* (Fig. 43A, B).

Variations in peloid content occur in each section and throughout the region, but little significance is attached to these variations. The variations most likely depend on whether grainstone or packstone was sampled. Few allochems called peloids were seen in lime mudstone matrix. Locally, the lower part of the Hitt Canyon Member contains beds filled with small, intensely micritized *Nuia*.

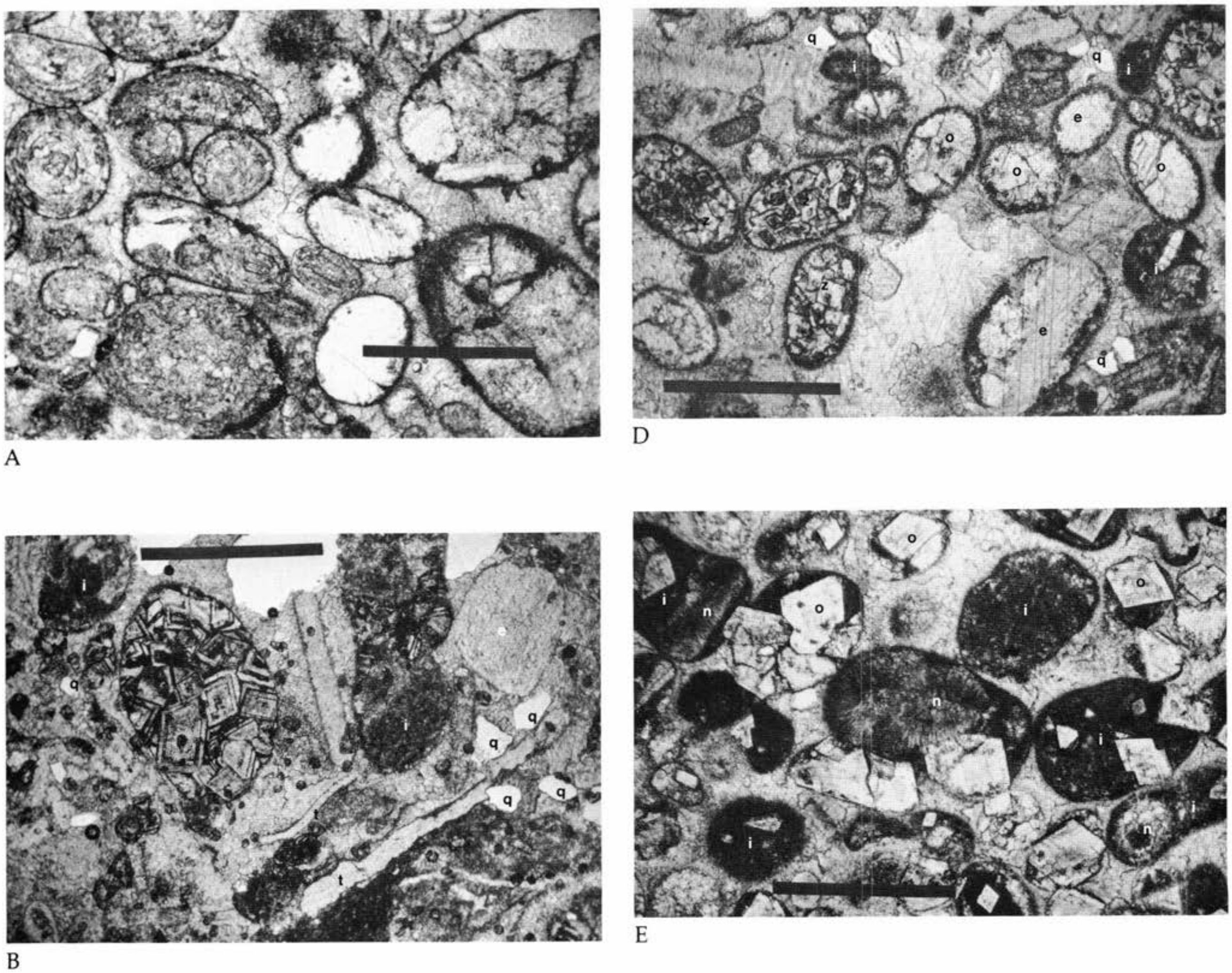

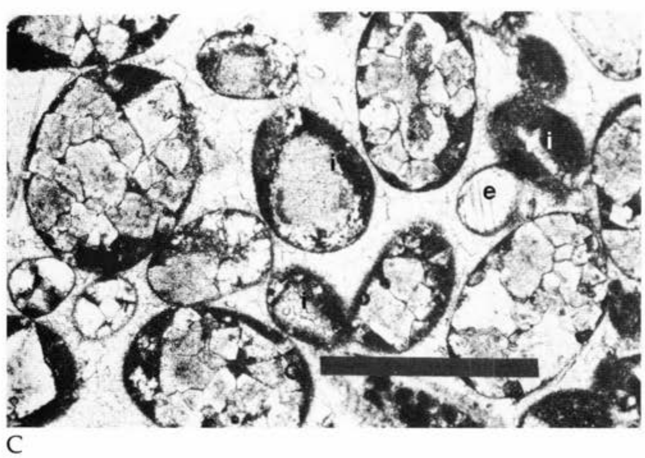

FIGURE 40—Thin sections of ooids. (A) Ooids with concentric structure and micritized rims (left), rounded echinoderm fragments with micritized rims (center), and ooids replaced by dolomite and showing little structure except micritized rims (right). In spar matrix. From Jose Member, Red Hills section. (B) Dolomitized ooid (left center), intraclasts (i), echinoderm (e), trilobite (t), and quartz (q) grains. From Jose Member, Snake Hills section. (C) Ooid grainstone containing oomoldic dolomite, rounded echinoderm fragments (e) with micritized rims, and intraclasts (i). From Jose Member, northwest Cooke's Range section. (D) Grainstone with zoned oomoldic dolomite (z), unzoned oomoldic dolomite (o), echinoderm fragments (e), intraclasts (i), and quartz (q) grains. From Jose Member, northwest Cooke's Range section. (E) Grainstone with oomoldic dolomite (o) and intraclasts (i) partly replaced by dolomite. Several intraclasts contain *Nuia* (n) fragments. From Jose Member, Cable Canyon section, southern Caballo Mountains. Bars = 1 mm.

Orthochemical constituents

Micrite

Micrite is microcrystalline ooze that occurs as fine particles less than 5 μ in diameter (Folk, 1959a). Most material considered as originally micrite in this study appears in thin sections as neomorphosed microspar. Regionally, the El Paso Formation contains mostly wackestone and pack-stone beds of a predominantly micrite matrix. The tables in Appendix **B** do not indicate true proportions of micrite and spar in the El Paso; one thin section may represent 5 m of apparently similar packstone, whereas another may represent only 0.1 m of grainstone with spar cement.

The origin of the micrite sediment in the El Paso For-

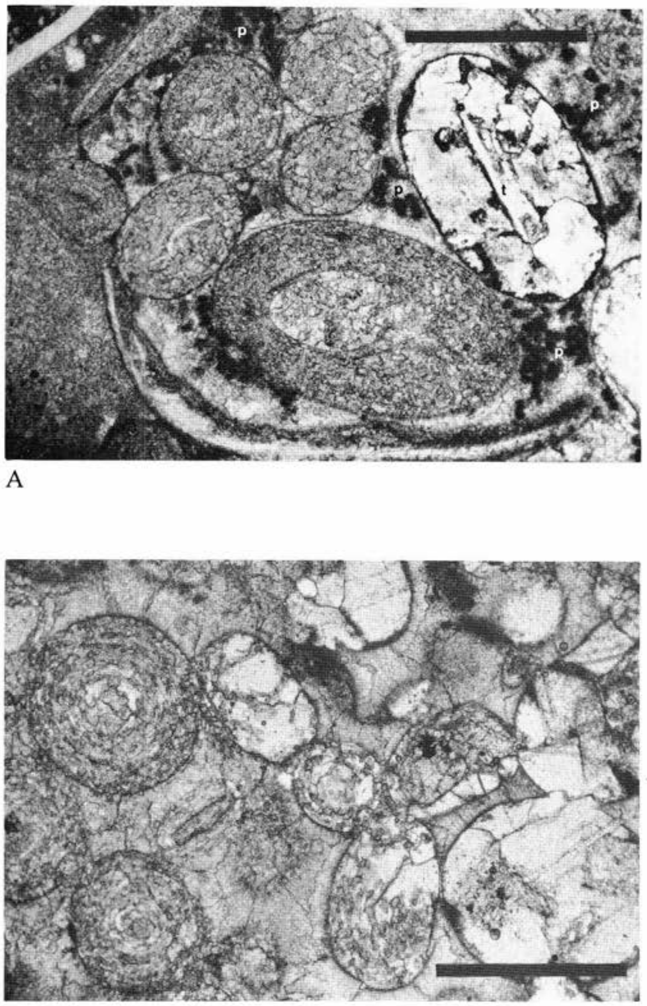

A

B

FIGURE 41—Thin sections of concentric ooids. (A) An ooid replaced by dolomite except for nucleus of trilobite (t) fragment, and peloidal (p) patches. From Jose Member, Ram Gorge section, Big Hatchet Mountains. (B) "Caught in the act." Concentric ooids (left), partly dolomitized ooids (lower center) and oomoldic dolomite (right). From Jose Member, Red Hills section. Bars = 1 mm.

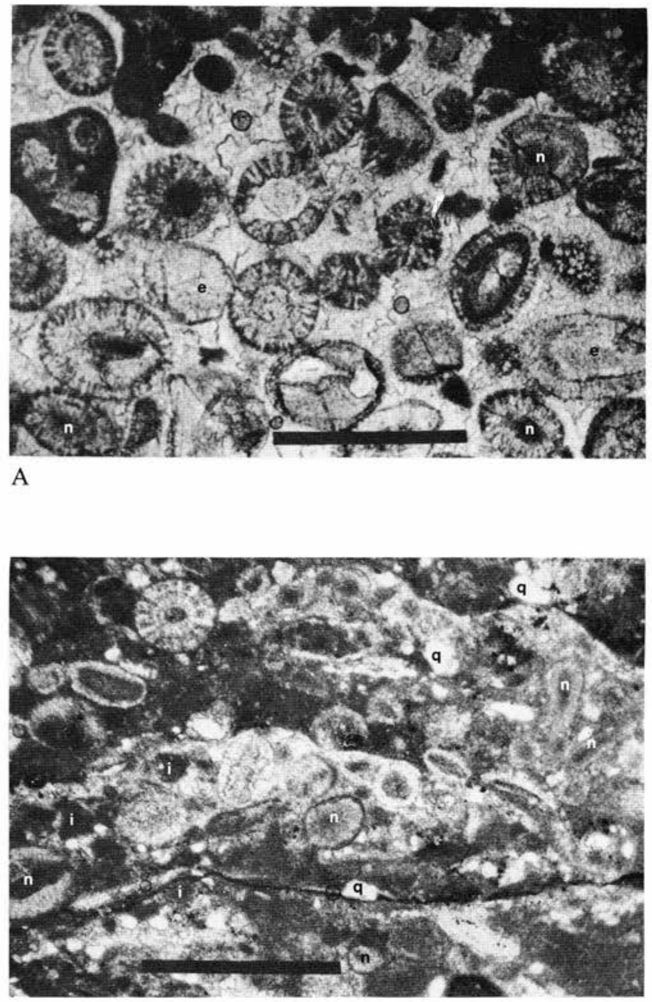

A

B

FIGURE 42—Thin sections of radial ooids. (A) Radial ooids, grapestone (upper left), intraclasts, and rounded echinoderm fragments (e). Several of the ooids have *Nuia* nuclei (n). From upper part of Hitt Canyon Member, Quartzite Ridge section. (B) Radial ooids (upper left), *Nuia* (n), quartz grains (q), and intraclasts (i). From Hitt Canyon Member, Kingston section. Bars = 1 mm.

mation is uncertain. Klement and Toomey (1967) suggested the micrite was produced by *Girvanella* boring and corrosion. However, bioclasts in wackestone and packstone have less micritized rims and are more angular than those in grainstone. Most micritic rock in the El Paso has been extensively bioturbated. The micrite was probably produced by some combination of algal boring and trituration of bioclasts during bioturbation, as suggested by Ginsburg (1964), Wolf (1965), Bathurst (1966), Klement and Toomey (1967), and others. Micrite in the cryptalgal mounds, then, represents settling from suspension of triturated material onto algal surfaces.

Spar

Sparry calcite is the clear component of a limestone that forms crystals more than 10 µ in size (Folk, 1959a). This type of calcite forms as cement in empty spaces within an allochem framework. Sparry calcite occurs in the El Paso Formation as grainstone cement (Figs. 32C, 42A), as cavity fillings (stromatactis) in the cryptalgal mounds (Fig. 12), and as casts of gastropod shells, *Pulchrilamina* (Fig. 35), sponges, and *Calathium*. Cement types in grainstone include syntaxial cement on echinoderm fragments and isopachous, crust, and scarce meniscus cements, as well as cavity-fill mosaics.

Dolomite

Dolomite content in the El Paso Formation ranges from very minor at some locales to 100% at others. Crystals range from 10 µ or less up to 1 mm in size. The average crystal size in dolostone is about 0.1 to 0.25 mm. Euhedral rhombs that replaced micritic material range from 0.01 to 0.5 mm and average about 0.2 mm. Rock that consists wholly of dolomite has anhedral crystals. Where dolomite occurs in burrows, intraclasts, stylolite seams, or chert, crystals tend to be euhedral.

The euhedral dolomite crystals occur as three general classes: (1) slightly dusty-brown to "dirty-gray" rhombs, (2) small, dark reddish-brown rhombs, and (3) zoned rhombs (Figs. 40B, 44). Zoning may be shown by (a) dark core and light outer zone, (b) light core and dark rim, or *(c)* a series of parallel rhomb-shaped zones of various thicknesses. Folk

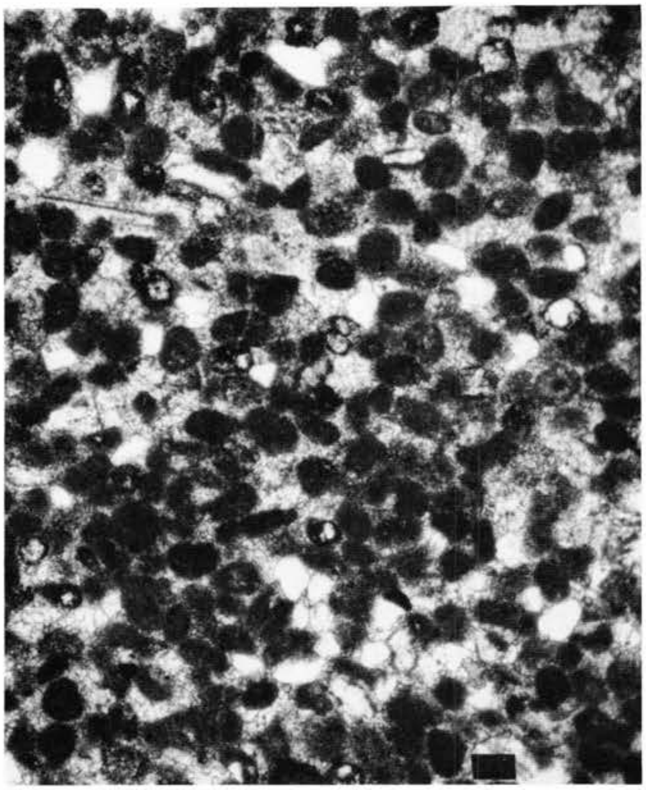

A

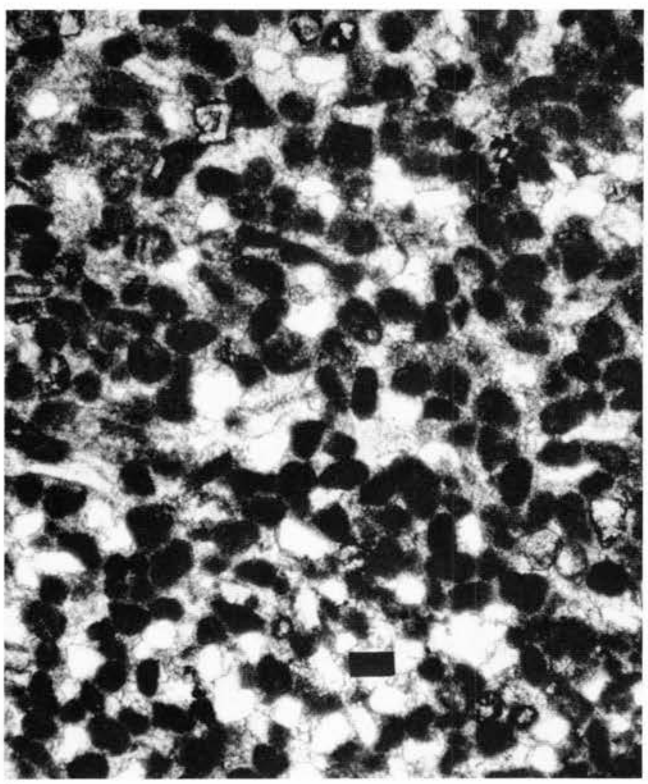

B

FIGURE 43—Thin sections of sandy (white grains) *Nuia* grainstone. (A) From Hitt Canyon Member, Ram Gorge section, Big Hatchet Mountains. The micritized *Nuia* grains are easily misidentified as peloids if a few *Nuia* are not still visible as in center right view. (B) From lower part of Hitt Canyon Member, Cable Canyon section, southern Caballo Mountains. Bars = 0.1 mm.

FIGURE 44—Thin section of zoned euhedral dolomite rhombs replacing micritic burrow filling. From upper part of McKelligon Member, Snake Hills section. Bar = 0.1 mm.

(1959b) attributed the dusty-brown appearance of dolomite in rocks of the Ellenburger Group to organic material and fluid inclusions. Katz (1971) studied zoned dolomite crystals of Jurassic age of similar appearance; he considered them to be early diagenetic. Calcian dolomite zones were formed by dilution of interstitial dolomitizing brines. On occasions this dilution was sufficient to cause dedolomitization and replacement of calcian dolomite by calcite. Periodically, shallow, stagnant reducing conditions led to the formation of ferroan dolomite zones. At periods of dilution during storms, oxygenated interstitial solutions oxidized the ferroan dolomite zones to hematite zones.

Quartz

Orthochemical quartz is present as microcrystalline chalcedony and chert and rarely as authigenic crystals replacing micrite in intraclasts (Fig. 45). Chert nodules and lenses are scarce in the El Paso Formation; they seem to be more common in the Padre Member in the Florida Mountains than elsewhere. Locally, small (1-3 cm) chert nodules appear to replace sponge and *Calathium* fragments. Ropy chert networks, resembling large (2-3 cm) burrows (Fig. 17B), occur commonly in the upper part of the Hitt Canyon Member and in the McKelligon Member as repeated zones 10 to 30 cm apart. The crypto- to microcrystalline chert contains bioclast ghosts and scattered, floating euhedral dolomite rhombs.

Cephalopod siphuncles are preserved in outcrops because of their silicified character. *Calathium* and *Pulchrilamina* typically are silicified on weathered rock surfaces, but in fresh samples neither organism is replaced by silica. Fragments of silicified gastropods, brachiopods, and echinoderms were rarely observed in outcrops. In thin sections, brachiopod and echinoderm clasts are seen to be partly replaced by chalcedony and chert. Two specimens of silicified *Archaeoscyphia* (K. Rigby, written commun. 1986) were collected from the Capitol Dome section. The source of the silica that forms the chalcedony and chert is believed to be the siliceous sponges.

Other minerals

Minor trace occurrences of glauconite were seen in several thin sections of basal beds in the Hitt Canyon Member from several locales. The bright green glauconite pellets and interstitial (squashed?) fillings average about 0.15 mm in di-

FIGURE 45—Thin section of authigenic euhedral quartz in large ooid. From Jose Member, Quartzite Ridge section. Bar = 0.1 mm.

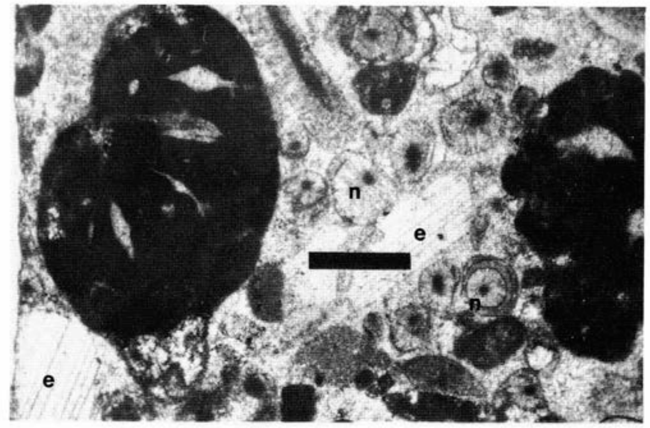

FIGURE 46—Thin section of green clay(?) or glauconite(?) grains associated with *Nuia* (n) and echinoderm (e) fragments. From Jose Member, Cox Mountain section. Bar = 1 mm.

ameter. Conspicuous glauconite peloids from the Jose Member northeast of Cox Mountain (Fig. 46) range up to 4 mm across. They appear to have desiccation cracks filled with spar and a few resemble grapestones.

Gypsum occurs in the silty upper part of the Hitt Canyon Member in the Victorio Mountains. Mostly present in trace amounts, gypsum makes up 2% of one thin section. The gypsum occurs mostly as tiny fibers less than 0.1 mm long, but in a couple of thin sections more tabular crystals attain subequal dimensions of 0.3 mm. No gypsum was observed at any other sections in the study area.

Dolomitization

The original El Paso Formation carbonate rocks were predominantly, if not completely, limestone. Folk (1959b) estimated that the original composition of the laterally equivalent Ellenburger Group was 60% micrite—allochem rock (packstone) and 30% micritic rock (wackestone and lime mudstone). Folk (1959b) also included about 3% biolithite (cryptalgal mounds) in his estimate. Sampling methods used in this study do not allow accurate estimates of rock types as proportions of the total volume of the El Paso. However, from the rock types shown in 310 thin sections of the El Paso sampled from two sections in the Florida Mountains, the original carbonate rocks were about 34% grainstone, 33% packstone, and 33% wackestone and lime mudstone. Although mounds are not abundant in the Florida Mountains, algal-mound rock is included as lime mud-stone.

Dolomitization has altered the primary sediments in various ways at different locales throughout the study area. Pervasive dolomitization has completely replaced El Paso Formation beds, including many *sponge-Calathium* mounds, in the Pedregosa Mountains, in the San Andres and Oscura Mountains north of Rhodes Canyon, in the Sacramento Mountains, and at Bishop Cap (Fig. 47). The El Paso is dominantly dolostone at Beach Mountain near Van Horn, Texas, in the southern San Andres Mountains, and at Bear Mountain and Lone Mountain near Silver City. At other locales the El Paso is dominantly limestone, but at some locales the El Paso may contain 10 to 100 m of dolostone. A few single beds of dolostone (0.1-10 m thick) are locally interbedded with limestone in the McKelligon and Padre Members in the Florida Mountains. The El Paso on the north slope of Cable Canyon is 98% limestone, whereas the El Paso within and on the south slope of Cable Canyon is predominantly dolostone. Nearly all burrow fillings in the El Paso are dolomitized. Dolomite crystals are also common in stylolite seams and micritic intraclasts.

Origins

No single theory will satisfactorily explain all the variations in dolomite distribution. Several earlier workers have proposed that some of the dolomite in the El Paso Formation is probably primary because it formed in supratidal environments (Hayes, 1975a; LeMone, 1976b; Lucia, 1968). Harris (1973) proposed a model for dolomitization of Lower Ordovician sediments in the eastern United States. His epicontinental-sea model showed that a shoreward-increasing salinity gradient, occurring in shallow restricted seas where evaporation is great, is responsible for the refluxing of magnesium-rich brine, which dolomitizes widespread subtidal carbonate sediments. The model demonstrated that clastic sediments along the shoreline interfinger seaward, in a few hundred miles, with dolostone, which, in another few **hun-**

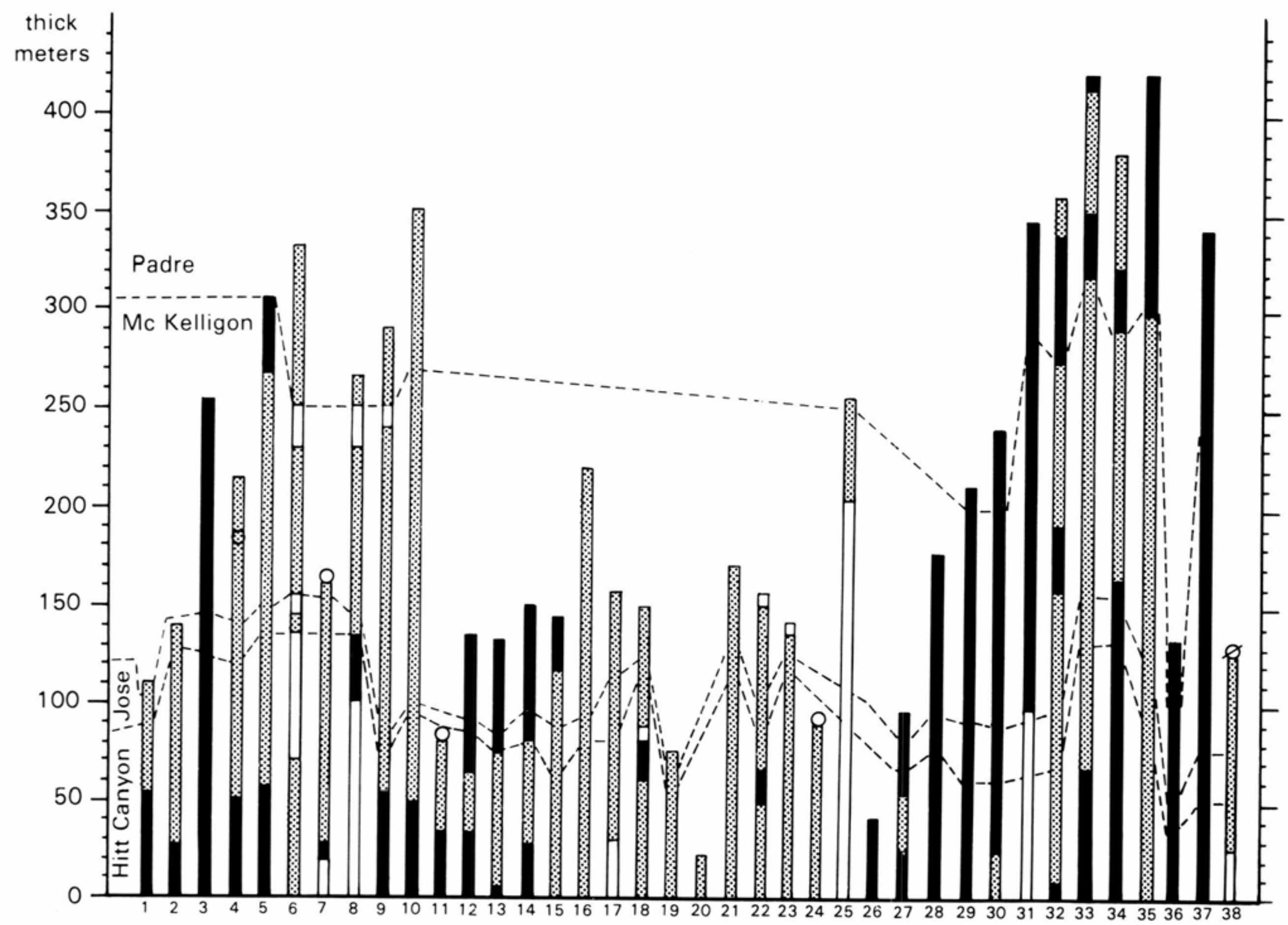

FIGURE 47—Chart showing distribution of limestone (dark shading) and dolostone (light shading) in members of the El Paso Formation at the 38 sections sampled (for locations see Fig. 1, Table 1). Parts of sections eliminated or not exposed due to faulting are not shaded. The El Paso is underlain by the Bliss Sandstone and overlain by the Montoya Formation at most of the locales. The exceptions are locale nos. 4, 7, 11, and 24, where alluvium (○) overlies the El Paso and locale 38 where Cretaceous sandstone (Ø) overlies the El Paso.

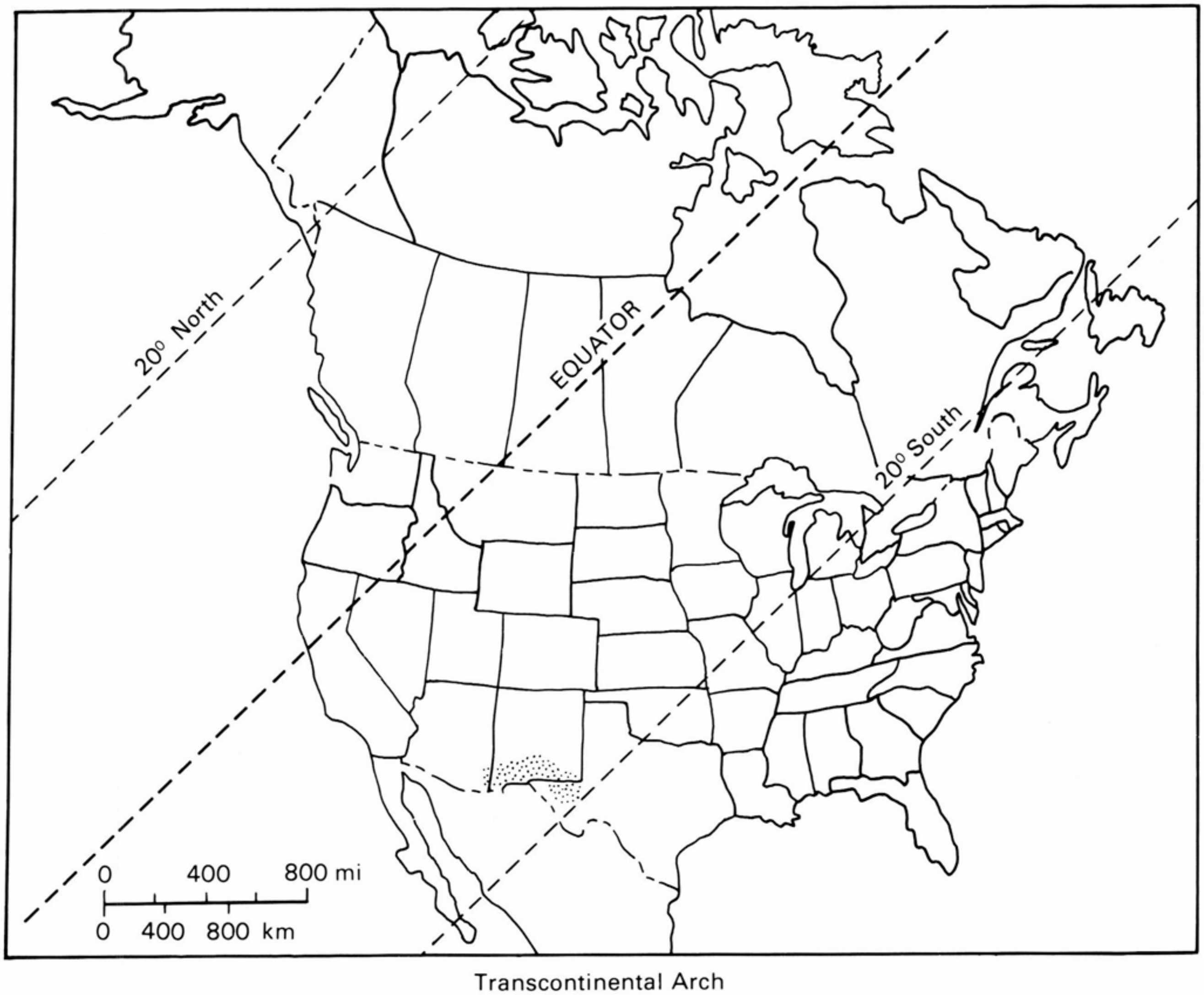

FIGURE 48—Map of North America showing area of study (dotted pattern) and interpreted position of Equator during Early Ordovician time (after Ross, 1976).

dred miles, grades into a limestone facies that forms a band tens of miles wide parallel to the shelf edge. Local influx of fresh water from land prevents the dolomitization of near-shore carbonate sediments. The free-mixing of waters with the sea lowers the salinity caused by evaporation and prevents the dolomitization of offshore carbonate sediments.

Ross (1976) utilized Harris's (1973) model to explain that Lower Ordovician sedimentation in the West was in shallow restricted seas in the horse latitudes (Fig. 48). Ross proposed that the Transcontinental Arch presented a barrier in Early Ordovician time between west Texas—southern New Mexico (about 15° S. latitude) and the well-circulated equatorial waters to the north-northwest. He proposed that this barrier accounted for the predominant dolostone lithology of the Ellenburger Group. He explained the normal-marine limestone lithology of the correlative Arbuckle Group in terms of the southern Oklahoma aulacogen providing circulation through the Transcontinental Arch (Ross, 1976: fig. 5). He did not attempt to explain the predominant occurrence of limestone in the El Paso Formation at the type section in the Franklin Mountains and in southern New Mexico. Lee and Friedman (1987) attributed the Ellenburger dolomitization to deep burial fluids.

Observations during this study show that much of the dolostone in the Caballo, Florida, Animas, and Peloncillo Mountains, the Klondike Hills, and the Kingston, Winston, and Silver City areas is of hydrothermal origin. El Paso Formation sections examined in these areas contain much silicification along fractures and, locally, completely silicified breccia. There are known mineral deposits closely associated with the dolostone, and commonly a dolostone bed or group of beds can be traced laterally into limestone. Excellent examples of the type change in lithology are present northwest of Capitol Dome, over the low ridge northeast of Victorio Canyon in the southeastern Florida Mountains, and at Cable Canyon in the southern Caballo Mountains.

Primary dolostone possibly may form beds in parts of the Jose and Padre Members in the Franklin Mountains and in the lower part of the Padre at Bishop Cap and in the southern San Andres and Sacramento Mountains. Hayes (1975a) described dolostone near Morenci, Arizona, and northwest to Nantac Rim (probably upper Hitt Canyon or Jose Member equivalents) that has features characteristic of primary dolostone. The Jose and Padre beds at the above locales in southern New Mexico and west Texas contain small- to medium-scale planar crossbeds (Fig. 22A, B) in silty to sandy dolostone. Also present are thinly laminated (algal-mat?) dolostone (Fig. 15) and interbedded intraclastic grainstone (intrasparrudite; intraformational chip or edgewise conglomerate). Some of the thinly laminated dolostone displays bird's-eye structure (fenestrae). Hayes (1975a) also reported mudcracks, tracks, and trails at Nantac Rim in east-central Arizona. These strata in the Jose and Padre are not generally burrowed and contain little evidence of fossil ghosts.

Late diagenetic processes probably account for much of the El Paso Formation dolostone. Where overlain by the Montoya or Martin Formations, the uppermost beds of the El Paso (regardless of which member) are dolomitized, except in the Florida, Peloncillo, and Dos Cabezas Mountains. Dolomitization of these uppermost beds indicates that the post-diagenetic processes were probably associated with the return of the seas that deposited the Montoya and Martin sediments. Land (1973) documented dolomitization after lithification. He inferred that the dolomitizing solution was mainly subsurface meteoric water mixed with about 10 to 25% marine water.

The lowermost beds in the El Paso Formation are also dolostone in most sections studied (Fig. 47). These bioclastic, sandy beds are gradationally underlain by Bliss Sandstone, thus representing an Early Ordovician transgressing sea. Dolomitization may have occurred by seawater—freshwater mixing (Badiozamani, 1973) along the shoreline soon after deposition. Dolostone interbeds in predominantly limestone sections may record temporary, local conditions of the water-mixing process. Garven (1985) and Garven and Freeze (1984) indicated that it is possible for deep, basinal brines to migrate updip for long distances toward basement highs. Their model may explain the predominantly dolostone sections at Bishop Cap and in the Sacramento and San Andres Mountains, as well as the dolomitized Hitt Canyon Member in the Franklin, Victorio, and Florida Mountains. All these areas were near or adjacent to basement highs during Early to Middle Ordovician time. The dolostone beds are generally pale yellowish brown to grayish orange, reflecting oxidized iron-bearing dolomite.

Dolomite crystals in burrow fillings are probably early to late diagenetic. They may have formed preferentially in the burrows, where there were high porosity and permeability. Morrow (1978) reported that micron-sized dolomite crystals may have formed in burrows during deposition. They may have acted as nuclei for selective precipitation of dolomite in late-diagenetic dilute solutions. Morrow (1978) also suggested that magnesium may have been retained preferentially by noncalcareous organic material in the burrows. Release of this magnesium during late diagenesis may have aided dolomitization of the burrow fillings. Kendall (1977) believed that Ordovician sediments may have been rich in magnesian calcite. Magnesium released during stabilization of calcite caused dolomitization of the more porous, permeable burrow fillings. Dedolomite(?) rhombs in many El Paso Formation burrow fillings indicate the presence of porous, permeable fillings into the late diagenetic stage. Zoned dolomite crystals in micritic intraclasts are believed to have formed after deposition of the grainstone sediment and before complete cementation.

Hardie (1987) pointed out deficiencies in present-day dolomitization models and recommended caution in attempting to explain the origin of massive dolostone sections. Data from detailed geochemical and cathode-luminoscope studies of El Paso Formation dolomites are needed before a more conclusive interpretation of their origins can be made.

Depositional environments

The El Paso Formation is a Lower Ordovician (Canadian) sequence of beds, laterally continuous with the Ellenburger Group, that was deposited on a wide epicontinental platform. Epeiric seas extended from southeastern Arizona, across southern New Mexico and west Texas, at least to central Texas (Cloud and Barnes, 1948). The platform probably was a homoclinal ramp (Read, 1985) that sloped gently (about 1 m/km) southward from the Transcontinental Arch that extended northeastward from central New Mexico (Ross, 1976). Apparently there was a local deepening (embayment or trough) near Marathon, Texas (Young, 1970). Otherwise, depositional lithofacies appear similar from Willcox, Arizona, to central Texas.

Two reported differences in lithology between the Ellenburger Group (Cloud and Barnes, 1948; Barnes et al., 1959) and the El Paso Formation (Clemons, 1987; this report) are the fauna and pellet-rich rock in the Ellenburger. The Ellenburger apparently had a more restricted fauna and softer sea floor than the El Paso. Caution is needed, however, in using pellet-rich sediment as a criterion for a soft-sea floor environment because *Nuia* was not recognized in the Ellenburger or the El Paso until 1965-66 (Toomey, 1965; Toomey and Klement, 1966). Previously, and to less extent until 1977 (Umphress, 1977), small (0.02-0.3 mm) *Nuia* was locally interpreted as ooids, peloids, or pellets (Fig. 43).

The southern extent of the Lower Ordovician platform is unknown. Thick upper Paleozoic and Mesozoic sections overlying the Ordovician rocks in northern Chihuahua make studies of the Ordovician difficult. Relations among Upper Cambrian—Lower Ordovician platform carbonate rocks reported 320 km south of El Paso (Bridges, 1964), 300 km south of Willcox (Stewart et al., 1984), and in northwestern Sonora (Lopez-Ramos, 1969) also are unknown.

There were several islands or southerly projecting peninsulas on the El Paso—Ellenburger ramp. Kottlowski et al. (1969, 1973) described land areas in the southern Franklin Mountains and Florida Mountains. They reported that Thunderbird rhyolite, a Precambrian landmass in the Franklin Mountains that was surrounded by Ordovician seas, was not covered until at least 230 m of El Paso Formation had been deposited. Apparently only a few meters of El Paso sediments, above approximately 50 m of Bliss Sandstone, were required to cover the Florida land area. A few potassium-feldspar grains are scattered throughout the lower 40 m of the Hitt Canyon Member of the El Paso Formation. Although potassium-rich volcanic rock fragments are common in El Paso sands in the Franklin Mountains, Stageman (1987) noted that El Paso sands at Beach Mountain do not contain any volcanic rock fragments. King (1965) described three sandy zones at Beach Mountain that contain well-rounded quartz and feldspar grains. The lowest sandy zone is in his "Division A" (lower part of the Hitt Canyon Member), the next higher sandy zone is at the top of "Division A" (Jose Member), and the highest sandy zone is near the top of "Division B" (probably equivalent to lower part of the Padre Member). The sand at Beach Mountain probably came from the north or northeast because the El Paso Formation in the Hueco Mountains is much less sandy than the sections in the Franklin Mountains and at Beach Mountain. Much of the sand in the Ellenburger Group in central Texas is eolian; its source probably lay to the east or southeast (Cloud and Barnes, 1948). The presence of peninsulas, islands, and shoaling areas complicated the facies distributions.

The El Paso Formation ramp subsided slowly and intermittently for about 15 to 25 m.y. as a minimum of 420 m of shallow-subtidal to supratidal carbonate sediments were deposited. Stylolitization and erosion(?) during several major regressions removed an unknown thickness of El Paso beds. The average rate of deposition of preserved rock was about 20-30 mm/1,000 yrs. Langenheim et al. (1962) reported a sedimentation rate of 24.3 mm/1,000 years for the Lower Ordovician in Nevada. Cloud and Barnes (1948), Lucia (1968, 1971), Hayes (1975a), Toomey and Nitecki (1979), LeMone (1976a, b), Loucks and Anderson (1985), and Kerans and Lucia (1989) have described transgressions, regressions, and the cyclic nature of the Early Ordovician seas during deposition of the El Paso.

Taking into consideration the detailed petrography of the members of the El Paso Formation and their mutual relations regionally, as well as the information acquired from the sedimentary structures, it is possible to infer their depositional environments more precisely than previously reported. Table 2 contains criteria (environmental indicators) useful in interpreting depositional environments (Shinn, 1983). The distribution and relative abundance of these environmental indicators throughout the El Paso are shown in Table 3. The following discussion pertains primarily to regional variations of the environmental indicators in each member.

The lower part of the Hitt Canyon Member does not vary much throughout the study area. One notable exception is the limited occurrence of ooids in the Kingston and Lake Valley areas; their presence probably indicates local shoaling episodes, possibly close to another island. Oncolites are ubiquitous in the Hitt Canyon, but are sparse in a few of the sections studied. They appear most abundant where other features indicate periods of nondeposition and possible development of hardgrounds (Brett and Brookfield, 1984), notably at Capitol Dome. The only occurrence of evaporite minerals is in the upper part of the Hitt Canyon in the Victorio Mountains; notably this section was one of only a few that contained no stromatolite mounds. Mud-cracks, fenestrae, cryptalgal laminites, and microcrystalline dolomite were not observed in the Hitt Canyon in the study area, but were reported by Hayes (1975a) in the upper part of the Hitt Canyon in eastern Arizona.

Small *sponge-Calathium* mounds occur only in a few sections of the Hitt Canyon or Jose Members, e.g. Ram Gorge. Stacked-hemispheroidal-stromatolite mounds are present in the upper part of the Hitt Canyon, the Jose, or the lower part of the McKelligon at most locales and are most abundant in the Cable Canyon, Red Hills, northwest Cooke's Range, and Klondike Hills sections. Small- to medium-scale crossbeds are present in the Jose only in the Franklin, Sacramento, and San Andres Mountains, probably adjacent to the peninsula or north-elongated island located between or east of these ranges. To the west, the Jose is relatively sand free. Cryptalgal laminites and microcrystalline dolomite in the Jose are also confined to the Franklin and San Andres Mountains.

The lower part of the McKelligon Member is typically distinguished by *sponge-Calathium* mounds, but they are sparse to absent locally (Fig. 7). They are notably sparse or missing at Beach Mountain, the Hueco, Peloncillo, and Florida Mountains, Snake Hills, Cooke's Range, and north of Ash Canyon in the San Andres Mountains. This variable distribution is difficult to explain unless rather specific water depth and bottom conditions are required for mound development. Whatever these conditions were, they were repeated many times in the southern Franklin Mountains and Caballo Mountains and apparently less frequently at the other locales studied. Dark/light color banding on 3-5-m scale in sections of the McKelligon at Ash and Hembrillo Canyons probably reflect some of the cyclicity represented in mound development to the south. The dark zones rep-

TABLE 2—Criteria used for interpretation of depositional environments. A, abundant; C, common; R, rare; H, high; M, medium or moderate; L, low; V, variable; ms, medium scale; ss, small scale; T, thick; t, thin; —, not observed.

Features	Supratidal	Intertidal	Shallow Subtidal	Deep Subtidal
Mudcracks	A	R	—	—
Fenestrae	A	R	—	—
Cryptalgal laminites	A	R	—	—
Evaporites	C	R	—	—
Microcrystalline dolomite	A	—	—	—
Oncolites	—	R	A	—
Cryptalgal mounds	—	A	C	—
Crossbedding	ss	ms	ms	R
Bedding	t	tM	MT	T
Vertical burrows	—	C	—	—
Horizontal burrows	—	R	A	C
Sponge—*Calathium* mounds	—	R	A	C
Fossil abundance	L	V	H	H
Fossil diversity	L	V	M	H
Intraclasts	A	A	A	R
Ooids	—	C	A	R
Spar/micrite	L	V	V	L

FIGURE 49—Beds in upper part of Padre Member at Scenic Drive section in southern Franklin Mountains.

resent deeper water and grade upward into light-colored rock formed in shallow, well-oxygenated water.

The Padre Member has been eroded from most areas, and so interpretations are based on sections observed in the southern locales from the Florida Mountains east to Beach Mountain. The Padre differs very little at all these locales, except in the Florida Mountains where sections do not contain supratidal indicators.

The El Paso Formation rocks in the Sacramento Mountains are somewhat anomalous. Pray (1961) measured and described 132 m of the El Paso at Agua Chiquita Canyon. This section is approximately one-third as thick as the sections measured in the southern Franklin Mountains and Hueco Mountains, but all four members of the El Paso appear to be present (Table 1). Sections of El Paso at Arrow, Mule, Dog, and Agua Chiquita Canyons in the Sacramento Mountains are all dolostone, and so no detailed petrography is possible. The thickest section of 132 m was measured and described by Pray (1961). Individual members in the El Paso in the Sacramento Mountains are tentatively identified by using the features listed in Tables 2 and 3 and correlating with sections to the west and southeast. Apparently this part of the platform subsided more slowly, or was covered intermittently by epeiric seas for shorter periods of time, than portions to the east and west.

Most, if not all, previous reports, including Clemons (1985, in press) referred to the El Paso Formation as a diachronous unit deposited by an eastward- or northeastward-advancing sea. In this report, evidence now supports an east-westtrending shoreline across southern New Mexico possibly to central Texas. Isopachs show northward depositional thinning of the Hitt Canyon, Jose, and probably the McKelligon Members (Figs. 3B, 3C). The Jose is a relatively thin shoal deposit that can be recognized from Willcox, Arizona, to central Texas. Although further work using conodonts is needed to determine its age, the Jose is probably not diachronous. Its age probably does not vary across southern New Mexico. A very distinctive, mottled, medium- to dark-gray oolite bed occurs in the Jose at Hembrillo Canyon, Cable Canyon, Red Hills, and Lake Valley sections along an east-west trend. If the seashore had advanced eastward, such key beds would be aligned north-south. Interestingly, the oolitic—hematitic facies in the underlying Bliss Formation has an east-west trend across New Mexico (Kelley, 1951; Kottlowski, 1963). Stageman (1987) also documented an east-west strand line during Bliss deposition. The eastward increase in sand content in the El Paso is localized by islands or peninsulas on the platform (described above).

After considerations of all the regional differences and environmental indicators present in the various members, the following sequence of transgressions, regressions, and depositional environments is proposed. This sequence differs little from Lucia (1968, 1971) and Hayes (1975a), but is refined and supported by evidence in the preceding sections of this report.

A gradual northward transgression of the sea continued in Early Ordovician time as most of the Hitt Canyon Member was deposited in shallow-subtidal waters. Locally, intertidal to supratidal conditions may have existed around the islands. Deposition was interrupted many times by scouring of storm-generated wave action. Deposition probably was faster than subsidence, at times forming many hardgrounds and small-scale disconformities. Southward regression started in late Hitt Canyon time as shallow-subtidal to intertidal, stacked hemispheroids formed. Supratidal conditions existed in east-central Arizona.

TABLE 3—Chart showing sedimentary features observed in the El Paso Formation. A, abundant; C, common; R, rare; H, high; M, medium or moderate; L, low; V, variable; ms, medium scale; ss, small scale; T, thick; t, thin; —, not observed.

Members	Mudcracks	Fenestrae	Cryptalgal laminites	Evaporites	Microcrystalline dolomite	Oncolites	Cryptalgal mounds	Crossbedding	Bedding	Vertical burrows	Horizontal burrows	Sponge-*Calathium* mounds	Fossil abundance	Fossil diversity	Intraclasts	Ooids	Spar/micrite
Upper Padre	—	—	—	—	—	—	—	—	tM	—	C	—	M	L	C	—	M
Lower Padre	C	C	A	—	A	—	—	A	t	—	R	—	L	L	R	—	L
Upper McKelligon	—	—	—	—	—	—	—	—	T	—	A	R	H	H	A	—	M
Lower McKelligon	—	—	—	—	—	—	C	—	M	—	A	A	H	H	A	—	M
Jose	—	—	R	—	R	R	R	C	t	R	R	R	M	L	A	A	H
Upper Hitt Canyon	R	R	R	R	R	A	C	—	t	—	A	R	H	H	A	—	H
Lower Hitt Canyon	—	—	—	—	—	C	—	C	t	—	C	—	M	M	C	R	M

Nondeposition and maybe some erosion adjacent to some of the islands accounts for the missing faunal zones in the Franklin Mountains.

In Jose time, a northward transgression gradually began. Throughout most of the region, the dark Jose Member was deposited in shallow-subtidal, shoaling water. Near some of the islands, intertidal environments transgressed into supratidal flats. Transgression continued as the McKelligon Member was deposited in shallow-subtidal environments. Regionally, sediments were deposited above the storm-wave base, and hundreds or thousands of times scour-and-fill features were formed. *Sponge-Calathium* mounds grew near shores, but were periodically cut by intertidal currents throughout McKelligon time.

Another, probably minor, regression occurred after the McKelligon Member was deposited. Regression and return of the sea accompanied supratidal deposits in the lower part of the Padre Member adjacent to a few still-existing islands. The presence of fine sand and silt in the shallow-subtidal Padre in the Florida Mountains indicates that regression did not proceed far. Upper beds of the Padre (Fig. 49) represent a more restricted shallow-subtidal—intertidal(?) environment. *Nuia* is rare and ostracods occur only in the Padre. Stricker and Carozzi (1973) reported similar occurrences of *Nuia* and ostracods in the Lower Ordovician Pogonip Group in Nevada. They stated that *Nuia* formed a dense population seaward of offshore bars and was dispersed landward and seaward by wave action.

Conclusions

(1) The El Paso Formation was deposited on a gradually and intermittently subsiding platform (homoclinal ramp) during the Early Ordovician.

(2) The El Paso is predominantly a subtidal deposit, but locally and temporally intertidal, and rarely supratidal, conditions prevailed.

(3) From the south, three major transgressions and two regressions of the sea took place during deposition of the El Paso. Open-marine conditions followed the first two transgressions, but a more restricted shelf lagoon environment followed the third transgression.

(4) Small-scale depositional cycles are interspersed with the transgressive—regressive deposits. The cycles may be attributed to variations in subsidence rates relative to depositional rates or to eustatic sea-level changes.

(5) Primary dolomite in the El Paso is rare. Dolomitization of primary calcium carbonate sediments occurred by several methods that include hydrothermal alteration, probable mixing of meteoric and sea water during diagenesis, and refluxion after lithification.

(6) Areal distribution of *sponge-Calathium* mounds and stacked hemispheroidal stromatolites appears random, but was probably controlled by water depths relative to islands and peninsulas(?) rather than by a regional strand line.

References

Aluka, M. I. J., 1984, Stratigraphy of Early Ordovician El Paso Group of the southern Hueco Mountains, Hudspeth County, Texas: unpublished PhD dissertation, The University of Texas, El Paso, 466 pp.

American Commission on Stratigraphic Nomenclature, 1961, Code of stratigraphic nomenclature: American Association of Petroleum Geologists Bulletin, v. 45, pp. 645-665.

Armstrong, A. K., Silberman, M. L., Todd, V. R., Hoggatt, W. C., and Carter, R. B., 1978, Geology of central Peloncillo Mountains, Hidalgo County, New Mexico: New Mexico Bureau of Mines and Mineral Resources, Circular 158, 19 pp.

Bachman, G. 0., 1965, Geologic map of the Capitol Peak NW quadrangle, Socorro County, New Mexico: U.S. Geological Survey, Miscellaneous Geologic Investigations Map 1-441, scale 1:31,680.

Bachman, G. 0., 1968, Geology of the Mockingbird Gap quadrangle, Lincoln and Socorro Counties, New Mexico: U.S. Geological Survey, Professional Paper 594-J, 43 pp.

Bachman, G. 0., and Myers, D. A., 1963, Geology of the Bear Peak NE quadrangle, Dona Ana County, New Mexico: U.S. Geological Survey, Miscellaneous Geologic Investigations Map 1-374, scale 1:31,680.

Bachman, G. 0., and Myers, D. A., 1969, Geology of the Bear Peak area, Dona Ana County, New Mexico: U.S. Geological Survey, Bulletin 1271-C, 46 pp.

Badiozamani, K., 1973, The Dorag dolomitization model-application to the Middle Ordovician of Wisconsin: Journal of Sedimentary Petrology, v. 43, pp. 965-984.

Ballman, D. L., 1960, Geology of the Knight Peak area, Grant County, New Mexico: New Mexico Bureau of Mines and Mineral Resources, Bulletin 70, 39 pp.

Barnes, V. E., Cloud, P. E., Jr., Dixon, L. P., Folk, R. L., Jonas, E. C., Palmer, A. R., and Tynan, E. J., 1959, Stratigraphy of the pre-Simpson Paleozoic subsurface rocks of Texas and southeast New Mexico: The University of Texas, Bureau of Economic Geology, Publication 5924, 2 v., 836 pp.

Bathurst, R. G. C., 1966, Boring algae, micrite envelopes and lithification of molluscan biosparites: Journal of Geology, v. 5, pp. 15-32.

Blankenship, J. C., Jr., 1972, Stratigraphy and petrology of the El Paso Formation in the Silver City Range, New Mexico: unpublished MS thesis, University of Houston, 101 pp.

Brett, C. E., and Brookfield, M. E., 1984, Morphology, faunas and genesis of Ordovician hardgrounds from southern Ontario, Canada: Paleogeography, Paleoclimatology, Paleoecology, v. 46, pp. 233-290.

Bridges, L. W., 1964, Stratigraphy of Minas Plomosas-Placer de Guadalupe area: West Texas Geological Society, Publication 6450, pp. 50-59.

Brown, G. A., 1982, Geology of the Mahoney mine-Gym Peak area, Florida Mountains, Luna County, New Mexico: unpublished MS thesis, New Mexico State University, Las Cruces, 82 pp.

Church, S. B., 1974, Lower Ordovician patch reefs in western Utah: Brigham Young University, Geology Studies, v. 21, pp. 41-62.

Clemons, R. E., 1982, Geology of Massacre Peak quadrangle, Luna County, New Mexico: New Mexico Bureau of Mines and Mineral Resources, Geologic Map 51, scale 1:24,000.

Clemons, R. E., 1984, Geology of Capitol Dome quadrangle, Luna County, New Mexico: New Mexico Bureau of Mines and Mineral Resources, Geologic Map 56, scale 1:24,000.

Clemons, R. E., 1985, Geology of South Peak quadrangle, Luna County, New Mexico: New Mexico Bureau of Mines and Mineral Resources, Geologic Map 59, scale 1:24,000.

Clemons, R. E., 1987, El Paso Formation-a Lower Ordovician carbonate deposit (abs.): American Association of Petroleum Geologists Bulletin, v. 71, p. 539.

Clemons, R. E., in press, Geology of the Florida Mountains, Luna County, New Mexico: New Mexico Bureau of Mines and Mineral Resources, Memoir 43.

Clemons, R. E., and Brown, G. A., 1983, Geology of Gym Peak quadrangle, Luna County, New Mexico: New Mexico Bureau of Mines and Mineral Resources, Geologic Map 58, scale 1:24,000.

Clemons, R. E., and Osburn, G. R., 1986, Geology of the Truth or Consequences region-an overview: New Mexico Geological Society, Guidebook to 37th Field Conference, pp. 69-82.

Cloud, P. E., Jr., and Barnes, V. E., 1948, The Ellenburger group of central Texas: The University of Texas, Bureau of Economic Geology, Publication 4621, 473 pp.

Cloud, P. E., Jr., and Barnes, V. E., 1957, Early Ordovician sea in central Texas; *in* Ladd, H. S. (ed.), Treatise on marine ecology and paleoecology: Geological Society of America, Memoir 67, v. 2, pp. 163-214.

Cooper, J. R., 1960, Reconnaissance map of the Willcox, Fisher Hills, Cochise, and Dos Cabezas quadrangles, Cochise and Graham Counties, Arizona: U.S. Geological Survey, Miscellaneous Field Studies Map MF-231, scale 1:62,500.

Corbitt, L. L., 1971, Structure and stratigraphy of the Florida Mountains, New Mexico: unpublished PhD dissertation, University of New Mexico, Albuquerque, 115 pp.

Cunningham, J. E., 1974, Geologic map and sections of Silver City quadrangle, New Mexico: New Mexico Bureau of Mines and Mineral Resources, Geologic Map 30, scale 1:24,000.

Darton, N. H., 1916, Geology and underground water of Luna County, New Mexico: U.S. Geological Survey, Bulletin 618, 188 pp.

Darton, N. H., 1917, Description of the Deming quadrangle, New Mexico: U.S. Geological Survey, Geologic Atlas, Folio 207, 15 pp.

Darton, N. H., 1928, "Red beds" and associated formations in New Mexico: U.S. Geological Survey, Bulletin 794, 356 pp.

Donnan, G. T., 1987, Stratigraphy and structural geology of the northern part of the northern Animas Mountains, Hidalgo County, New Mexico: unpublished MS thesis, New Mexico State University, Las Cruces, 121 pp.

Drewes, H., and Thorman, C. H., 1980a, Geologic map of the Steins quadrangle and the adjacent part of the Vanar quadrangle, Hidalgo County, New Mexico: U.S. Geological Survey, Miscellaneous Geologic Investigations Map 1-1220, scale 1:24,000.

Drewes, H., and Thorman, C. H., 1980b, Geologic map of the Cotton City quadrangle and the adjacent part of the Vanar quadrangle, Hidalgo County, New Mexico: U.S. Geological Survey, Miscellaneous Geologic Investigations Map 1-1221, scale 1:24,000.

Dunham, R. J., 1962, Classification of carbonate rocks according to depositional texture: American Association of Petroleum Geologists, Memoir 1, pp. 108-121.

Epis, R. C., 1958, Early Paleozoic strata in southeastern Arizona: American Association of Petroleum Geologists Bulletin, v. 42, pp. 2750-2756.

Epis, R. C., and Gilbert, C. M., 1957, Early Paleozoic strata in southeastern Arizona: American Association of Petroleum Geologists Bulletin, v. 41, pp. 2223-2242.

Ethington, R. L., and Clark, D. L., 1964, Conodonts from the El Paso Formation (Ordovician) of Texas and Arizona: Journal of Paleontology, v. 38, pp. 685-704.

Ethington, R. L., and Clark, D. L., 1971, Lower Ordovician conodonts in North America; *in* Sweet, W. C., and Bergstrom, S. M. (eds.), Symposium on conodont biostratigraphy: Geological Society of America, Memoir 127, pp. 63-82.

Evans, K. V., and Clemons, R. E., 1987, U-Pb geochronology of the Florida Mountains, New Mexico-new evidence for latest Cambrian-earliest Ordovician alkalic plutonism (abs.): Geological Society of America, Abstracts with Programs, v. 19, pp. 657658.

Evans, K. V., and Clemons, R. E., 1988, Cambrian-Ordovician (500 Ma) alkalic plutonism in southwestern New Mexico-U-Th-Pb isotopic data from the Florida Mountains: American Journal of Science, v. 288, pp. 735-755.

Flower, R. H., 1953, Paleozoic sedimentary rocks of southwestern New Mexico: New Mexico Geological Society, Guidebook to 4th Field Conference, pp. 106-112.

Flower, R. H., 1957, Studies of the Actinoceratida: New Mexico Bureau of Mines and Mineral Resources, Memoir 2, 101 pp.

Flower, R. H., 1958, Cambrian-Mississippian beds of southern New Mexico: Roswell Geological Society, Guidebook 11, pp. 61-78.

Flower, R. H., 1959, Cambrian-Devonian beds of southern New Mexico: Permian Basin Section, Society of Economic Paleontologists and Mineralogists, and Roswell Geological Society, Joint Conference Guidebook in the Sacramento Mountains, pp. 154-171.

Flower, R. H., 1964, The nautiloid order Ellesmeroceratida (Cephalopoda): New Mexico Bureau of Mines and Mineral Resources, Memoir 12, 234 pp.

Flower, R. H., 1965, Early Paleozoic of New Mexico: New Mexico

Geological Society, Guidebook to 16th Field Conference, pp. 112-131.

Flower, R. H., 1969, Early Paleozoic of New Mexico and El Paso region: El Paso Geological Society, Ordovician Symposium, pp. 31-101.

Flügel, E., 1982, Microfacies analysis of limestones: Springer-Verlag, New York, 633 pp.

Folk, R. L., 1959a, Practical petrographic classification of limestones: American Association of Petroleum Geologists Bulletin, v. 43, pp. 1-38.

Folk, R. L., 1959b, Thin-section examination of pre-Simpson Paleozoic rocks; *in* Stratigraphy of the pre-Simpson Paleozoic subsurface rocks of Texas and southeast New Mexico: University of Texas, Bureau of Economic Geology, Publication 5924, pp. 95-130.

Garven, G., 1985, The role of regional fluid flow in the genesis of the Pine Point deposit, western Canada sedimentary basin: Economic Geology, v. 80, pp. 307-324.

Garven, G., and Freeze, R. A., 1984, Theoretical analysis of the role of groundwater flow in the genesis of stratabound ore deposits: American Journal of Science, v. 284, part 1, pp. 1085-1124; part 2, pp. 1125-1174.

Gastil, R. G., and Miller, R. H., 1981, Lower Paleozoic strata on the Pacific plate of North America: Nature, v. 292, pp. 828-830.

Gillerman, E., 1958, Geology of the central Peloncillo Mountains, Hidalgo County, New Mexico, and Cochise County, Arizona: New Mexico Bureau of Mines and Mineral Resources, Bulletin 57, 152 pp.

Ginsburg, R. N., 1964, South Florida carbonate sediments: Geological Society of America Convention, Miami Beach, Florida, Field Trip No. 1 Guidebook, 72 pp.

Harbour, R. L., 1972, Geology of the northern Franklin Mountains, Texas and New Mexico: U.S. Geological Survey, Bulletin 1298, 129 pp.

Hardie, L. A., 1987, Perspectives on dolomitization-a critical view of some current views: Journal of Sedimentary Petrology, v. 57, pp. 166-183.

Harris, L. D., 1973, Dolomitization model for Upper Cambrian and Lower Ordovician carbonate rocks in the eastern United States: U.S. Geological Survey, Journal of Research, v. 1, pp. 63-78.

Hayes, P. T., 1972, Stratigraphic nomenclature of Cambrian and Lower Ordovician rocks of easternmost Arizona and adjacent westernmost New Mexico: U.S. Geological Survey, Bulletin 1372-B, 21 pp.

Hayes, P. T., 1975a, Cambrian and Ordovician rocks of southern Arizona and New Mexico and westernmost Texas: U.S. Geological Survey, Professional Paper 873, 98 pp.

Hayes, P. T., 1975b, Selected stratigraphic sections of Cambrian and Ordovician rocks in Arizona, New Mexico, and western Texas: U.S. Geological Survey, Open-file Report 75-178, 51 pp.

Hedlund, D. C., 1977, Geology of the Hillsboro and San Lorenzo quadrangles, Sierra and Grant Counties, New Mexico: U.S. Geological Survey, Miscellaneous Field Studies Map MF-900A, scale 1:48,000.

Hedlund, D. C., 1978, Geologic map of the Werney Hill quadrangle, Grant County, New Mexico: U.S. Geological Survey, Miscellaneous Field Studies Map MF-1038, scale 1:24,000.

Hendricks, L., 1964, Stratigraphic summary of the Ellenburger Group of north Texas; *in* Symposium on the Arbuckle: Tulsa Geological Society Digest, v. 32, pp. 119-125.

Hill, J. D., 1956, Paleozoic stratigraphy of the Mud Springs Mountains, Sierra County, New Mexico: unpublished MS thesis, University of New Mexico, Albuquerque, 72 pp.

Hintze, L. F., 1973, Lower and Middle Ordovician stratigraphic sections in the Ibex area, Millard County, Utah: Brigham Young University, Geology Studies, v. 20, pp. 3-36.

Horowitz, A. S. and Potter, P. E., 1971, Introductory petrography of fossils: Springer-Verlag, New York, 302 pp.

Jahns, R. H., 1955, Geology of the Sierra Cuchillo, New Mexico: New Mexico Geological Society, Guidebook to 6th Field Conference, pp. 158-174.

Jicha, H. L., Jr., 1954, Geology and mineral deposits of Lake Valley quadrangle, Grant, Luna, and Sierra Counties, New Mexico: New Mexico Bureau of Mines and Mineral Resources, Bulletin 37, 93 pp.

Jones, S. M., and Bacheller, W. D., 1953, Measured sections near Dos Cabezas, Arizona: New Mexico Geological Society, Guidebook to 4th Field Conference, p. 149.

Jones, W. R., Hernon, R. M., and Moore, S. L., 1967, General geology of Santa Rita quadrangle, Grant County, New Mexico: U.S. Geological Survey, Professional Paper 555, 144 pp.

Katz, A., 1971, Zoned dolomite crystals: Journal of Geology, v. 79, pp. 38-51.

Kelley, V. C., 1951, Oolitic iron deposits of New Mexico: American Association of Petroleum Geologists Bulletin, v. 35, pp. 21992228.

Kelley, V. C., and Furlow, J. W., 1965, Lower Paleozoic wedge edges in south-central New Mexico-new control: Geological Society of America Bulletin, v. 76, pp. 689-694.

Kelley, V. C., and Silver, C., 1952, Geology of the Caballo Mountains: University of New Mexico, Albuquerque, Publication in Geology, no. 4, 286 pp.

Kendall, A. C., 1977, Origin of dolomite mottling in Ordovician limestones from Saskatchewan and Manitoba: Bulletin of Canadian Petroleum Geology, v. 25, pp. 480-504.

Kendall, A. C., and Tucker, M. E., 1973, Radiaxial fibrous calcite: a replacement after acicular carbonate: Sedimentology, v. 20, pp. 365-389.

Kerans, C., and Lucia, F. J., 1989, Recognition of second, third, and fourth/fifth order scales of cyclicity in the El Paso Group and their relation to genesis and architecture of Ellenburger reservoirs: Permian Basin Section, Society of Economic Paleontologists and Mineralogists.

King, P. B., 1965, Geology of the Sierra Diablo region, Texas: U.S. Geological Survey, Professional Paper 480, 185 pp.

King, P. B., King, R. E., and Knight, J. B., 1945, Geology of Hueco Mountains, El Paso and Hudspeth Counties, Texas: U.S. Geological Survey, Oil and Gas Investigations Preliminary Map 36, scale 1:63,360.

Klement, K. W., and Toomey, D. F., 1967, Role of the blue-green alga *Girvanella* in skeletal grain destruction and lime-mud formation in the Lower Ordovician of west Texas: Journal of Sedimentary Petrology, v. 37, pp. 1045-1051.

Kottlowski, F. E., 1960, Summary of Pennsylvanian sections in southwestern New Mexico and southeastern Arizona: New Mexico Bureau of Mines and Mineral Resources, Bulletin 66, 187 pp.

Kottlowski, F. E., 1963, Paleozoic and Mesozoic strata of southwestern and south-central New Mexico: New Mexico Bureau of Mines and Mineral Resources, Bulletin 79, 100 pp.

Kottlowski, F. E., Flower, R. H., Thompson, M. L., and Foster, R. W., 1956, Stratigraphic studies of the San Andres Mountains, New Mexico: New Mexico Bureau of Mines and Mineral Resources, Memoir 1, 132 pp.

Kottlowski, F. E., Kuellmer, F. J., and Jones, W. R., 1953, Road log from Las Cruces to Silver City: New Mexico Geological Society, Guidebook to 5th Field Conference, pp. 29-63.

Kottlowski, F. E., LeMone, D. V., and Foster, R. W., 1969, Early Ordovician highlands of Precambrian rocks and their associated facies: El Paso Geological Society, Guidebook 3, pp. 134-142.

Kottlowski, F. E., LeMone, D. V., and Foster, R. W., 1973, Remnant mountains in Early Ordovician seas of the El Paso region, Texas and New Mexico: Geology, v. 1, pp. 137-140.

Krieger, M. H., 1968, Stratigraphic relations of the Troy Quartzite (younger Precambrian) and the Cambrian formations in southeastern Arizona: Arizona Geological Society, Guidebook III, pp. 23-32.

Kuellmer, F. J., 1954, Geologic section of the Black Range at Kingston, New Mexico: New Mexico Bureau of Mines and Mineral Resources, Bulletin 33, 100 pp.

Land, L. S., 1973, Contemporaneous dolomitization of middle Pleistocene reefs by meteoric water, North Jamaica: Marine Science Bulletin, v. 23, pp. 64-92.

Langenheim, R. L., Carss, B. W., Kennerly, J. B., McCutcheon, V. A. and Waines, R. H., 1962, Paleozoic section in Arrow Canyon Range, Clark County, Nevada: American Association of Petroleum Geologists Bulletin, v. 46, pp. 592-609.

Lee, Y. I., and Friedman, G. M., 1987, Deep-burial dolomitization in the Ordovician Ellenburger Group carbonates, west Texas and southeastern New Mexico: Journal of Sedimentary Petrology, v. 57, pp. 544-557.

LeMone, D. V., 1969, Cambrian-Ordovician in El Paso border region: New Mexico Bureau of Mines and Mineral Resources, Circular 104, pp. 17-25.

LeMone, D. V., 1974, The Lower Ordovician Florida Mountains Formation stratotype, Luna County, New Mexico: El Paso Geological Society, Guidebook 8, pp. 36-46.

LeMone, D. V., 1975, Correlation aspects of the Ordovician of the southwestern United States; *in* Hills, J. M. (ed.), Exploration from the mountains to the basins: El Paso Geological Society, Guidebook 9, pp. 169-196.

LeMone, D. V., 1976a, Cyclic digitate algae of the Canadian (Lower Ordovician) Jose Formation, southern Franklin Mountains, El Paso County, Texas: El Paso Geological Society, Quinn Memorial Volume, pp. 11-24.

LeMone, D. V., 1976b, The Lower Ordovician Florida Mountains Formation of the Franklin Mountains, El Paso County, Texas: El Paso Geological Society, Quinn Memorial Volume, pp. 25-33.

LeMone, D. V., 1980, Stratigraphy of the Franklin Mountains, Texas and New Mexico: American Association of Petroleum Geologists, Southwest Section Annual Meeting, Guidebook, 55 pp.

Lindgren, W., 1905, The copper deposits of the Clifton-Morenci district, Arizona: U.S. Geological Survey, Professional Paper 43, 375 pp.

Lochman-Balk, C., 1958, The Capitol Dome section, Florida Mountains: Roswell Geological Society, Guidebook 11, pp. 47-52.

Logan, B. W., Rezak, R., and Ginsburg, R. N., 1964, Classification and environmental significance of algal stromatolites: Journal of Geology, v. 72, pp. 68-83.

Lopez-Ramos, E., 1969, Marine Paleozoic rocks of Mexico: American Association of Petroleum Geologists Bulletin, v. 53, pp. 23992417.

Loucks, R. G., and Anderson, J. H., 1985, Depositional facies and porosity development in Lower Ordovician Ellenburger Dolomite, Puckett Field, Pecos County, Texas; *in* Roehl, P. 0., and Choquette, P. W. (eds.), Carbonate petroleum reservoirs: Springer-Verlag, New York, pp. 19-37.

Lucia, F. J., 1968, Sedimentation and paleogeography of the El Paso Group: West Texas Geological Society, Guidebook 68-55a, pp. 61-75.

Lucia, F. J., 1971, Lower Paleozoic history of the western Diablo Platform, west Texas and south-central New Mexico: Permian Basin Section, Society of Economic Paleontologists and Mineralogists, Field Conference Guidebook of Robledo Mountains and Franklin Mountains, pp. 174-214.

Lynn, G. C., 1975, Stratigraphic correlation of the El Paso and Montoya Groups in the Vittorio Mountains, the Snake Hills, and the Big Florida Mountains in southwestern New Mexico: unpublished MS thesis, University of Arizona, Tucson, 115 pp.

Mamet, B., and Roux, A., 1982, Sur le mode de croissance de *Nuia,* algue incertae sedis: Geubias, no. 15, fast. 6, pp. 959-965.

Maslov, V. P., 1956, Fossil calcareous algae of the U.S.S.R.: Akademiya Nauk SSSR, Institut Geologichnykh Nauk Trudy, v. 160, 301 pp., 96 pls., 9 tables (in Russian).

Mason, J. T., 1976, The geology of the Caballo Peak quadrangle, Sierra County, New Mexico: unpublished MS thesis, University of New Mexico, Albuquerque, 131 pp.

Morrow, D. W., 1978, Dolomitization of lower Paleozoic burrow-fillings: Journal of Sedimentary Petrology, v. 48, pp. 295-306.

Nitecki, M. H., 1986, Receptaculitids and their relationship to other problematic fossils: Oxford Monographs on Geology, no. 5, pp. 27-34.

North American Commission on Stratigraphic Nomenclature, 1983, North American stratigraphic code: American Association of Petroleum Geologists Bulletin, v. 67, pp. 841-875.

Paige, S., 1916, Description of the Silver City quadrangle, New Mexico: U.S. Geological Survey, Geological Atlas, Folio 199, 19 pp.

Pratt, B. R., 1982, Stromatolitic framework of carbonate mudmounds: Journal of Sedimentary Petrology, v. 52, pp. 1203-1227.

Pratt, B. R., 1984, *Epiphyton* and Renalcis-diagenetic microfossils from calcification of coccoid blue-green algae: Journal of Sedimentary Petrology, v. 54, pp. 948-971.

Pratt, B. R., and James, N. P., 1982, Cryptalgal-metazoan bioherms of Early Ordovician age in the St. George Group, western Newfoundland: Sedimentology, v. 29, pp. 543-569.

Pratt, W. P., 1967, Geology of the Hurley west quadrangle, Grant County, New Mexico: U.S. Geological Survey, Bulletin 1241-E, 91 pp.

Pray, L. C., 1961, Geology of the Sacramento Mountains escarpment, Otero County, New Mexico: New Mexico Bureau of Mines and Mineral Resources, Bulletin 35, 144 pp.

Read, J. F., 1985, Carbonate platform facies models: American Association of Petroleum Geologists Bulletin, v. 69, pp. 1-21. Repetski, J. E., 1982, Conodonts from El Paso Group (Lower Ordovician) of westernmost Texas and southern New Mexico: New Mexico Bureau of Mines and Mineral Resources, Memoir 40, 121 pp.

Richardson, G. B., 1904, Report of a reconnaissance in Trans-Pecos Texas, north of the Texas and Pacific Railway: University of Texas Mineral Survey, Bulletin 9, 119 pp.

Richardson, G. B., 1908, Paleozoic formations in Trans-Pecos Texas: American Journal of Science, 4th series, v. 25, pp. 474-484.

Richardson, G. B., 1909, Description of the El Paso quadrangle, Texas: U.S. Geological Survey, Geologic Atlas, Folio 166, 11 pp.

Riding, R., and Toomey, D. F., 1972, The sedimentological role of *Epiphyton* and *Renalcis* in Lower Ordovician mounds, southern Oklahoma: Journal of Paleontology, v. 46, pp. 509-519.

Rigby, J. K., 1965, Stratigraphy and Porifera of Ordovician rocks near Columbia icefields, Jasper National Park, Alberta, Canada: Brigham Young University, Geology Studies, v. 12, pp. 165-184.

Ross, R. J., 1976, Ordovician sedimentation in the western United States; *in* Bassett, M. G. (ed.), The Ordovician System-proceedings of a paleontological association symposium, Birmingham, Sept. 1974: University of Wales Press and National Museum of Wales, Cardiff, pp. 73-105.

Rupert, M. G., 1986, Structure and stratigraphy of the Klondike Hills, southwestern New Mexico: unpublished MS thesis, New Mexico State University, Las Cruces, 138 pp.

Sabins, F. F., 1957, Stratigraphic relations in Chiricahua and Dos Cabezas Mountains, Arizona: American Association of Petroleum Geologists Bulletin, v. 41, pp. 466-510.

Sandberg, P. A., 1975, New interpretations of Great Salt Lake ooids and of ancient non-skeletal carbonate mineralogy: Sedimentology, v. 22, pp. 497-537.

Sandberg, P. A., 1983, An oscillating trend in Phanerozoic non-skeletal carbonate mineralogy: Nature, v. 305, pp. 19-22.

Schuchert, C., 1955, Atlas of paleogeographic maps of North America: John Wiley & Sons, New York, 177 pp.

Seager, W. R., 1973, Geologic map and sections of Bishop Cap-Organ Mountains area, New Mexico: New Mexico Bureau of Mines and Mineral Resources, Geologic Map 29, scale 1:24,000.

Seager, W. R., 1981, Geology of Organ Mountains and southern San Andres Mountains, New Mexico: New Mexico Bureau of Mines and Mineral Resources, Memoir 36, 97 pp.

Seager, W. R., Hawley, J. W., and Clemons, R. E., 1971, Geology of San Diego Mountain area, Dona Ana County, New Mexico: New Mexico Bureau of Mines and Mineral Resources, Bulletin 97, 38 pp.

Sheehan, P. M., and Schiefelbein, D. R. J., 1984, The trace fossil *Thalassinoides* from the Upper Ordovician of the eastern Great Basin-deep burrowing in the early Paleozoic: Journal of Paleontology, v. 58, pp. 440-447.

Shinn, E. A., 1983, Tidal flat environment; *in* Scholle, P. A., Bebout, D. G., and Moore, C. H. (eds.), Carbonate depositional environments: American Association of Petroleum Geologists, Memoir 33, pp. 171-210.

Shoji, R., and Folk, R. L., 1964, Surface morphology of some limestone types as revealed by electron microscope: Journal of Sedimentary Petrology, v. 34, pp. 144-155.

Soule, J. M., Structural geology of northern part of Animas Mountains, Hidalgo County, New Mexico: New Mexico Bureau of Mines and Mineral Resources, Circular 125, 15 pp.

Stageman, J. C., 1987, Depositional facies and provenance of lower Paleozoic sandstones of the Bliss, El Paso, and Montoya Formations, southern New Mexico and west Texas: unpublished MS thesis, New Mexico State University, Las Cruces, 101 pp.

Stauffer, K. W., 1962, Quantitative petrographic study of Paleozoic carbonate rocks, Caballo Mountains, New Mexico: Journal of Sedimentary Petrology, v. 32, pp. 357-396.

Stewart, J. H., McMenamin, M. A. S., and Morales-Ramirez, J. M., 1984, Upper Proterozoic and Cambrian rocks in the Caborca region, Sonora, Mexico-physical stratigraphy, biostratigraphy, paleocurrent studies, and regional relations: U.S. Geological Survey, Professional Paper 1309, 36 pp.

Stricker, G. D., and Carozzi, A. V., 1973, Carbonate microfacies of the Pogonip Group (Lower Ordovician) Arrow Canyon Range, Clark County, Nevada, U.S.A.: Societe National des Petroles d'Aquitaine, Bulletin du Centre de Recherches de Pau, v. 7, no. 2, pp. 499-541.

Swett, K., 1964, Petrology and paragenesis of the Ordovician Manitou Formation along the Front Range of Colorado: Journal of Sedimentary Petrology, v. 34, pp. 615-624.

Toomey, D. E, 1964, Ellenburger (Lower Ordovician) sponge beds of central Texas: Tulsa Geological Society Digest, v. 32, pp. 98111.

Toomey, D. F., 1965, A problematical organism from the Lower Ordovician (El Paso Group) of west Texas (abs.): Geological Society of America, Annual Meetings Program, pp. 174.

Toomey, D. F., 1967, Additional occurrences and extension of strati-graphic range of the problematical micro-organism *Nuia:* Journal of Paleontology, v. 41, pp. 1457-1461.

Toomey, D. F., 1970, An unhurried look at a Lower Ordovician mound horizon, southern Franklin Mountains, west Texas: Journal of Sedimentary Petrology, v. 40, pp. 1318-1334.

Toomey, D. F., 1978, Observations on the Monument Spring Member of the Lower Ordovician Marathon Formation, Marathon region, southwest Texas: Permian Basin Section, Society of Economic Paleontologists and Mineralogists, Publication 78-17, pp. 215-221.

Toomey, D. F., 1981, Organic-buildup constructional capability in Lower Ordovician and late Paleozoic mounds; *in* Gray, J., Boucot, A. J., and Berry, W. R. N. (eds.), Communities of the past: Hutchinson Ross Publication, Stroussburg, Pennsylvania, pp. 35-68.

Toomey, D. F., and Babcock, J. A., 1983, Precambrian and Paleozoic algal carbonates, west Texas—southern New Mexico: Colorado School of Mines, Golden, Professional Contribution No. 11, 345 pp.

Toomey, D. F., and Ham, W. E., 1967, *Pulchrilamina,* a new mound-building organism from Lower Ordovician rocks of west Texas and southern Oklahoma: Journal of Paleontology, v. 41, pp. 981-987.

Toomey, D. F., and Klement, K. W., 1966, A problematical micro-organism from the El Paso Group (Lower Ordovician) of west Texas: Journal of Paleontology, v. 40, pp. 1304-1311.

Toomey, D. F. and Nitecki, M. H., 1979, Organic buildups in the Lower Ordovician (Canadian) of Texas and Oklahoma: Fieldiana Geology, New Series, no. 2, 181 pp.

Umphress, A. M., 1977, Lithostratigraphic zonation of the Ellenburger Group within the Belco Hickman No. 13 well, Barnhart Field, Reagan uplift, Texas: unpublished MA thesis, University of Texas, Arlington, 156 pp.

Webby, B. D., 1986, *Pulchrilamina:* Oxford Monographs on Geology, no. 5, pp. 148-166.

Wolf, K. H., 1965, "Grain-diminution" of algal colonies to micrite: Journal of Sedimentary Petrology, v. 35, pp. 420-427.

Yochelson, E. L. and Bridge, J., 1957, The Lower Ordovician gastropod *Ceratopea: U .S* . Geological Survey, Professional Paper 294H, pp. 281-304.

Young, L. M., 1970, Early Ordovician sedimentary history of Marathon Geosyncline, Trans-Pecos Texas: American Association of Petroleum Geologists Bulletin, v. 54, pp. 2303-2316.

Zeller, R. A., Jr., 1965, Stratigraphy of the Big Hatchet Mountains area, New Mexico: New Mexico Bureau of Mines and Mineral Resources, Memoir 16, 128 pp.

Appendix A

Other El Paso Formation sections

Some outcrops of the El Paso Formation were examined in the field and compared with descriptions in the literature, but were not sampled. Locations, references, and approximate thicknesses of these sections are listed in Table A1. Reasons for not selecting these sections for sampling and more detailed study included: (1) dolomitization (sections 1, 3, 4, 5, 6, 7, 9, 12, 13, and 14); (2) silicification and brecciation (sections 5, 6, 7, 8, 9, and 13); and (3) similarity with nearby sections that were sampled (sections 2, 4, 8, 10, 11, and 15).

TABLE A1—Approximate thicknesses of the El Paso Formation sections that were not sampled.

Location and references	Approximate thickness (m)
1. Morenci, Arizona (Lindgren, 1905; Hayes, 1972, 1975b)	113
2. South Ridge, Caballo Mountains (Kelley and Silver, 1952; Hayes, 1975b)	124
3. Capitol Peak, northern San Andres Mountains (Bachman, 1965)	61
4. Little San Nicholas Canyon, southern San Andres Mountains (Bachman and Myers, 1963, 1969)	232
5. Mule Canyon, Sacramento Mountains (Pray, 1961)	50
6. Dog Canyon, Sacramento Mountains (Pray, 1961)	60
7. Northern Animas Mountains (Zeller, 1965; Soule, 1972; Donnan, 1987)	174
8. Central Peloncillo Mountains, east end of Wood Canyon (Gillerman, 1958; Armstrong et al., 1978; Drewes and Thorman, 1980b)	166
9. Molinas Canyon, southern Caballo Mountains (Kelley and Silver, 1952; Hayes, 1975a)	103
10. Mescal Canyon, Big Hatchet Mountains (Zeller, 1965; Hayes, 1975b)	326
11. Chaney Canyon, Big Hatchet Mountains (Zeller, 1965)	200
12. Blue Mountain, Arizona (Sabins, 1957)	136
13. Apache Pass, southeast end of Dos Cabezas Mountains (Sabins, 1957)	104
14. 4.8 km southeast of Blue Mountain (Sabins, 1957)	218
15. 7.2 km east of Pumping Station, southern Hueco Mountains (Aluka, 1984)	314
16. Southern Swisshelm Mountains, 16 km north of Douglas, Arizona (Epis and Gilbert, 1957; Epis, 1958)	188

Appendix B

Quantitative analyses of thin sections

Quantitative analyses of El Paso Formation thin sections from 29 locales are listed in the following tables. Rocks in the other nine of the 38 sections sampled (sections 2, 3, 19, 20, 26, 29, 31, 36, and 37 in Figs. 1 and 47 and Table 1) were too neomorphosed or dolomitized to permit reliable identification of allochems.

Tables B1-B29 show the percentages of the constituents comprising more than 99% of the rocks. The grain-solid volumes are based on 300-point grids on each thin section (Flügel, 1982). A trace (tr) indicates that a constituent is present in a thin section, but represented no more than one point in the count.

TABLE B1—Dos Cabezas Mountains (section 1: Fig. 1 and Table 1).

Thickness above base of section (m)	Brachio-pods	Echino-derms	Gastro-pods	*Nuia*	Ostracods	Sponge spicules	Trilobites	Intraclasts	Pellets and peloids	Ooids	Quartz silt and sand	Spar cement	Micrite matrix
McKelligon Member													
111	tr	12	2	tr	–	–	6	52	–	–	tr	28	–
108	–	3	1	30	–	–	2	21	–	–	–	24	19
107	tr	6	5	–	–	12	3	3	–	–	–	3	68
106	–	tr	1	–	–	4	1	–	–	–	–	8	86
102	–	10	–	38	–	–	2	2	–	–	–	44	4
Jose Member													
99	–	21	–	11	–	–	5	7	9	–	–	47	–
98	–	10	–	2	–	–	11	25	8	–	–	44	–
89	1	11	–	1	–	–	17	2	30	–	tr	38	–
Hitt Canyon Member													
83	1	13	4	5	–	tr	4	22	–	–	–	30	23
82	–	5	–	–	–	–	4	–	24	–	–	–	67
81	–	21	10	6	–	–	3	29	–	–	–	31	–
80	–	3	2	1	–	–	4	3	–	–	–	18	69
79	–	21	13	4	–	–	1	27	–	–	–	34	–
78	–	13	5	2	–	–	2	63	–	–	–	15	–
77	–	8	2	18	–	7	5	1	–	–	–	15	44
74	–	12	–	4	–	–	7	10	17	–	–	44	6
71	tr	8	9	5	–	–	8	12	3	–	2	33	20
70	–	16	–	13	–	–	5	3	12	–	–	51	–
67	tr	10	–	1	–	–	6	24	16	–	–	43	–
62	–	6	–	4	–	–	2	–	36	–	–	52	–
61	–	4	2	12	–	2	3	–	4	–	–	10	63
59	1	5	1	2	–	–	10	–	23	–	–	–	58
58	–	11	1	7	–	–	6	–	17	–	1	57	–
(underlain by 58 m of sandy dolostone)													

TABLE B2—Central Peloncillo Mountains (section 4: Fig. 1 and Table 1).

Thickness above base of section (m)	Brachio-pods	Echino-derms	Gastro-pods	*Nuia*	Ostracods	Sponge spicules	Trilobites	Intraclasts	Pellets and peloids	Ooids	Quartz silt and sand	Spar cement	Micrite matrix
McKelligon Member													
(alluvium cover)													
175	–	8	–	–	–	10	4	–	–	–	–	–	78
168	–	10	–	5	–	–	5	35	–	–	–	45	–
153	tr	3	5	–	–	5	4	–	–	–	–	3	80
145	–	23	–	7	–	–	5	12	–	–	2	43	8
Jose Member													
138	–	2	–	–	–	–	3	23	–	24	–	48	–
137	–	3	5	–	–	–	8	30	–	8	–	46	–
130	–	7	–	–	–	–	4	12	31	–	3	32	11
122	tr	8	11	–	–	–	11	42	–	–	1	25	2

TABLE B2—(continued)

Thickness above base of section (m)	Brachio-pods	Echino-derms	Gastro-pods	*Nuia*	Ostracods	Sponge spicules	Trilobites	Intraclasts	Pellets and peloids	Ooids	Quartz silt and sand	Spar cement	Micrite matrix
Hitt Canyon Member													
115	1	13	4	5	–	–	–	22	–	–	–	42	13
100	tr	8	1	2	–	3	2	50	–	–	–	34	–
92	–	2	2	2	–	5	1	18	–	–	–	39	31
85	–	4	1	–	–	3	1	–	–	–	–	4	87
77	–	2	7	1	–	7	6	–	–	–	–	–	77
70	–	10	tr	4	–	–	1	48	–	–	–	37	–
62	–	9	–	3	–	–	5	50	–	–	–	33	–
55	–	18	–	6	–	–	2	5	16	–	–	24	29
47	–	3	4	–	–	–	5	69	–	–	1	18	–
40	–	3	3	1	–	–	2	52	4	–	tr	35	–
31	–	23	8	2	–	tr	4	33	–	–	–	30	–
25	tr	7	–	3	–	–	4	59	5	–	tr	22	–
20	–	14	–	–	–	8	5	–	tr	–	–	2	71
10	–	12	–	8	–	–	2	7	37	–	tr	34	–
(underlain by 10+ m of dolostone)													

TABLE B3—Ram Gorge (section 5: Fig. 1 and Table 1).

Thickness above base of section (m)	Brachio-pods	Echino-derms	Gastro-pods	*Nuia*	Ostracods	Sponge spicules	Trilobites	Intraclasts	Pellets and peloids	Ooids	Quartz silt and sand	Spar cement	Micrite matrix
McKelligon Member													
(overlain by 35 m of dolostone)													
270	tr	1	–	tr	–	2	1	2	–	–	–	14	80
262	tr	1	1	–	–	3	–	3	–	–	–	2	90
255	tr	5	–	–	–	3	tr	5	–	–	–	5	82
247	–	2	3	–	–	5	2	1	–	–	–	8	79
240	–	tr	–	tr	–	2	tr	4	–	–	–	14	80
232	–	4	–	–	–	–	2	56	–	–	–	36	2
225	–	1	–	–	–	9	1	–	6	–	–	2	81
217	–	41	–	–	–	–	1	–	5	–	–	12	41
210	–	1	tr	–	–	9	2	–	–	–	–	–	88
202	–	tr	–	–	–	6	tr	16	–	–	–	1	77
195	–	37	–	tr	–	–	1	–	5	–	–	28	29
187	–	15	1	2	–	20	3	5	3	–	–	10	41
180	–	3	–	1	–	1	tr	3	20	–	–	15	57
172	tr	59	–	–	–	–	1	7	–	–	–	27	6
165	–	17	5	–	–	–	6	12	–	–	–	13	47
158	tr	46	–	1	–	–	7	8	–	–	–	24	14
157	–	tr	–	–	–	5	1	–	–	–	–	18	76
150	–	4	3	–	–	9	3	1	–	–	–	4	76
Jose Member													
142	tr	21	1	–	–	–	8	12	11	–	1	46	–
138	–	tr	3	–	–	–	1	17	–	20	1	12	46
Hitt Canyon Member													
136	tr	31	tr	9	–	–	2	7	–	–	–	41	10
135	tr	6	2	5	–	3	2	1	5	–	8	8	60
129	tr	2	7	–	–	–	1	63	11	–	–	13	3
127	tr	2	1	1	–	–	2	21	41	–	3	29	–
120	1	9	1	13	–	–	1	42	–	–	–	33	–
119	tr	1	tr	–	–	–	1	2	–	–	–	9	86
112	–	5	tr	tr	–	4	2	7	–	–	–	15	67
105	–	7	2	42	–	–	1	2	–	–	–	33	13
100	–	8	5	3	–	2	1	11	10	–	–	31	29
97	–	7	–	59	–	–	–	–	–	–	–	27	7
90	–	5	–	50	–	–	–	–	–	–	–	9	36
82	–	9	–	50	–	–	–	1	–	–	tr	33	7
75	–	33	–	11	–	–	1	2	–	–	–	53	–
67	tr	26	–	17	–	2	2	9	3	–	2	22	17
60	1	12	–	15	–	2	2	2	8	–	2	26	30
52	–	47	–	1	–	–	–	–	2	–	1	49	–
(underlain by 52 m of dolostone)													

TABLE B4—Klondike Hills (section 6: Fig. 1 and Table 1).

Thickness above base of section (m)	Brachio- pods	Echino- derms	Gastro- pods	*Nuia*	Ostracods	Sponge spicules	Trilobites	Intraclasts	Pellets and peloids	Ooids	Quartz silt and sand	Spar cement	Micrite matrix
Padre Member													
*82	1	1	–	–	tr	13	3	1	–	–	–	1	80
70	–	3	–	–	–	16	4	2	3	–	6	11	55
58	1	10	–	–	4	–	16	20	–	–	1	37	11
46	–	1	1	1	–	8	1	15	–	–	–	18	55
38	–	1	–	6	–	13	1	9	7	–	–	25	38
30	–	3	–	5	–	6	2	19	–	–	–	18	47
24	–	5	1	1	–	1	3	7	–	–	tr	12	70
20	–	3	2	4	–	17	3	2	–	–	tr	10	59
14	–	4	1	11	–	10	3	–	2	–	tr	8	61
7	4	3	–	10	–	3	2	1	4	–	1	11	61
0	–	8	tr	–	–	19	6	2	13	–	tr	14	38
McKelligon Member													
*76	2	7	5	–	tr	5	4	6	1	–	–	8	62
75	tr	2	1	–	1	–	9	41	6	–	tr	33	7
72	5	13	2	–	tr	2	11	13	2	–	tr	33	19
70	tr	12	3	9	1	10	3	2	–	–	–	10	50
69	1	9	–	–	tr	7	3	7	13	–	tr	13	47
67	tr	24	3	–	–	–	6	12	9	–	–	46	–
64	1	12	2	–	tr	–	9	47	–	–	–	29	–
62	tr	19	1	–	tr	1	3	11	16	–	tr	29	20
61	tr	27	2	2	–	–	4	17	11	–	tr	37	–
59	tr	7	3	1	tr	12	5	–	1	–	–	3	68
56	tr	3	tr	–	tr	8	1	6	–	–	–	16	66
52	tr	9	4	3	–	–	3	25	15	–	–	41	–
49	–	–	tr	–	–	tr	–	–	–	–	–	–	100
43	tr	15	3	2	–	–	12	38	–	–	–	30	–
41	–	2	1	41	–	–	5	16	–	–	–	35	–
38	–	3	1	7	–	8	1	5	–	–	–	23	52
34	–	21	1	5	–	–	2	37	–	–	–	34	–
32	tr	7	–	40	–	–	2	19	–	–	–	32	–
30	–	1	1	1	–	4	–	30	8	–	–	29	26
27	tr	4	1	4	–	–	2	51	–	–	–	38	–
24	1	2	2	–	–	4	5	3	–	–	–	2	81
18	–	10	1	5	–	6	1	49	2	–	–	26	–
15	–	1	1	3	–	5	2	4	–	–	–	11	73
5	–	3	–	–	–	25	3	2	–	–	–	7	60
0	1	3	–	–	–	–	16	25	–	–	–	33	22
Jose Member													
*10	–	1	1	2	–	–	–	58	–	–	–	38	–
8	–	5	1	6	–	–	–	48	–	–	tr	26	14
6	–	36	2	3	–	–	9	11	–	9	4	26	–
4	–	15	4	3	–	–	5	30	–	–	1	42	–
2	–	14	1	2	–	–	2	31	–	6	1	43	–
1	–	14	3	–	–	–	5	34	–	13	–	31	–
Hitt Canyon Member													
*70	–	2	5	1	–	8	–	15	–	–	–	18	51
67	–	1	tr	–	–	3	2	–	–	–	–	21	73
61	–	1	3	2	–	11	1	–	–	–	–	–	82
60	–	15	4	4	–	1	2	26	–	–	–	15	33
57	–	7	5	–	–	15	6	1	–	–	–	–	66
55	–	9	9	–	–	8	8	17	–	–	–	18	31
51	–	6	11	–	–	12	3	6	–	–	–	8	54
47	–	2	3	1	–	4	1	–	–	–	–	–	89
43	–	1	–	28	–	–	1	29	–	–	–	23	18
37	tr	6	–	–	–	–	9	46	3	–	tr	36	–
35	–	5	1	1	–	8	3	5	13	–	–	20	44
32	–	5	2	tr	–	13	3	2	–	–	–	5	70
25	tr	10	tr	1	–	–	1	49	–	–	tr	39	–
20	tr	5	–	4	–	–	5	39	–	–	tr	23	24
14	–	1	tr	10	–	13	1	4	17	–	1	18	35
10	–	7	–	56	–	–	2	–	–	–	tr	35	–
7	–	4	tr	35	–	5	1	7	–	–	tr	25	23
3	1	2	tr	–	–	7	7	1	17	–	2	19	44
0	–	2	–	–	–	8	1	5	20	–	3	29	32

*Structural deformation prohibits measuring a complete section. These four partial sections contain no repetitions, but amount deleted is unknown.

TABLE B5—Victorio Mountains (section 7: Fig. 1 and Table 1).

Thickness above base of section (m)	Brachio-pods	Echino-derms	Gastro-pods	*Nuia*	Ostracods	Sponge spicules	Trilobites	Intraclasts	Pellets and peloids	Ooids	Quartz silt and sand	Spar cement	Micrite matrix
McKelligon Member													
(overlain by 6 m of limestone and alluvium)													
118	tr	8	1	–	–	5	1	24	–	–	–	33	28
Jose Member													
116	–	12	3	7	–	–	4	43	–	2	tr	29	–
114	–	3	1	11	–	–	1	28	–	4	1	34	17
112	–	5	6	8	–	2	2	5	–	1	1	–	70
110	–	8	–	–	–	–	4	10	13	15	1	28	21
108	–	6	tr	21	–	–	–	13	–	21	tr	39	–
106	–	2	–	–	–	–	2	12	–	45	1	38	–
104	–	2	7	–	–	–	2	11	–	30	1	31	16
101	tr	4	26	–	–	–	6	2	–	–	1	14	47
Hitt Canyon Member													
100	–	11	2	12	–	tr	2	26	–	–	tr	32	15
99	–	8	–	15	–	1	1	–	–	–	2	10	63
91	–	7	6	1	–	–	6	20	–	–	1	26	33
85	–	4	2	8	–	4	2	–	–	–	2	–	78
77	tr	5	tr	12	–	2	2	–	–	–	2	–	77
69	tr	7	–	2	–	3	6	–	–	–	1	–	81
61	–	12	1	29	–	–	8	7	–	–	–	43	–
55	–	7	–	14	–	tr	1	17	11	–	tr	46	4
(underlain by 55 m of intensely neomorphosed limestone and dolostone; fault contact)													

TABLE B6—Snake Hills (section 8: Fig. 1 and Table 1).

Thickness above base of section (m)	Brachio-pods	Echino-derms	Gastro-pods	*Nuia*	Ostracods	Sponge spicules	Trilobites	Intraclasts	Pellets and peloids	Ooids	Quartz silt and sand	Spar cement	Micrite matrix
Padre Member													
*15	1	11	–	–	1	10	7	8	7	–	–	13	42
11	1	7	–	–	1	13	7	2	6	–	–	13	50
7	tr	5	–	–	–	6	5	10	4	–	tr	17	53
0	1	6	1	–	2	11	4	18	tr	–	–	24	33
McKelligon Member													
*125	–	tr	–	40	–	–	5	18	–	–	–	37	–
117	–	3	1	41	–	–	1	6	–	–	–	43	5
110	1	3	2	–	–	–	7	46	–	–	–	41	–
106	–	4	6	–	–	5	4	9	–	–	–	8	64
102	–	1	2	–	–	7	3	30	–	–	–	35	22
93	tr	2	7	–	–	11	3	tr	–	–	–	4	73
91	1	8	14	–	–	1	4	3	–	–	tr	6	63
85	1	2	7	–	–	12	2	2	–	–	–	14	60
79	–	2	1	tr	–	4	2	28	3	–	tr	24	36
78	1	1	tr	1	–	3	2	32	5	–	–	26	29
77	–	tr	–	1	–	–	5	29	16	–	–	47	2
68	tr	2	–	tr	–	7	3	27	–	–	–	24	37
67	tr	5	1	–	–	17	5	3	2	–	1	5	61
59	1	9	4	–	–	3	4	8	–	–	–	5	66
Jose Member													
45	–	19	4	–	–	–	8	27	–	–	–	42	–
38	tr	4	6	–	–	4	10	10	tr	4	tr	23	39
33	1	13	4	5	–	5	3	15	–	–	2	13	39
Hitt Canyon Member													
(underlain by 33 m of dolostone; lowest dolostone covered by alluvium)													

*Incomplete section: base not exposed and unknown thickness missing near top.

TABLE B7—Capitol Dome (section 9: Fig. 1 and Table 1).

Thickness above base of section (m)	Brachio-pods	Echino-derms	Gastro-pods	*Nuia*	Ostracods	Sponge spicules	Trilobites	Intraclasts	Pellets and peloids	Ooids	Quartz silt and sand	Spar cement	Micrite matrix
Padre Member													
290	1	29	–	tr	–	–	2	24	–	–	–	23	21
285	8	7	1	–	–	–	6	33	–	–	–	21	24
270	tr	3	13	tr	1	5	2	6	–	–	–	24	46
263	1	3	tr	–	tr	3	1	–	–	–	–	–	92
260	–	1	1	–	–	8	1	3	4	–	–	–	82
257	1	5	10	–	–	3	7	–	–	–	–	–	74
254	1	9	2	–	–	7	3	–	–	–	1	3	74
249	–	3	tr	–	2	–	1	–	16	–	3	47	28
McKelligon Member													
248	2	6	1	8	–	–	1	22	–	–	–	21	39
244	1	10	2	2	–	6	2	tr	–	–	–	4	73
243	2	8	1	3	–	2	2	–	–	–	2	–	80
236	2	11	3	8	–	–	2	39	–	–	–	35	–
219	–	6	3	6	–	4	1	3	–	–	–	8	69
209	1	10	3	2	–	18	tr	tr	–	–	–	–	66
201	3	12	7	tr	–	7	4	tr	–	–	–	–	67
196	–	13	7	4	–	5	tr	–	–	–	–	7	64
186	–	8	2	5	–	3	2	26	–	–	–	20	34
170	1	7	–	5	–	9	2	22	–	–	–	14	40
162	3	3	8	8	–	4	4	9	–	–	–	9	52
157	2	1	3	1	–	3	2	–	–	–	–	–	88
151	3	5	3	–	–	8	3	tr	–	–	–	1	77
142	1	7	4	1	–	13	4	5	–	–	–	7	58
134	1	3	3	1	–	8	2	–	–	–	–	2	80
128	tr	6	2	2	–	11	4	8	–	–	–	10	57
118	2	8	12	1	–	5	3	4	–	–	tr	11	54
112	–	4	4	2	–	10	3	2	–	–	–	5	70
104	–	2	4	–	–	–	2	55	–	–	–	31	6
98	–	5	2	3	–	7	1	–	–	–	–	2	80
89	–	11	8	tr	–	9	5	8	–	–	–	16	43
Jose Member													
82	1	8	2	1	–	8	7	–	–	–	–	35	38
80	–	10	2	–	–	–	18	5	–	12	4	24	25
79	–	7	1	–	–	4	3	4	–	–	1	6	74
77	–	1	1	–	–	8	1	–	–	–	1	6	82
Hitt Canyon Member													
69	–	4	1	8	–	–	1	64	–	–	1	21	–
61	–	7	1	7	–	–	4	25	–	–	–	29	27
56	tr	3	2	1	–	–	3	27	–	–	–	18	46
(underlain by 53 m of dolostone)													

TABLE B8—Victorio Canyon (section 10: Fig. 1 and Table 1).

Thickness above base of section (m)	Brachio-pods	Echino-derms	Gastro-pods	*Nuia*	Ostracods	Sponge spicules	Trilobites	Intraclasts	Pellets and peloids	Ooids	Quartz silt and sand	Spar cement	Micrite matrix
Padre Member													
350	1	33	11	–	–	–	3	5	–	4	–	38	5
346	4	23	6	–	1	–	6	4	6	–	–	27	23
341	tr	39	5	–	1	–	3	9	–	3	–	40	–
338	1	4	–	–	tr	tr	4	38	9	–	tr	44	–
329	–	10	1	–	tr	16	1	–	2	–	–	5	65
325	tr	2	3	–	tr	7	4	–	–	–	–	–	83
319	2	1	16	–	tr	8	3	4	–	–	–	5	61
315	tr	12	5	–	1	7	3	1	–	–	–	2	69
307	tr	4	tr	–	–	7	tr	1	–	–	6	4	78
298	tr	2	1	–	–	13	16	8	–	–	tr	26	34
294	tr	2	6	–	–	4	5	3	12	–	1	12	55
289	tr	6	24	–	–	–	9	5	4	–	3	25	24
283	tr	4	21	–	–	–	7	4	2	–	1	41	20
274	–	6	2	1	–	7	2	–	–	–	2	25	55
269	–	16	2	8	–	–	1	46	–	–	–	27	–
McKelligon Member													
266	–	11	2	1	–	11	1	5	–	–	1	9	59
260	–	20	3	1	–	5	2	2	–	–	–	8	59
251	–	1	1	tr	–	9	1	4	–	–	–	5	79
242	–	1	1	–	–	7	1	2	–	–	–	–	88
235	–	3	3	3	–	3	1	–	–	–	–	–	87
225	tr	5	2	1	–	11	3	–	–	–	–	2	76
220	–	2	–	66	–	–	1	–	–	–	–	27	4
208	–	1	3	3	–	8	2	–	–	–	–	2	81
202	tr	4	4	2	–	7	6	–	–	–	–	2	75
196	1	1	5	1	–	5	1	–	–	–	–	–	86
190	1	7	–	–	–	–	2	56	–	–	–	34	–
182	2	7	1	19	–	–	3	29	–	–	–	39	–
175	tr	3	9	1	–	2	3	19	–	–	–	15	48
165	tr	3	5	–	–	6	2	27	–	–	–	23	34
159	tr	5	20	–	–	8	4	–	–	–	–	–	63
147	–	4	10	1	–	12	2	–	–	–	–	–	71
142	–	2	12	–	–	8	1	10	–	–	–	10	57
133	–	4	9	–	–	4	2	–	–	–	–	4	77
125	1	7	5	tr	–	5	4	8	–	–	–	13	57
121	–	5	4	1	–	3	2	41	–	–	–	21	23
112	–	9	2	1	–	–	8	29	–	–	–	26	25
106	tr	3	3	tr	–	4	4	–	–	–	–	–	86
97	–	12	5	–	–	4	8	4	–	–	–	7	60
Jose Member													
96	–	4	4	–	–	–	2	5	–	45	tr	40	–
95	–	5	5	–	–	5	9	2	–	–	tr	10	64
94	–	8	3	–	–	–	5	20	–	27	2	31	4
Hitt Canyon Member													
91	–	5	2	13	–	1	2	–	–	–	1	3	73
83	–	3	–	3	–	–	1	–	37	–	tr	56	–
78	–	–	–	1	–	9	tr	–	–	–	tr	12	78
67	–	5	2	27	–	–	2	25	–	–	–	39	–
62	tr	8	13	4	–	–	5	11	–	–	–	21	38
57	–	5	–	18	–	2	7	11	–	–	–	41	16
51	1	9	5	1	–	2	4	3	2	–	1	4	68
(underlain by 49 m of dolostone)													

TABLE B9—Werney Hill (section 11: Fig. 1 and Table 1).

Thickness above base of section (m)	Brachio-pods	Echino-derms	Gastro-pods	*Nuia*	Ostracods	Sponge spicules	Trilobites	Intraclasts	Pellets and peloids	Ooids	Quartz silt and sand	Spar cement	Micrite matrix
Hitt Canyon Member													
(overlain by alluvium)													
78	–	7	2	12	–	–	3	41	2	–	–	33	–
75	tr	17	–	8	–	–	3	2	3	–	1	14	52
70	tr	19	15	2	–	–	7	8	13	–	1	20	15
67	tr	3	3	3	–	9	1	7	–	–	–	17	57
64	–	tr	–	–	–	4	tr	–	–	–	–	24	72
60	–	1	3	3	–	18	4	2	–	–	–	4	65
53	tr	5	1	2	–	3	5	13	15	–	tr	41	15
52	1	2	1	1	–	10	4	6	4	–	tr	7	64
45	–	5	–	2	–	8	6	21	9	–	tr	31	18
37	–	9	–	21	–	–	5	17	–	–	tr	44	4
(underlain by 37 m of dolostone and interbedded sandstone)													

TABLE B10—Bear Mountain (section 12: Fig. 1 and Table 1).

Thickness above base of section (m)	Brachio-pods	Echino-derms	Gastro-pods	*Nuia*	Ostracods	Sponge spicules	Trilobites	Intraclasts	Pellets and peloids	Ooids	Quartz silt and sand	Spar cement	Micrite matrix
(overlain by 52 m of dolostone)													
Hitt Canyon Member													
(overlain by 20 m of dolostone)													
63	–	25	4	1	–	–	6	37	–	–	–	–	26
58	tr	16	–	19	–	–	11	3	–	–	–	51	–
57	tr	26	–	2	–	–	5	2	–	–	–	65	–
55	–	2	tr	tr	–	12	4	6	–	–	tr	12	64
51	tr	1	1	4	–	13	1	23	–	–	–	10	47
47	tr	7	8	1	–	–	11	44	–	–	tr	29	–
46	–	1	–	–	–	7	–	–	–	–	tr	19	73
41	–	7	–	15	–	3	7	–	5	–	1	31	31
35	tr	12	–	7	–	5	3	1	–	–	2	37	33
34	–	6	–	21	–	–	5	–	tr	–	tr	40	28
33	tr	2	tr	–	–	15	7	6	5	–	–	16	49
(underlain by 33 m of dolostone)													

TABLE B11—Chloride Flat (section 13: Fig. 1 and Table 1).

Thickness above base of section (m)	Brachio-pods	Echino-derms	Gastro-pods	*Nuia*	Ostracods	Sponge spicules	Trilobites	Intraclasts	Pellets and peloids	Ooids	Quartz silt and sand	Spar cement	Micrite matrix
(overlain by 55 m of dolostone)													
Hitt Canyon Member													
(overlain by 2 m of dolostone)													
75	tr	3	1	–	–	tr	4	64	–	–	–	22	6
67	tr	28	1	2	–	–	3	25	–	–	tr	41	–
60	–	2	1	22	–	3	1	3	4	–	–	13	51
52	–	6	3	20	–	4	tr	–	–	–	–	3	64
45	–	15	4	5	–	12	2	5	–	–	–	13	44
37	–	9	–	tr	–	9	2	–	tr	–	1	5	74
31	–	22	–	12	–	–	5	–	7	–	tr	54	–
30	–	13	–	16	–	2	2	–	23	–	1	35	8
22	tr	11	–	7	–	3	2	–	15	–	tr	38	24
15	–	23	–	2	–	1	2	–	19	–	tr	45	8
8	–	3	–	14	–	–	3	–	20	–	3	54	3
(underlain by 7 m of dolostone)													

TABLE B12—Lone Mountain (section 14: Fig. 1 and Table 1).

Thickness above base of section (m)	Brachio-pods	Echino-derms	Gastro-pods	*Nuia*	Ostracods	Sponge spicules	Trilobites	Intraclasts	Pellets and peloids	Ooids	Quartz silt and sand	Spar cement	Micrite matrix
overlain by 54 m of dolostone)													
Jose Member													
(overlain by 15 m of dolostone)													
81	–	5	1	8	–	–	2	32	–	18	1	33	–
Hitt Canyon Member													
73	–	2	4	13	–	5	2	2	–	–	1	8	63
58	tr	8	1	5	–	8	5	5	21	–	–	18	29
50	1	17	14	2	–	–	7	18	–	–	–	41	–
43	–	–	–	–	–	14	tr	–	–	–	tr	3	83
35	1	16	–	5	–	3	9	1	–	–	2	10	53
27	–	9	–	13	–	9	3	–	–	–	tr	–	66
(underlain by 27 m of sandy dolostone)													

TABLE B13—San Lorenzo (section 15: Fig. 1 and Table 1).

Thickness above base of section (m)	Brachio-pods	Echino-derms	Gastro-pods	*Nuia*	Ostracods	Sponge spicules	Trilobites	Intraclasts	Pellets and peloids	Ooids	Quartz silt and sand	Spar cement	Micrite matrix
McKelligon Member													
(overlain by 18 m of dolostone)													
128	tr	1	2	–	–	20	4	–	3	–	–	6	64
122	1	1	1	–	–	21	5	–	4	–	–	4	63
114	tr	1	17	–	–	12	5	3	–	–	–	17	45
108	–	5	1	2	–	17	1	15	–	–	–	17	42
107	tr	5	2	1	–	13	3	9	–	–	–	10	57
100	–	tr	–	–	–	3	–	–	–	–	–	22	75
95	–	8	2	1	–	9	1	42	3	–	–	22	12
92	–	5	7	–	–	7	2	32	–	–	–	26	21
Jose Member													
88	–	4	1	–	–	–	5	–	30	–	6	–	54
84	–	–	–	–	–	–	2	–	29	–	7	–	62
82	–	tr	–	–	–	–	6	14	11	36	1	32	–
79	–	4	tr	1	–	–	tr	65	–	–	1	29	–
76	–	2	–	3	–	tr	–	55	–	–	–	25	15
75	–	4	–	34	–	–	–	29	–	–	–	33	–
69	tr	1	2	9	–	12	1	3	–	–	1	6	65
Hitt Canyon Member													
63	–	10	–	38	–	–	4	9	–	–	–	39	–
61	tr	8	–	24	–	–	5	2	–	–	–	54	7
58	–	4	1	tr	–	–	1	65	–	–	–	29	–
54	tr	tr	–	–	–	1	tr	–	–	–	–	2	97
50	–	11	–	–	–	7	4	–	15	–	–	26	37
47	tr	2	tr	–	–	4	3	7	–	–	–	6	78
45	–	1	1	–	–	–	tr	54	–	–	–	31	13
44	1	5	6	tr	–	–	11	16	9	–	tr	10	42
41	tr	tr	tr	–	–	10	2	–	–	–	tr	3	85
40	tr	2	3	2	–	19	3	2	–	–	–	6	63
37	–	4	–	2	–	16	4	6	5	–	–	15	48
36	tr	11	–	5	–	–	10	–	12	–	–	58	4
34	–	1	–	13	–	–	1	42	5	–	–	30	8
30	–	17	–	2	–	11	7	6	5	–	–	31	21
27	–	4	–	12	–	11	3	–	–	–	–	–	70
26	–	9	–	3	–	–	3	57	3	–	–	25	–
22	–	6	–	2	–	13	7	2	9	–	tr	18	43
15	1	21	2	1	–	–	21	7	7	1	tr	30	9
11	–	5	tr	10	–	12	3	4	–	–	tr	5	61
7	–	4	1	17	–	7	4	8	–	–	3	8	48
4	–	13	–	4	–	tr	8	–	13	–	2	53	7
2	–	15	–	–	–	5	6	17	–	–	1	28	28
0	–	12	–	1	–	6	6	16	–	–	4	29	26

TABLE B14—Northwest Cooke's Range (section 16: Fig. 1 and Table 1).

Thickness above base of section (m)	Brachio-pods	Echino-derms	Gastro-pods	*Nuia*	Ostracods	Sponge spicules	Trilobites	Intraclasts	Pellets and peloids	Ooids	Quartz silt and sand	Spar cement	Micrite matrix
McKelligon Member													
223	–	10	1	2	–	5	3	22	–	–	–	32	25
210	–	6	2	1	–	8	2	–	1	–	–	4	76
200	–	3	3	1	–	13	2	4	–	–	–	12	62
190	tr	1	1	1	–	10	1	–	4	–	–	6	76
185	tr	1	2	–	–	16	1	1	–	–	–	7	72
180	–	–	–	tr	–	12	–	–	–	–	–	5	83
175	–	2	6	–	–	9	5	4	20	–	–	28	25
170	tr	3	5	1	–	15	2	5	–	–	–	7	62
160	tr	17	4	–	–	3	3	16	–	–	–	16	41
155	tr	3	1	tr	–	7	4	16	–	–	–	24	45
150	–	2	4	tr	–	14	3	5	–	–	–	8	64
140	–	7	11	tr	–	13	2	2	–	–	–	4	61
130	–	–	10	–	–	2	1	12	–	–	–	–	75
120	–	tr	1	–	–	2	4	44	–	–	–	31	18
115	tr	5	5	–	–	7	4	4	–	–	–	15	60
110	–	2	4	1	–	5	1	9	–	–	tr	17	61
105	–	5	2	–	–	22	2	3	–	–	tr	14	52
100	tr	8	3	–	–	8	1	3	–	–	–	7	70
Jose Member													
92	–	1	tr	–	–	–	2	53	–	8	tr	36	–
85	–	6	4	4	–	3	2	6	–	10	3	8	54
81	–	4	1	1	–	14	2	13	–	–	2	15	48
Hitt Canyon Member													
80	–	2	1	5	–	–	1	72	–	–	–	19	–
75	–	1	1	31	–	–	–	38	–	–	–	29	–
70	–	4	tr	–	–	7	4	18	–	–	–	23	44
65	1	6	3	tr	–	5	9	1	9	–	1	10	55
60	–	13	–	10	–	1	13	–	–	–	1	–	62
55	–	8	–	2	–	–	1	52	–	–	–	37	–
50	4	23	–	tr	–	–	10	–	–	–	8	42	13
45	3	13	1	–	–	21	9	2	–	–	2	18	31
40	–	5	tr	27	–	–	2	37	–	–	tr	29	–
35	–	5	–	13	–	5	2	4	–	–	2	12	58
23	–	2	–	30	–	–	2	tr	–	–	3	15	48
8	–	8	–	–	–	tr	11	2	8	–	3	14	54

TABLE B15—Quartzite Ridge (section 17: Fig. 1 and Table 1).

Thickness above base of section (m)	Brachio-pods	Echino-derms	Gastro-pods	*Nuia*	Ostracods	Sponge spicules	Trilobites	Intraclasts	Pellets and peloids	Ooids	Quartz silt and sand	Spar cement	Micrite matrix
McKelligon Member													
*134	tr	7	1	tr	–	8	3	7	–	–	–	11	63
124	1	7	1	tr	–	9	1	1	–	–	–	–	80
111	tr	8	2	4	–	11	1	9	–	–	–	10	55
99	–	3	2	tr	–	13	2	–	–	–	–	17	63
Jose Member													
82	–	–	–	–	–	–	1	13	–	54	tr	32	–
79	–	1	–	1	–	4	tr	tr	–	–	1	28	65
74	–	1	1	–	–	–	1	12	–	44	1	36	4
73	–	8	–	4	–	–	tr	67	–	–	–	21	–
67	–	1	–	7	–	–	–	71	–	–	tr	21	–
65	–	5	1	22	–	–	1	43	–	–	tr	28	–
Hitt Canyon Member													
*59	–	3	1	13	–	–	1	50	–	–	–	26	6
57	–	6	–	66	–	–	tr	6	–	–	–	21	1
52	–	8	–	22	–	–	–	–	43	–	tr	17	10
50	–	5	1	1	–	–	1	44	–	–	–	6	42
45	–	14	tr	33	–	–	3	6	–	–	–	27	17
35	–	tr	–	–	–	9	tr	–	–	–	–	7	84
29	tr	3	2	tr	–	21	1	–	1	–	–	2	70
22	–	19	–	tr	–	–	1	22	4	–	4	41	9
13	–	6	tr	1	–	–	tr	42	2	20	tr	29	–
5	–	1	tr	22	–	–	1	–	7	–	9	–	60

*Base of El Paso not exposed; first sample 5 m above fault contact mostly covered by alluvium.

TABLE B16—Kingston (section 18: Fig. 1 and Table 1).

Thickness above base of section (m)	Brachio-pods	Echino-derms	Gastro-pods	*Nuia*	Ostracods	Sponge spicules	Trilobites	Intraclasts	Pellets and peloids	Ooids	Quartz silt and sand	Spar cement	Micrite matrix
McKelligon Member													
*149	–	2	–	3	–	5	2	43	–	–	–	16	29
141	–	–	–	–	–	6	–	–	–	–	–	5	89
134	–	2	–	1	–	7	2	13	–	–	–	11	64
Jose Member													
126	tr	9	–	–	–	–	6	33	–	18	–	34	–
125	–	7	5	1	–	–	5	–	–	51	–	31	–
124	tr	7	–	30	–	–	8	11	–	–	–	44	–
Hitt Canyon Member													
120	–	2	tr	7	–	–	5	5	–	–	5	10	66
113	–	1	–	9	–	4	6	3	–	–	3	34	40
105	–	2	–	–	–	8	3	–	–	–	–	5	82
98	tr	8	2	1	–	–	4	51	–	–	–	34	–
90	–	13	2	46	–	–	1	4	–	–	–	34	–
83	–	4	2	–	–	9	1	tr	–	–	–	1	83
75	–	1	–	–	–	4	1	–	–	–	–	10	84
68	–	5	–	–	–	4	8	6	tr	–	5	35	37
61	–	5	2	4	–	5	3	tr	–	–	–	–	81
(break in section; dolostone overlies lower 60 m)													
*60	tr	5	4	1	–	14	3	14	–	–	–	9	50
53	–	4	6	3	–	4	1	4	8	–	–	16	54
45	–	4	–	–	–	29	6	–	10	–	–	–	51
38	tr	4	–	13	–	–	1	18	–	4	4	23	33
37	tr	5	–	10	–	–	1	27	–	–	–	34	23
30	–	2	1	8	–	12	2	–	10	–	2	7	56
23	–	7	–	1	–	–	tr	55	–	–	–	37	–
15	–	4	1	9	–	11	2	13	–	–	1	11	48
2	–	2	–	13	–	10	–	17	–	–	2	14	42

*Probably no repeated section, but unknown thickness probably deleted at 60 m.

TABLE B17—Mud Springs Mountains (section 21: Fig. 1 and Table1).

Thickness above base of section (m)	Brachio-pods	Echino-derms	Gastro-pods	*Nuia*	Ostracods	Sponge spicules	Trilobites	Intraclasts	Pellets and peloids	Ooids	Quartz silt and sand	Spar cement	Micrite matrix
McKelligon Member													
(overlain by 8 m of dolostone)													
164	tr	5	3	tr	–	3	4	–	–	–	1	6	78
158	tr	1	5	–	–	tr	2	–	–	–	tr	52	40
156	–	3	4	tr	–	tr	tr	–	–	–	–	45	48
146	–	1	2	tr	–	–	tr	50	–	–	–	29	18
137	–	2	1	–	–	4	1	–	–	–	tr	28	64
Jose Member													
128	–	2	1	–	–	–	2	41	–	13	2	39	–
125	–	9	–	–	–	–	2	46	–	–	3	40	–
117	–	4	–	12	–	–	1	20	–	–	1	40	22
Hitt Canyon Member													
108	–	4	–	24	–	–	1	15	–	–	tr	33	23
107	tr	4	1	1	–	1	2	–	–	–	2	7	82
102	–	4	–	38	–	–	1	16	–	–	–	36	5
88	–	1	–	–	–	2	tr	–	–	–	1	4	92
80	1	15	1	1	–	1	3	9	–	–	tr	32	37
74	1	8	–	6	–	2	4	4	–	–	3	40	32
67	–	3	–	8	–	–	1	54	–	–	–	21	13
59	–	2	–	1	–	14	8	33	–	–	tr	39	3
51	–	9	–	21	–	–	4	2	1	–	3	11	49
44	–	6	–	3	–	1	4	8	2	–	12	40	14
36	–	6	–	42	–	–	1	–	–	–	6	24	21
26	–	7	–	15	–	–	6	28	4	–	9	15	16
(underlain by 24 m of dolomitic, sandy limestone)													

TABLE B18—Cable Canyon (section 22: Fig. 1 and Table 1).

Thickness above base of section (m)	Brachio-pods	Echino-derms	Gastro-pods	*Nuia*	Ostracods	Sponge spicules	Trilobites	Intraclasts	Pellets and peloids	Ooids	Quartz silt and sand	Spar cement	Micrite matrix
McKelligon Member													
(overlain by 18 m of dolostone; fault contact)													
131	tr	3	–	–	–	19	1	3	10	–	–	17	47
127	–	3	tr	tr	–	–	2	65	–	–	–	30	–
122	–	4	–	tr	–	–	1	69	–	–	–	26	–
119	–	3	1	tr	–	40	tr	1	–	–	–	3	52
117	–	10	2	tr	–	8	2	19	–	–	–	22	37
116	–	6	6	–	–	7	1	5	–	–	–	15	60
113	–	5	6	–	–	9	3	7	–	–	–	8	62
108	–	3	4	tr	–	19	1	1	–	–	–	4	68
106	–	2	4	tr	–	21	1	3	–	–	tr	8	61
104	–	12	–	–	–	–	1	37	7	–	–	43	–
102	–	3	8	–	–	6	2	5	–	–	–	4	72
101	–	5	1	–	–	27	tr	–	–	–	1	–	66
97	–	tr	–	–	–	6	–	–	–	–	–	12	82
96	–	23	8	–	–	–	5	38	–	–	tr	26	–
Jose Member													
94	–	–	4	–	–	–	1	51	–	16	tr	28	–
85	–	1	2	–	–	tr	tr	38	–	10	2	30	17
84	–	6	6	–	–	–	4	23	–	–	3	35	23
83	–	5	8	1	–	5	–	40	–	–	1	35	5
82	–	2	1	–	–	–	–	14	–	45	–	38	–
Hitt Canyon Member													
80	tr	2	11	2	–	6	1	2	–	–	tr	5	71
78	–	4	3	3	–	13	1	4	–	–	–	6	66
76	–	9	1	30	–	–	3	21	–	–	–	6	30
74	–	3	1	9	–	2	1	53	–	–	tr	18	12
72	–	1	1	6	–	24	1	4	–	–	–	8	55
69	–	1	tr	5	–	17	1	5	–	–	tr	6	65
66	–	11	10	20	–	1	2	5	–	–	–	21	30
49	–	1	–	–	–	9	–	–	–	–	–	–	90
46	1	5	3	tr	–	6	3	21	–	–	–	19	42
41	–	1	–	22	–	–	1	53	–	–	–	23	–
35	–	4	2	46	–	–	1	11	–	–	–	27	9
27	–	7	–	32	–	4	4	–	–	–	1	27	25
24	tr	8	tr	17	–	3	8	4	–	–	4	42	14
12	–	5	–	9	–	2	5	–	–	–	6	45	28
5	tr	4	–	49	–	–	3	–	–	–	4	40	–

TABLE B19—Red Hills (section 23: Fig. 1 and Table 1).

Thickness above base of section (m)	Brachio-pods	Echino-derms	Gastro-pods	*Nuia*	Ostracods	Sponge spicules	Trilobites	Intraclasts	Pellets and peloids	Ooids	Quartz silt and sand	Spar cement	Micrite matrix
McKelligon Member													
(fault contact)													
134	–	4	tr	–	–	4	1	32	–	–	–	31	28
127	–	7	4	–	–	–	5	39	–	–	–	31	14
Jose Member													
122	–	–	1	–	–	–	4	29	–	29	1	36	–
121	tr	tr	tr	–	–	–	2	11	–	55	tr	32	–
119	–	4	1	–	–	2	tr	10	–	22	1	12	48
111	–	tr	2	tr	–	–	3	66	–	–	–	29	–
Hitt Canyon Member													
108	–	3	2	1	–	9	2	13	–	–	–	7	63
105	–	2	–	6	–	10	tr	4	–	–	1	4	73
104	–	3	2	1	–	19	1	6	–	–	tr	7	61
99	–	7	–	3	–	–	1	–	24	–	tr	48	17
96	–	1	–	22	–	3	tr	16	–	–	tr	25	33
91	–	2	–	17	–	10	1	3	–	–	–	11	56
88	tr	1	–	37	–	–	–	25	–	–	–	37	–
85	–	18	–	1	–	–	5	–	–	–	–	27	49
81	–	1	–	50	–	–	tr	11	–	–	–	28	10
78	tr	6	–	34	–	–	2	6	–	–	–	41	11
73	–	9	–	32	–	–	1	22	–	–	–	36	–
70	–	2	–	tr	–	11	2	–	–	–	1	1	83
69	–	5	tr	1	–	–	tr	62	–	–	–	25	7
66	–	9	–	2	–	2	2	36	–	–	–	28	21
61	–	7	1	8	–	5	1	4	–	–	3	11	60
58	–	1	tr	tr	–	9	tr	tr	–	–	tr	5	85
49	–	tr	–	–	–	11	tr	–	–	–	–	4	85
44	–	16	tr	8	–	–	2	34	–	–	–	25	15
43	–	4	–	3	–	3	tr	tr	23	–	–	51	16
35	–	6	tr	12	–	1	tr	1	–	–	3	19	58
30	–	11	–	19	–	2	2	–	–	–	3	29	34
15	–	4	–	4	–	–	1	9	19	–	4	26	33
8	–	4	–	32	–	–	1	–	–	–	2	41	20
3	–	11	–	9	–	–	4	35	–	–	2	39	–
0	1	22	–	3	–	–	19	–	–	–	2	29	24

TABLE B20—San Diego Mountain (section 24: Fig. 1 and Table 1).

Thickness above base of section (m)	Brachio-pods	Echino-derms	Gastro-pods	*Nuia*	Ostracods	Sponge spicules	Trilobites	Intraclasts	Pellets and peloids	Ooids	Quartz silt and sand	Spar cement	Micrite matrix
Hitt Canyon Member													
(upper part covered by alluvium)													
88	–	3	tr	1	–	3	1	12	3	–	–	10	67
85	–	7	3	7	–	–	3	15	3	–	–	20	42
82	–	6	1	1	–	–	6	33	–	–	–	29	24
79	–	6	–	3	–	2	2	4	2	–	tr	4	77
76	–	3	2	2	–	2	4	4	–	–	–	2	81
73	–	9	2	4	–	1	4	18	–	–	tr	23	39
72	–	2	–	1	–	–	1	53	2	–	–	25	16
69	–	13	3	6	–	2	3	10	4	–	tr	3	56
67	–	3	–	9	–	–	5	3	3	–	–	23	54
61	–	7	1	13	–	2	6	10	–	–	1	4	56
55	–	4	–	32	–	–	–	1	–	–	6	5	52
52	–	8	–	12	–	1	2	4	2	–	–	14	57
43	tr	5	–	15	–	2	6	13	5	–	3	23	28
37	–	5	–	17	–	–	2	1	1	–	3	25	46
30	–	12	–	3	–	–	4	–	–	–	3	12	66
20	–	2	–	21	–	–	2	2	1	–	11	3	58
10	–	5	–	1	–	–	3	2	19	–	9	55	6
2	–	8	–	1	–	–	22	3	5	–	tr	36	25

TABLE B21—Robledo Mountains (section 25: Fig. 1 and Table 1).

Thickness above base of section (m)	Brachio-pods	Echino-derms	Gastro-pods	*Nuia*	Ostracods	Sponge spicules	Trilobites	Intraclasts	Pellets and peloids	Ooids	Quartz silt and sand	Spar cement	Micrite matrix
Padre Member													
*34	1	8	–	1	–	–	1	33	–	–	–	48	8
32	–	1	1	–	–	5	1	–	–	–	–	2	90
McKelligon Member													
29	tr	1	–	–	–	–	4	3	11	–	1	15	65
28	–	6	–	–	–	–	2	8	2	–	–	25	57
25	–	7	1	–	–	2	3	10	10	–	tr	28	39
22	–	16	2	–	–	–	1	9	1	–	–	37	34
18	–	1	1	–	–	1	tr	4	–	–	–	3	90
16	–	11	1	1	–	2	1	21	1	–	–	14	48
12	–	2	–	1	–	8	1	1	2	–	–	2	83
8	–	1	–	2	–	–	–	4	–	–	–	46	47
4	–	3	–	18	–	2	3	6	1	–	–	8	59
0	1	8	1	–	–	2	1	–	–	–	–	8	79
(break in section)													
*18	–	7	1	1	–	4	2	11	1	–	–	4	69
16	–	4	2	1	–	5	1	12	–	–	–	2	73
13	tr	5	1	3	–	4	2	7	–	–	–	3	75
11	tr	3	–	13	–	1	8	9	6	–	–	38	22
8	–	2	1	5	–	2	1	4	–	–	–	4	81
3	–	1	1	4	–	1	tr	3	5	–	–	3	82
0	–	tr	1	–	–	4	1	7	–	–	–	–	87

*Incomplete, faulted section. No repetition, but unknown thickness missing at base and above lower segment.

TABLE B22—Rhodes Canyon (section 27: Fig. 1 and Table 1).

Thickness above base of section (m)	Brachio-pods	Echino-derms	Gastro-pods	*Nuia*	Ostracods	Sponge spicules	Trilobites	Intraclasts	Pellets and peloids	Ooids	Quartz silt and sand	Spar cement	Micrite matrix
(overlain by 29 m of dolostone)													
Hitt Canyon Member													
(overlain by 16 m of dolostone)													
50	–	3	tr	–	–	–	5	68	–	–	1	21	2
46	–	5	4	1	–	6	4	5	–	–	tr	4	71
41	–	9	7	tr	–	14	5	2	–	–	2	5	56
39	–	6	5	tr	–	5	7	3	–	–	2	3	69
37	–	5	6	4	–	4	3	1	–	–	2	4	71
34	–	4	10	2	–	4	6	5	–	–	2	3	64
30	–	9	1	–	–	9	6	3	–	–	tr	3	69
28	–	10	7	–	–	1	3	22	–	–	tr	13	44
26	–	15	3	–	–	–	3	34	–	–	tr	35	10
(underlain by 26 m of sandy dolostone)													

TABLE B23—Hembrillo Canyon (section 28: Fig. 1 and Table 1).

Thickness above base of section (m)	Brachio-pods	Echino-derms	Gastro-pods	*Nuia*	Ostracods	Sponge spicules	Trilobites	Intraclasts	Pellets and peloids	Ooids	Quartz silt and sand	Spar cement	Micrite matrix
(overlain by 82 m of dolostone)													
Jose Member													
(overlain by 1 m of dolostone)													
94	–	1	2	–	–	–	1	17	–	50	1	28	–
Hitt Canyon Member													
67	–	1	1	–	–	3	1	–	–	–	tr	3	91
62	–	9	10	1	–	7	8	–	–	–	tr	–	65
57	–	4	12	1	–	8	8	–	–	–	tr	6	61
51	–	10	9	1	–	tr	10	7	–	–	tr	7	56
45	tr	4	–	13	–	2	4	38	–	–	1	29	9
40	1	6	2	10	–	–	5	29	–	–	tr	36	11
35	tr	5	8	14	–	9	4	–	–	–	tr	3	57
31	1	14	4	9	–	–	6	16	–	–	2	34	12
29	1	11	7	12	–	–	9	14	–	–	3	34	9
(underlain by 29 m of sandy dolostone)													

TABLE B24—Ash Canyon (section 30: Fig. 1 and Table 1).

Thickness above base of section (m)	Brachio-pods	Echino-derms	Gastro-pods	*Nuia*	Ostracods	Sponge spicules	Trilobites	Intraclasts	Pellets and peloids	Ooids	Quartz silt and sand	Spar cement	Micrite matrix
(overlain by 177 m of dolostone)													
Hitt Canyon Member													
(overlain by 30 m of dolostone)													
30	–	2	1	45	–	–	1	7	2	–	–	38	4
24	–	4	–	5	–	1	3	–	4	–	6	35	42
21	–	4	2	30	–	–	2	2	9	–	1	37	13
9	1	7	2	10	–	1	12	4	3	–	4	13	43
8	tr	5	–	23	–	–	5	1	6	–	21	30	9
6	1	4	–	1	–	2	8	5	7	–	9	19	45
5	–	6	2	8	–	–	6	2	21	–	15	40	–
2	–	2	–	62	–	–	2	–	–	–	5	27	2
1	–	2	–	66	–	–	1	–	–	–	3	28	2
base	–	4	–	42	–	–	2	–	–	–	1	48	3

TABLE B25—Hitt Canyon (section 32: Fig. 1 and Table 1).

Thickness above base of section (m)	Brachio-pods	Echino-derms	Gastro-pods	*Nuia*	Ostracods	Sponge spicules	Trilobites	Intraclasts	Pellets and peloids	Ooids	Quartz silt and sand	Spar cement	Micrite matrix
Padre Member													
355	–	1	1	–	1	1	2	–	–	–	–	–	94
340	–	5	1	–	–	1	4	8	16	–	tr	8	57
326	–	2	1	–	–	7	2	8	6	–	–	3	71
309	–	2	1	–	–	–	1	–	45	–	tr	26	25
McKelligon Member													
274	–	4	2	–	–	5	1	5	–	–	tr	3	80
250	–	17	–	1	–	–	–	40	3	–	–	29	10
240	–	7	1	–	–	1	3	31	–	–	–	10	47
236	tr	7	1	–	–	–	3	16	3	–	tr	58	12
228	tr	5	–	–	–	–	2	9	34	–	tr	–	50
220	1	13	1	2	–	–	1	36	5	–	–	35	6
213	–	3	–	2	–	9	2	8	6	–	–	3	67
205	–	2	1	2	–	2	1	12	1	–	tr	8	71
198	–	2	tr	7	–	6	1	7	1	–	–	4	72
190	–	tr	2	2	–	1	2	2	1	–	–	2	88
183	–	6	3	4	–	tr	1	34	–	–	–	24	28
168	–	tr	tr	1	–	3	2	4	2	–	–	1	87
160	–	4	1	–	–	–	2	8	2	–	–	6	77
130	–	2	1	2	–	6	2	11	1	–	–	7	68
122	–	2	–	–	–	–	2	39	9	–	–	40	8
118	–	5	3	1	–	–	3	29	2	–	–	29	28
114	–	10	1	5	–	–	2	18	6	–	1	20	37
Jose Member													
98	–	9	1	1	–	1	3	23	10	–	1	34	17
92	–	11	1	8	–	–	–	7	1	–	2	5	65
88	–	1	1	6	–	2	1	7	–	11	1	4	66
85	–	2	2	5	–	–	1	13	2	16	2	19	38
80	–	–	–	3	–	–	2	2	1	47	–	28	17
76	–	4	2	8	–	4	3	9	2	–	1	7	60
72	–	4	2	8	–	4	3	9	2	–	1	7	60
66	–	4	–	50	–	–	1	2	9	–	1	28	5
Hitt Canyon Member													
60	–	2	–	7	–	6	1	3	4	–	–	3	74
47	–	1	–	1	–	3	2	3	1	–	–	–	89
38	–	5	2	1	–	2	2	20	1	–	–	–	67
32	–	6	1	22	–	–	1	18	8	–	1	19	24
24	–	1	–	–	–	7	1	–	–	–	tr	–	91
23	–	15	–	2	–	–	4	27	9	–	–	32	11
15	–	2	–	23	–	–	1	27	3	–	3	31	10
8	–	4	–	6	–	–	5	3	36	–	3	4	39
1	2	9	–	30	–	–	4	1	7	–	1	8	38

TABLE B26—El Paso type section (section 33: Fig. 1 and Table 1).

Thickness above base of section (m)	Brachio-pods	Echino-derms	Gastro-pods	*Nuia*	Ostracods	Sponge spicules	Trilobites	Intraclasts	Pellets and peloids	Ooids	Quartz silt and sand	Spar cement	Micrite matrix
Padre Member													
(overlain by 8 m of dolostone)													
412	tr	15	3	16	tr	–	2	21	5	–	–	38	–
405	4	4	–	5	–	6	4	12	8	–	–	17	40
397	–	2	–	–	tr	5	1	1	2	–	–	7	82
390	–	7	6	–	–	–	3	3	23	–	–	22	36
382	3	8	–	–	1	–	6	25	47	–	–	3	13
375	–	–	–	–	1	7	1	–	–	–	–	–	91
367	2	5	2	–	–	3	5	7	15	–	–	9	52
360	–	–	11	–	–	2	3	4	3	–	–	–	77
352	–	1	3	–	2	4	1	2	2	–	–	5	80
McKelligon Member													
307	15	12	1	–	–	4	6	4	4	–	–	27	27
300	–	2	1	–	–	19	1	1	–	–	–	–	76
292	1	3	3	–	–	7	6	1	8	–	–	2	69
285	–	14	–	1	–	–	3	40	10	–	–	32	–
277	–	8	1	1	–	–	3	28	5	–	–	51	3
270	–	6	2	1	–	3	3	1	10	–	1	4	69
262	tr	8	–	5	–	5	1	20	10	–	–	9	42
255	–	2	1	1	–	5	3	9	4	–	–	–	75
247	–	6	1	1	–	10	6	6	3	–	–	8	59
240	–	12	2	6	–	4	1	5	1	–	–	3	66
232	–	2	5	2	–	10	3	3	1	–	–	–	74
225	–	3	2	10	–	9	–	15	9	–	–	8	44
217	–	2	1	–	–	13	5	16	27	–	–	12	24
210	–	7	2	1	–	14	2	20	9	–	–	14	31
202	–	2	2	2	–	31	2	–	6	–	–	–	55
195	–	5	2	12	–	10	5	4	19	–	–	6	37
187	–	2	2	3	–	2	1	33	6	–	–	24	27
180	–	4	1	–	–	22	2	2	9	–	–	7	53
172	–	11	2	1	–	17	1	4	6	–	–	3	55
165	–	3	3	1	–	30	1	2	2	–	–	5	53
Jose Member (not sampled) and Hitt Canyon Member													
120	1	5	1	5	–	1	2	9	6	–	4	13	53
112	–	4	3	6	–	6	2	10	1	–	tr	14	54
105	–	2	–	55	–	–	1	3	–	–	–	39	–
97	1	1	3	–	–	10	2	–	39	–	–	8	36
75	1	17	1	–	–	11	3	5	11	–	–	5	46
(underlain by 75 m of dolostone and sandstone)													

TABLE B27—Scenic Drive (section 34: Fig. 1 and Table 1).

Thickness above base of section (m)	Brachio-pods	Echino-derms	Gastro-pods	*Nuia*	Ostracods	Sponge spicules	Trilobites	Intraclasts	Pellets and peloids	Ooids	Quartz silt and sand	Spar cement	Micrite matrix
Padre Member													
(overlain by 2 m of dolostone)													
378	1	25	1	–	1	–	8	2	–	–	–	7	55
371	1	8	–	2	1	–	5	11	5	–	–	20	47
365	–	2	–	–	1	6	2	2	1	–	–	2	84
360	3	10	–	–	–	–	11	2	1	–	–	18	55
353	2	3	3	–	–	–	9	22	1	–	–	8	52
345	1	9	–	–	–	–	2	44	4	–	–	35	5
338	–	–	3	–	1	2	3	2	–	–	–	5	84
332	–	3	–	4	–	1	2	19	10	–	–	13	48
330	–	4	3	3	1	3	4	19	9	–	–	12	42
323	–	3	–	–	1	5	1	11	4	–	–	4	71
317	–	1	2	–	–	3	2	48	–	–	–	–	44
315	–	1	1	1	1	–	1	49	1	–	–	22	23
285	–	1	–	–	–	–	1	4	47	–	–	26	21

TABLE B27—(continued)

Thickness above base of section (m)	Brachio-pods	Echino-derms	Gastro-pods	*Nuia*	Ostracods	Sponge spicules	Trilobites	Intraclasts	Pellets and peloids	Ooids	Quartz silt and sand	Spar cement	Micrite matrix
McKelligon Member													
271	–	1	1	–	–	7	1	1	–	–	–	–	89
269	2	4	–	–	–	–	4	10	29	–	–	28	23
262	–	6	1	–	–	–	1	47	3	–	–	22	20
254	tr	2	tr	–	–	6	4	10	3	–	–	1	74
250	1	2	1	2	–	–	1	43	6	–	–	34	10
240	–	1	–	1	–	3	–	42	2	–	–	24	27
231	–	13	2	3	–	1	3	9	1	–	–	20	48
224	1	2	2	2	–	4	3	8	2	–	–	3	73
216	1	2	1	2	–	3	1	34	–	–	–	19	37
213	–	1	1	–	–	4	1	24	2	–	–	23	44
207	–	4	–	–	–	4	4	38	28	–	–	20	2
201	–	6	–	3	–	–	–	50	–	–	–	41	–
195	–	2	2	3	–	7	–	18	2	–	–	9	57
192	–	2	1	–	–	16	–	9	1	–	–	–	71
182	–	6	2	2	–	10	2	7	3	–	–	6	62
178	–	3	–	6	–	3	1	1	3	–	–	–	83
175	–	5	–	4	–	5	1	26	6	–	–	12	41
170	–	2	1	2	–	6	2	6	22	–	–	11	48
168	–	2	2	2	–	8	2	–	–	–	–	2	82
(underlain by 168 m of dolostone and sandstone)													

TABLE B28—South Hueco Mountains (section 35: Fig. 1 and Table1).

Thickness above base of section (m)	Brachio-pods	Echino-derms	Gastro-pods	*Nuia*	Ostracods	Sponge spicules	Trilobites	Intraclasts	Pellets and peloids	Ooids	Quartz silt and sand	Spar cement	Micrite matrix
(overlain by 117 m of dolostone)													
McKelligon Member													
(overlain by 18 m of dolostone)													
285	–	–	–	–	–	2	2	7	22	–	2	54	11
282	1	5	–	–	–	–	3	54	–	–	1	36	–
280	1	1	3	–	–	9	2	–	–	–	–	5	79
278	–	2	4	–	–	8	3	1	–	–	–	5	77
275	–	–	5	–	–	9	2	22	14	–	–	37	11
270	tr	4	2	1	–	16	1	–	–	–	–	3	73
265	–	1	–	2	–	14	1	8	–	–	tr	7	67
260	–	5	–	–	–	6	3	25	–	–	–	35	26
255	–	2	1	tr	–	12	1	22	–	–	tr	19	43
250	–	4	9	1	–	13	4	–	–	–	–	2	67
240	tr	11	–	–	–	3	6	14	–	–	–	21	42
235	1	6	–	1	–	–	2	38	–	–	–	37	15
230	–	2	1	–	–	2	1	3	9	–	1	18	63
225	1	4	8	1	–	tr	8	–	–	–	–	5	73
220	–	4	4	1	–	8	3	–	–	–	–	–	80
210	–	3	3	tr	–	4	6	7	–	–	–	9	68
205	–	2	3	1	–	5	3	7	–	–	–	11	68
200	–	4	7	–	–	9	6	1	1	–	–	8	64
190	–	6	4	–	–	–	1	33	–	–	–	18	38
180	1	4	–	–	–	–	6	20	1	–	–	19	49
175	3	4	5	–	–	–	12	9	–	–	–	8	59
170	1	6	11	–	–	6	3	8	–	–	–	7	58
165	–	1	–	tr	–	8	3	13	5	–	–	34	36
160	6	1	8	–	–	5	11	5	–	–	–	10	54
150	2	1	6	–	–	5	13	12	5	–	–	27	29
140	2	6	2	–	–	8	7	10	7	–	–	18	40
130	–	6	–	1	–	–	5	6	34	–	–	48	–
Jose Member													
120	–	4	–	5	–	–	1	–	35	–	7	48	–
110	1	26	5	–	–	–	4	31	–	–	–	33	–
100	–	1	4	2	–	–	3	7	–	12	2	18	51
Hitt Canyon Member													
90	–	6	1	2	–	–	16	13	–	–	2	52	8
70	–	1	3	11	–	4	3	9	–	–	2	16	51
50	–	3	–	23	–	8	2	2	–	–	3	13	46
40	–	3	–	1	–	2	1	1	–	–	5	9	78
30	–	7	–	21	–	–	8	3	7	–	5	49	–
20	–	4	–	24	–	5	1	–	–	–	2	21	43
10	1	6	–	24	–	–	4	8	1	–	8	38	10
base	1	10	–	25	–	–	5	–	–	–	13	46	–

TABLE B29—Cox Mountain (section 38: Fig. 1 and Table 1).

Thickness above base of section (m)	Brachio-pods	Echino-derms	Gastro-pods	*Nuia*	Ostracods	Sponge spicules	Trilobites	Intraclasts	Pellets and peloids	Ooids	Quartz silt and sand	Spar cement	Micrite matrix
(eroded and overlain by Cretaceous sandstone)													
McKelligon Member													
93	1	1	1	–	–	17	3	8	–	–	–	9	60
90	–	–	–	–	–	22	1	9	–	–	–	16	52
85	tr	3	–	–	–	–	2	29	–	–	–	35	31
80	1	5	6	tr	–	8	6	10	–	–	–	12	52
77	–	7	6	–	–	2	10	9	2	–	–	9	55
75	–	4	4	–	–	–	9	12	7	–	1	30	33
70	–	–	3	–	–	–	6	19	–	–	tr	38	34
65	–	3	5	2	–	–	4	26	–	–	–	22	38
60	–	5	–	5	–	–	1	39	–	–	–	31	19
Jose Member													
55	–	tr	1	–	–	–	1	6	–	38	–	37	17
50	–	–	1	–	–	–	tr	4	–	51	–	25	19
45	–	–	8	–	–	–	2	5	35	–	1	49	–
41	–	7	–	–	–	–	1	22	–	–	tr	23	47
Hitt Canyon Member													
36	–	1	–	5	–	–	2	44	–	–	tr	25	23
34	–	4	1	7	–	3	tr	8	–	–	4	12	61
33	–	5	tr	15	–	–	2	32	–	–	2	40	4
32	–	9	4	19	–	–	1	32	–	–	tr	35	–
31	tr	10	3	3	–	tr	3	11	–	–	6	20	44
30	–	tr	tr	–	–	–	tr	46	–	–	–	54	–
20	–	1	1	4	–	–	2	38	–	–	1	24	29
15	–	1	1	4	–	–	1	42	–	–	2	18	31
10	–	3	2	3	–	–	1	5	1	–	1	20	64
5	–	1	–	–	–	–	2	34	7	13	2	39	2
3	–	–	2	–	–	–	4	46	5	–	2	26	15
0	–	–	–	–	–	–	6	9	18	–	3	53	11
(base not exposed; under alluvium)													

Selected conversion factors*

TO CONVERT	MULTIPLY BY	TO OBTAIN
Length		
inches, in	2.540	centimeters, cm
feet, ft	3.048×10^{-1}	meters, m
yards, yds	9.144×10^{-1}	m
statute miles, mi	1.609	kilometers, km
fathoms	1.829	m
angstroms, Å	1.0×10^{-8}	cm
Å	1.0×10^{-4}	micrometers, μm
Area		
in^2	6.452	cm^2
ft^2	9.29×10^{-2}	m^2
yds^2	8.361×10^{-1}	m^2
mi^2	2.590	km^2
acres	4.047×10^3	m^2
acres	4.047×10^{-1}	hectares, ha
Volume (wet and dry)		
in^3	1.639×10^1	cm^3
ft^3	2.832×10^{-2}	m^3
yds^3	7.646×10^{-1}	m^3
fluid ounces	2.957×10^{-2}	liters, l *or* L
quarts	9.463×10^{-1}	l
U.S. gallons, gal	3.785	l
U.S. gal	3.785×10^{-3}	m^3
acre-ft	1.234×10^3	m^3
barrels (oil), bbl	1.589×10^{-1}	m^3
Weight, mass		
ounces avoirdupois, avdp	2.8349×10^1	grams, gr
troy ounces, oz	3.1103×10^1	gr
pounds, lb	4.536×10^{-1}	kilograms, kg
long tons	1.016	metric tons, mt
short tons	9.078×10^{-1}	mt
oz mt^{-1}	3.43×10^1	parts per million, ppm
Velocity		
ft sec^{-1} (= ft/sec)	3.048×10^{-1}	m sec^{-1} (= m/sec)
mi hr^{-1}	1.6093	km hr^{-1}
mi hr^{-1}	4.470×10^{-1}	m sec^{-1}
Pressure, stress		
lb in^{-2} (= lb/in^2), psi	7.03×10^{-2}	kg cm^{-2} (= kg/cm^2)
lb in^{-2}	6.804×10^{-2}	atmospheres, atm
lb in^{-2}	6.895×10^3	newtons (N)/m^2, N m^{-2}
atm	1.0333	kg cm^{-2}
atm	7.6×10^2	mm of Hg (at 0° C)
inches of Hg (at 0° C)	3.453×10^{-2}	kg cm^{-2}
bars, b	1.020	kg cm^{-2}
b	1.0×10^6	dynes cm^{-2}
b	9.869×10^{-1}	atm
b	1.0×10^{-1}	megapascals, MPa
Density		
lb in^{-3} (= lb/in^3)	2.768×10^1	gr cm^{-3} (= gr/cm^3)
Viscosity		
poises	1.0	gr cm^{-1} sec^{-1} *or* dynes cm^{-2}
Discharge		
U.S. gal min^{-1}, gpm	6.308×10^{-2}	l sec^{-1}
gpm	6.308×10^{-5}	m^3 sec^{-1}
ft^3 sec^{-1}	2.832×10^{-2}	m^3 sec^{-1}
Hydraulic conductivity		
U.S. gal day^{-1} ft^{-2}	4.720×10^{-7}	m sec^{-1}
Permeability		
darcies	9.870×10^{-13}	m^2
Transmissivity		
U.S. gal day^{-1} ft^{-1}	1.438×10^{-7}	m^2 sec^{-1}
U.S. gal min^{-1} ft^{-1}	2.072×10^{-1}	l sec^{-1} m^{-1}
Magnetic field intensity		
gausses	1.0×10^5	gammas
Energy, heat		
British thermal units, BTU	2.52×10^{-1}	calories, cal
BTU	1.0758×10^2	kilogram-meters, kgm
BTU lb^{-1}	5.56×10^{-1}	cal kg^{-1}
Temperature		
°C + 273	1.0	°K (Kelvin)
°C + 17.78	1.8	°F (Fahrenheit)
°F − 32	5/9	°C (Celsius)

**Divide by* the factor number to reverse conversions.
Exponents: for example 4.047×10^3 (see acres) = 4,047; 9.29×10^{-2} (see ft^2) = 0.0929.

Editor: Jennifer Boryta
Susan Welch

Drafters: Kathy Campbell
Jan Thomas

Typeface: Palatino

Presswork: Miehle Single Color Offset
Harris Single Color Offset

Binding: Saddlestitched with softbound cover

Paper: Cover on 12-pt. Kivar
Text on 70-lb white Mountie matte

Ink: Cover—PMS 320
Text—Black

Quantity: 1000